Research & Development

2014

Mechanical Engineering Letters, Szent István University

Annual Technical-Scientific Journal of the Mechanical Engineering Faculty,
Szent István University, Gödöllő, Hungary

HU ISSN 2060-3789

Páter K. u. 1., Gödöllő, H-2103 Hungary
dekan@gek.szie.hu, www.gek.szie.hu,

Volume 11 (2014)

Selected Collection from the Research Results of Year 2014

Contents

Institute for Mechanics and Machinery

Professor Dr. István SZABÓ,
Director of the Institute

Dear Reader,
The Institute of Mechanics and Machinery is one of the teaching and research units of the Faculty of Mechanical Engineering at Szent István University, Gödöllő integrating activities of three departments:

- Department of Mechanics and Technical Drawing
- Department of Machine Construction
- Department of Agricultural- and Food-industrial machines.

Teaching and research programs are supported by two external departments as well

- Department of Biotechnics hosted by Onchotherm Ltd.
- Department of Farm Mechanization at National Institute of Agriculture Research and Innovation

IMM also hosts the Engineering Information Technology Center, a 2000 m^2 teaching and research facility of the Faculty of Mechanical Engineering.

The Institute is engaged in teaching of undergraduate and graduate courses in all programs of the Faculty and also has been active in various postgraduate trainings. Courses range from introductory level subjects (ie. technical drawings, statics, strength of materials, machine element design etc.) to more advanced areas like machine construction, engineering modeling, computer aided engineering and analyses, farm machinery and bio-systems engineering. It is our aim to provide all students with the skills to understand mechanical properties of machineries, their design and creative contribution to developing mechanical systems.

Research activities of staff members reflect the scientific interest of the three departments and this effort became integral part of our work. Articles published in this volume of Mechanical Engineering Letters may give a snapshot of the research programs that were carried out in 2014, but due to the limitations it is only a partial coverage of the results we had. I do hope that reading the following pages can be intellectually challenging for professionals of similar fields of interest and might inspire co-operation and joint research with us.

Dr István SZABÓ
director

On the Discrete Element Modeling of Agricultural Granular Materials

István OLDAL, István KEPPLER, Adrienn BABLENA,
Ferenc SAFRANYIK, Attila VARGA
Department of Mechanics and Technical Drawing,
Institute for Mechanics and Machinery

Abstract

Discrete element method based modelling of granular material – solid body interaction is demonstrated in our article. Silo outflow, screw auger performance optimisation and soil-tool interaction modelling results are discussed.

Keywords

Discrete element method, granular material, silo, drying, soil

1. Introduction

Most of the materials used in the agricultural crop production with capital importance are treated and stored in a form of granulates. Soil and agricultural products interact with the tools and equipment used to manipulate and store them. This interaction causes the load of the tools and of the agricultural product. The practicing engineer has to know how granular materials behave so as to be able to examine and control their mechanical behaviour. The design cost of the process can be greatly decreased if we are able to model properly the given mechanical phenomena, as the number of control experiments should be reduced by appropriate numerical modelling.

The Discrete Element Method (DEM) is a fairly new proceeding to model the mechanical properties bulk materials. By the use of DEM, the model problem is solved by applying and solving the equation of motion on each singular particle of the bulk material assembly.

In our article we would like to give an outlook to the research activities of our research group's work on the different applications of discrete element method based applied engineering research. The research group was established at 2012, and since then different publications were written: soil-tool interaction, particle motion inside dryers, silo outflow were examined beside others. In this article we would demonstrate our results related to vibrating silos, soil-wheel interaction and mixing screws. In all of the three topics there is the interaction between granular material and some other facilities is examined: storage silo wall, wheel interface of screw interface are interacting with the granular

assembly, experiments and DEM modelling techniques are used for describing the granular material's behaviour during the interaction.

2. Dicrete Element Method

The Discrete Element Method (DEM) is a fairly new proceeding to model the mechanical properties of bulk materials. By the use of DEM, the model problem is solved by applying and solving the equation of motion on each singular particle of the bulk material assembly (Cundall and Strack, 1979).
For modeling the mechanical behavior of the granular material, we used EDEM discrete element software with "Hertz Mindlin with bonding" contact model (EDEM, 2012). In this model, the particles are glued with a finite sized bond.

3. Applications for agricultural

3.1. Outflow from silos

In almost all fields of industry large, vertical containers (called silos) are used for storing particulate raw materials. The geometry and the surface conditions of the silo and the mechanical properties of the stored material define the flow mode (mass- or funnel flow). Whereas one of the most important design parameter of these storage equipment is the discharge rate several theories were formed to determine this parameter, nevertheless none of them are able to describe the discharge process with adequate accuracy in all cases of flow modes. Relying upon these findings the aim of this work is to create and validate a discharge model based on Discrete Element Method (DEM) then to compare this with analytical models and laboratory experiments in term of different flow modes.

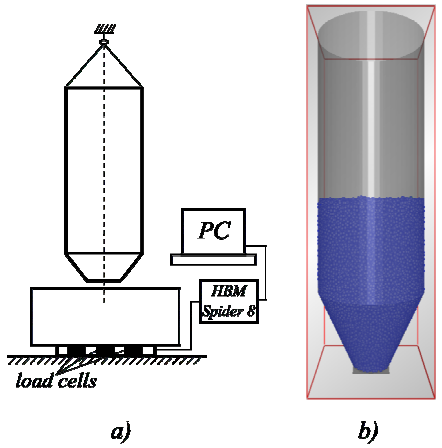

Figure 2. The measuring arrangement and the DEM model

To validate the DEM model and to compare this with analytical models laboratory experiments was carried out in term of different flow modes with wheat. During the simulation the Hertz-Mindlin no slip contact model uses a spring-dashpot model to describe interaction of the particles. This contact model is elastic and non-linear and takes into account viscous and frictional damping and it was used to simulate particle-particle and particle-wall contacts [Tsuji et al., 1992]. In modeling the micromechanical parameters and the particle model of wheat by Keppler et al. [2012] were carried out.

In case of laboratory experiments the mass of the discharged wheat was measured by three load cells. The measurements were repeated five times in case of every model silo. The goal of the measurements was the determination of the amount of outflowing wheat as a function in time. The mass change functions were determined by also the simulations and these were compared with the measurement results.

In the simulation process the first step was the randomly generation of all of the particles. The generated particles were allowed to fall under gravity; this step was the filling of silo. During the filling process the outlet of the silo was closed. The next step was the emptying of the silo. When the particles reach a static state (the amount of motion energy is about zero) then the outlet of the silo was opened and all of the particles were discharged. To the end of the filling process the bulk reaches a static state (his energy of motion is about zero).

Results

On the Figure 3 the particles were painted according to their vertical velocity. Vertical velocity of the blue particles is minimal and the vertical velocity of red particles is maximal.

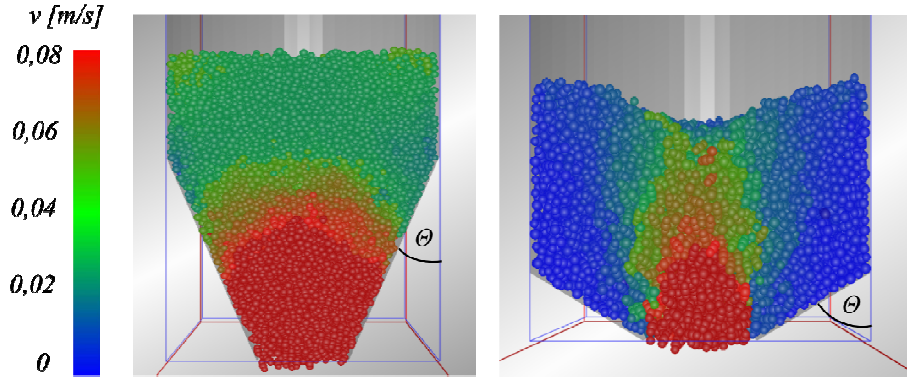

Figure 3. Flow modes based on the simulation

According to literature [Jenike, 1895] in case of a conical bin with low half angle the flow modes is mass flow, and in case of high half angle the motion is

confined to the vertical region of the granular assembly above the aperture – funnel flow.

3.2. Optimisation of screw auger performance

In drying processes of agricultural grains, the main problem is the uneven distribution of moisture content in the material assembly. To reduce the inhomogenity of the material there are numerous methods. In case of dryers with storing system a grain blender is fixed on top of the silo by which it is possible to reduce the inhomogeneity (*Figure 4*.) [Beke, 2002]. The mixig process consists of the superposition of three motions. The holder which is fixed on the top of the silo performs circular motion around the axis of the silo, while the two augers on the holder perform periodic motion along the holder and rotate about their own axes [Varga, 2013].

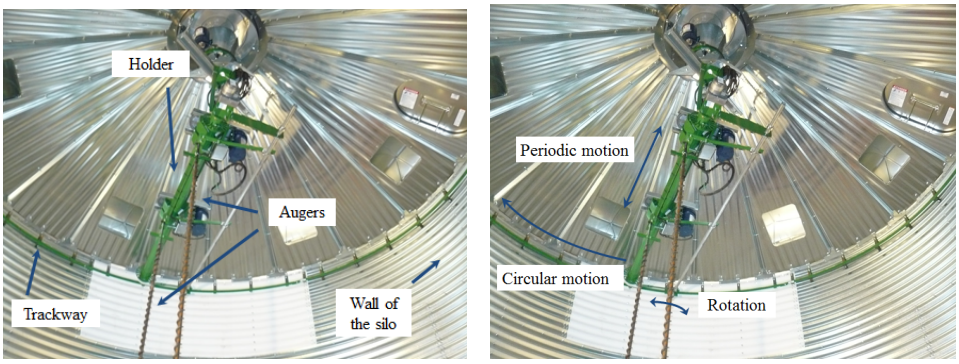

Figure 4. The structure and the motions of the grain blender

Our aim is to determine the kinematical parameters of screw augers needed to set optimal mixing performance. To reach this goal, we made experiments and numerical simulations to create an adequate kinematical model of screw auger-granular material.

We used DEM to get the proper kinematical model. For simulation process we used the model of wheat particles used by [Keppler et al. 2012].

The aim of our simulation was the determination of the volume of material mixed arround the rotating screw. (*Figure 5.*) [Szabó, 2013].

By introducing the so called effective radius of screw augers, it is possible to compare the different types of augers. (*Figure 6*). Another important concept is the mixing efficiency of the augers, which is the ratio of effective radius and the radius of the augers leaf. Five simulations were compared. We varied the angular velocity and diameter of auger and determined the changing of the effective radius. The augers diameter was 65, 97,5 and 130 mm. The different rotation speeds were 50, 100 és 150 1/min. The results are showed by *Table 1*. To evaulate efficienties , the distance between the augers axes and the container

wall was divided into ten equal parts. On the ten intervals, the average vertical velocities were determined. By fitting polynomial on the resulting points the effective radius is determined.

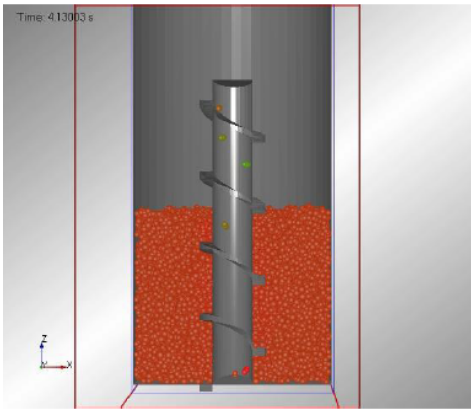

Figure 5. The discrete element modell

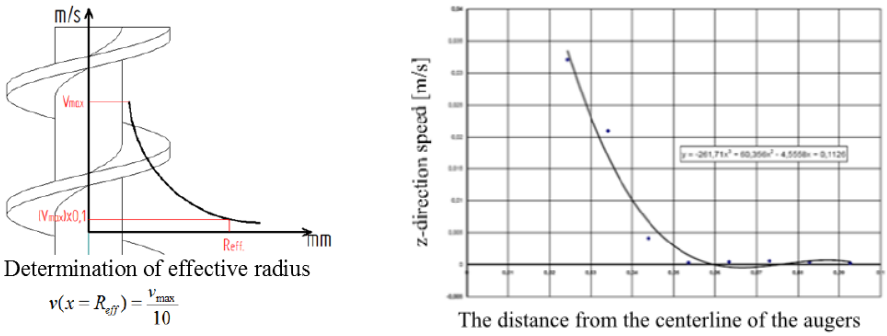

Figure 6. Interpretation of the effective radius

Table 1. Results of the simulation

d [mm]	n [1/min]	vmax [m/s]	Reff [m]
65	50	0,0321	0,0495
65	100	0,0821	0,0488
65	150	0,0881	0,0525
97,5	50	0,0462	0,0642
130	50	0,0344	0,1061

Conclusions from the comparison of the effective radius: at a given auger's leaf diameter, the increase of the speed does not lead to a change in the effective radius. The increase of auger's leaf diameter has caused more spectacular change. For the 130 mm diameter augers leaf has already more than twice the effective radius, than 65 mm in diameter. It can be concluded that in case of constant rotation speed, the increase of auger's leaf diameter increases the effective radius.

3.3. Modeling of soil-wheel interaction

Mechanical modeling of soil-wheel interaction has been examined for a long time. The main task is to determinate forces acting on the moving wheel. Analitical methods to solve this problem are mostly coming from experiments [Bekker, 1956].

The aim of this work is to determinate performance losses during wheel moving. To reach this aim the first particle movement was examined with discrete element method on the basis of experimental studies from literature.

The base of these experiments is determination of trajectories of soil particles from literature. Fukami et al. (2006) were found that trajectories of these particles under the wheel were spirals. In this experiment was performed with 3.9% and 20.9% slip.

Discrete element model os soil-wheel interaction was established for examination of particle motion (Figure 7).

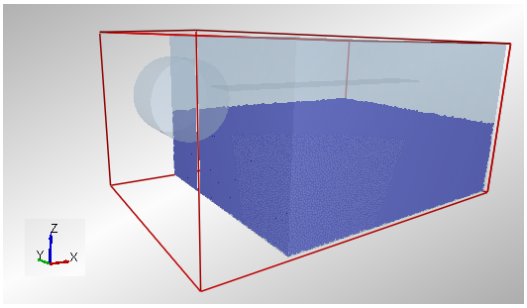

Figure7. The discrete element model

For examination of particle motion under the wheel according to figure 8.a, 15 pieces of particles were picked (3 pieces per row) and vertical movement (Z) was examined as a function of horizontal movement (X). On figure 8.b pressure distribution can be seen under the wheel.

In figure 3.a.-c. distribution of ΔU, ΔX and ΔZ, and their model functions can be seen. ΔU is the displacement of the particle in every time step, ΔX and ΔZ are X and Z components of the displacement. According to Fukami et al. (2006) ΔU can be modelled with a Gaussian function, ΔX is the first and ΔZ is the second derivative of ΔU.

In this case (for one particle) the model functions, where the parameters were calculated by matlab are the following:

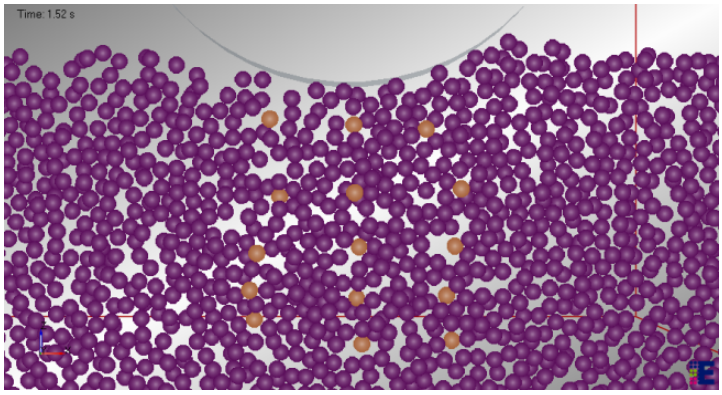

Figure 8.a Picked particles

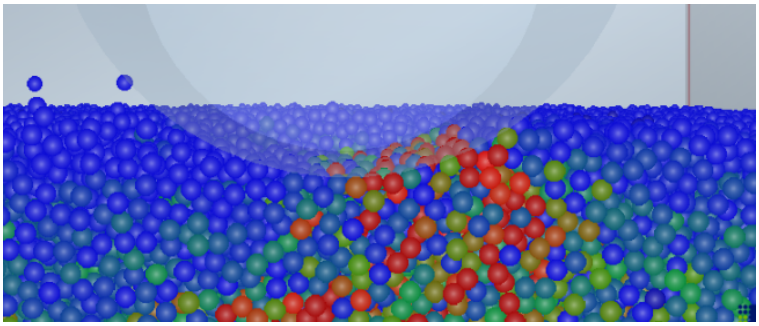

Figure 8.b Pressure distribution under the wheel

$$\Delta U(x) = 6.174 \cdot 10^{-4} \exp\left[-\frac{(x-0.6061)^2}{2 \cdot 4.343^2} \right]$$

$$\left(R^2 = 0.8037\right)$$

$$\Delta X(x) = -1.397 \cdot 10^{-4} \cdot (x+4.255) \cdot \exp\left[-\frac{(x+1.702)^2}{2 \cdot 3.372^2} \right]$$

$$\left(R^2 = 0.8366\right)$$

$$\Delta Z(x) = -4.726 \cdot 10^{-4} \cdot \left((x-4.311)^2 - 12.93\right) \cdot \exp\left[-\frac{(x-2.079)^2}{2 \cdot 2.638^2} \right]$$

$$\left(R^2 = 0.6279\right)$$

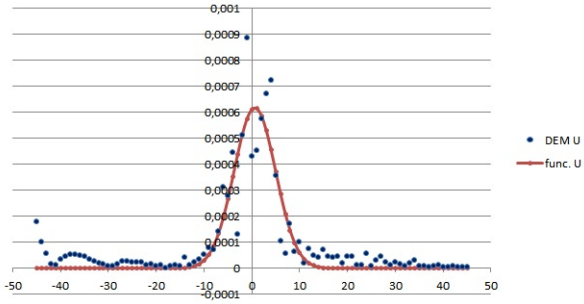

Figure 9.a Distribution of ΔU

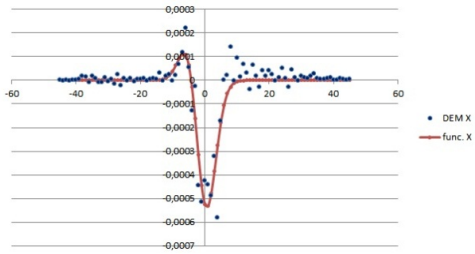

Figure 9.b Distribution of ΔX

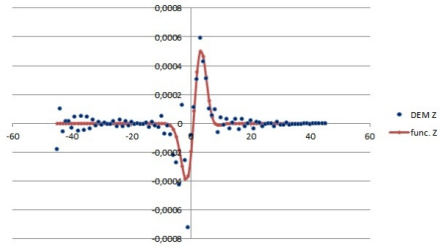

Figure 9.c Distribution of ΔZ

For calculating effort trajectory length was determinated. Trajectory of particles from the same height was averaged then a particle was picked which trajectory was nearest to average value. After this distances were represented in figure 10.a as a function of height in such a way that parameter s and h were divided wheel radius so non-dimensional parameters were represented.

Determination of forces acted of particles is also necessary but during discrete element modeling these were determinated by the program. In figure 10.b these force values can be seen in function of particle vertical position.

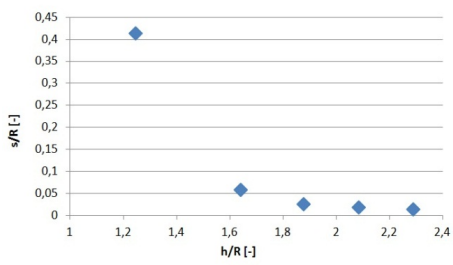

Figure 10/a. Distance in function of height

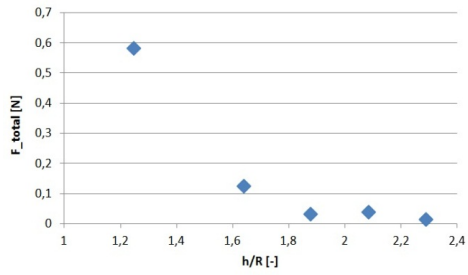

Figure 10/b. Force in function of height

Conclusion

The discrete element method is suitable for modeling the moving of granular materials in closed and open space. Three applications was introduced in this work. All of the them describe the interaction between granular material and other facilities: storage silo wall, wheel interface and screw interface are interacting with the granular assembly.

Conclusions of silo modeling:

- Based on the results of laboratory experiments and numerical simulations the mass of the discharged material in function of time are linear in all cases. This means, that the discharge rate is constant, consequently this is independent of the filling level of silo. This means that the numerical model is suitable for right modeling the physical phenomenon.
- Based on the mass-times values the discharge rate was determined in all cases. The difference between the DEM model and measurements is less than 5% also in case of a funnel flow and also in case of mass.
- The available analytical models are unable to describe the mass flow discharge with adequate accuracy. But this numerical model for silo discharge is suitable for describe the outflow process with an adequate accuracy also in case of mass flow.
- With the numerical model the whole discharge process can be described, still in case of an emptying bin. One of the analytical models is not able to describe the process in this non-stationary case.

Conclusion of screw auger modeling:

- The discrete element method is suitable for modeling the granular-motion created by stirring augers in the silodryer;
- Introducing the concept of the effective radius, it is possible to compare the individual auger-constructions;
- At a given auger geometry the increasing of angular velocity does not necessarily lead to a significant change of the effective.

Conclusion of soil-wheel interaction modeling

- Using discrete element method particle trajectories can be examined.
- Trajectory of a particle under moving wheel is a spiral. The distance in spite of particle height measured from the wheel shows declining tendency.
- Values of forces acted on particles increase depth also decreased.
- In following experiments – knowing trajectories and forces – wheel effort will be determined.

Important conclusion of our researches that DEM modeling always needs validation. Long-term aim of this research area is creation of DEM material model which can be used for applications without model validations.

References

[1] Keppler I., Hudoba Z., Oldal I., Csatar A., Fenyvesi L.: Discrete element modeling of vibrating tillage tools, Engineering Computations, Accepted Research Paper, 20-Mar-2014.
[2] Istvan Keppler: Failure analysis of pebble bed reactors during earthquake by discrete element method, Nuclear Engineering and Design, Volume 258, May 2013, Pages 102–106. http://dx.doi.org/10.1016/j.nucengdes.2013.01.028
[3] Istvan Keppler, Laszlo Kocsis, Istvan Oldal, Istvan Farkas, Attila Csatar, Grain velocity distribution in a mixed flow dryer, Advanced Powder Technology 23 (2012), pp. 824-832,
[4] Istvan Oldal, Istvan Keppler, Bela Csizmadia, Laszlo Fenyvesi, Outflow properties of silos: The effect of arching, Advanced Powder Technology 23 (2012) pp. 290-297.
[5] Beverloo, R. (1961). The flow of granular solids through orifices. Chemical Engineering Science, 15(262), 260-269.
[6] Jenike, A.W., Johansson, J.R., Carson, J.W. (1973). Bin loads – part 2: Concepts. ASME Journal of Engineering for Industry, 95(1), 1-5.
[7] Janssen, H.A. (1895). Getreidedruck in Silozellen. Z. Ver. Dt. Ing., 39, 1045-1049.
[8] Johanson, J.R. (1965). Method of calculating rate of discharge from hoppers and bins. SME of AIME, Transactions, 232, 69-80.
[9] Tsuji, Y., Tanaka, T., Ishida; T. (1992). Lagrangian numerical simulation of plug flow of cohesionless particles in a horizontal pipe. Powder Technology, 71, 259-270.
[10] Arun S. M, Beke J (2002): Gyakorlati szárítás, Szaktudás Kiadó Ház, Budapest, (in Hungarian).
[11] Varga A (2013): Bolygatott ágyas szárítóberendezés keverőrendszerének tervezése, Diplomamunka, Gödöllő, (in Hungarian)
[12] Istvan Keppler, Laszlo Kocsis, Istvan Oldal, Istvan Farkas, Attila Csatar (2012): Grain velocity distribution in a mixed flow dryer, Advanced Powder Technology 23, pp. 824-832
[13] Szabó M. (2013): Vastagrétegű szárítók szemcsemozgás viszonyainak elemzése diszkrét elemek módszerével, TDK dolgozat, Gödöllő, (in Hungarian)
[14] Bekker M. G. (1956): Theory of land locomotion, Michigan, University of Michigan Press, 520. o.
[15] Fukami K. et al. (2006): Mathematical models for soil displacement under a rigid wheel, Journal of Terramechanics Vol. 43, No. 3, pp. 287-301.

Information entropy prediction

Zoltán BLAHUNKA, Zoltán BÁRTFAI, Dezső FAUST
Department of Agricultural and Food-industrial Machines,
Institute for Mechanics and Machinery

Abstract

In the agricultural practice numerous methods used for describing the soil surface. Many of them are standardised, and because of it precise, but difficult to use and time consuming. Our experimental method is based on the usage of mobile robots as a field equipment and the method is based on calculating the exponential regression of entropy-time function.

Keywords

mobile robot, soil surface, information entropy

1. Introduction

Stochastic processes are always changing. Measurement seems endless. Our aim is to find a stable state, where we know everything about the process and the further measurement will not give more information.

Our stochastic process is the **soil surface**. Clots have different size there is different distance between them. When we are measuring the surface we are also calculating the **information entropy** of the surface's parameters distribution. The information entropy shows us how much new information we get by the measurement. When entropy is stabilized, we get all available information from soil surface.

To forecast the sufficient level we calculate the exponential regression of the entropy by time. The regression has very high coefficient (over 90%). 5T means 3% different below the estimated maximum. When R^2 is over 90%, 5T forecast the sufficient length of measurement.

2. Method

There are many methods to measure the soil surface, starting with the profilograph method, laser scanners and 3D air photos.

Our method works with IMU (Blahunka & Faust, 2013). Testing all inputs (3D accelerometer, 3D angle speed) finally we use the angle speed over the y axis (horizontal sideway). Integrating this angle speed, we are able to calculate the height different between front and rear axle (Blahunka, Faust, Bártfai, & Lefánti, 2011).

Figure 1. Mobile robot on the field

At the beginning we used IMU (Wang, 2006) accelerometer for detecting soil surface. The IMU devices measure the total acceleration. It is equal the kinetic acceleration and the part of gravity depending on the 3D position of the device. In the static state it shows only the position, but in moving state it is not possible to determine the position of mobile robot platform. That is why we use angular velocity.

Figure 2. Analog Devices 16365 IMU device

The angular velocity shows only position changing, independent from kinetically acceleration. It is useful for detect clot on agricultural soil surface.

To log and control the measurement we use a standard laptop, and wifi router.

The whole measurement system consists of:

- a mobile robot with IMU device
- a laptop for controlling, logging
- wifi access point (for wireless connection)
- (optional power supply parts, inverter, battery)

The surface classification process is the following:
- setup the measurement system,
- put or drive the mobile robot to the inspected surface
- start the IMU logging
- drive the robot on a straight line (while the sufficient distance covered)
- stop the robot
- stop the IMU logging (save the results)

The IMU device is placed as ordered in ISO8855:2011 (Coutinho, 2013). It is a right handed, 3 dimensional coordinates system. X axle shows to front, Y axle shows to the left and Z axle shows up. For detecting the level difference between the front and rear axis the angular velocity over the y axis is the best choice.

The complete measurement consists of the following steps:
- read the measured channels (acceleration, angular velocity)
- integrating the angular velocity to get the angle
- using the axle distance calculate the height
- histogram of heights (extended distance between clods, 2 dimensional histogram)
- calculating distribution based on histogram (probabilities)
- informatical entropy (Shannon & Weaver, 1949)
- exponential regression of entropy (Seber & Wild, 2005)
- based on regression parameters estimate, forecast the sufficient distance.

3. Entropy

The entropy shows how much new information we get. Shannon defines it at 1949 (Shannon & Weaver, 1949).

$$H = -\sum p_i \log_2 p_i \tag{1}$$

Equation 1 shows the entropy for discrete events. p_i–s are the probabilities of events. Because of $\log_2$ the entropy is calculated by binary bits.

How can the entropy changing (increasing, decreasing)? To calculate the entropy we need a distribution (probabilities for all events). The entropy depends on the number of the events, probabilities. With the same number of events the entropy is higher when the probabilities are the same. Let's see two examples: coin, dice.

4. Coin

The coin has two events. At first we use normal coin, both side has the same probability. Calculating the entropy for this case gives 1. Throwing a (normal) coin gives us 1 bit new information.

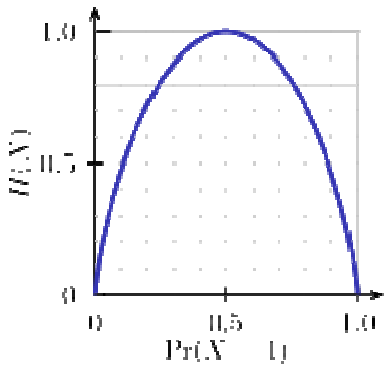

Figure 3. Entropy for two events (coin), source: (Wikipedia contributors, 2012)

However if we cheat, the probabilities are not the same. One side has a bigger probability. This way the entropy is smaller. Worst case the coin fallen always at one side. At this case the entropy is 0. We know the result, there is no new information by the measurement.

5. Dice

The dice has 6 sides. All sides have the same probability. This way the entropy is equal log26.

Big question of dice? How many times should we throw to get the 1/6 probabilities? For example: 1000. 1000 is not divisible by 6, that mean not all events will be 1/6. Every throwing makes a new distribution and new entropy. The entropy has a limit, the theoretical value $\log_2 6$. We can get this value when all events have the same probability. If we are lucky it can be after 6 throwing. But for 7th throwing the entropy will deceasing.

We use this experience to define the optimal length of (stochastic) measurement.

We are calculating the height distribution of the soil surface. The information entropy of the distribution shows u show much information we get. During the measurement this entropy shows a saturating exponential function.

$$H(T) = H_{\infty}(1 - e^{(t6T)})$$

The exponential regression calculates two parameters: H_∞ and T. We are also calculating the R^2 for validation.

- H_∞ is the theoretical entropy maximum (at infinite)
- This control theory parameter shows when the function reach the H_∞ if it growing by the constant value at the starting point
- R^2 is the coefficient determination

Exponential regression makes high R^2, over 90%. Based on equation, measuring for 5T time ensures that we reach the H_∞ 97%.

Why is it a saturating function? At the start position there is no distribution, the entropy value is 0. The first phase is while the distribution starting to fill up. While all used position is filled the information entropy growing. At the finishing phase all distribution values are valid, there are no big changing on entropy. At final phase the distribution is stabilizing the information entropy getting constant.

6. Results

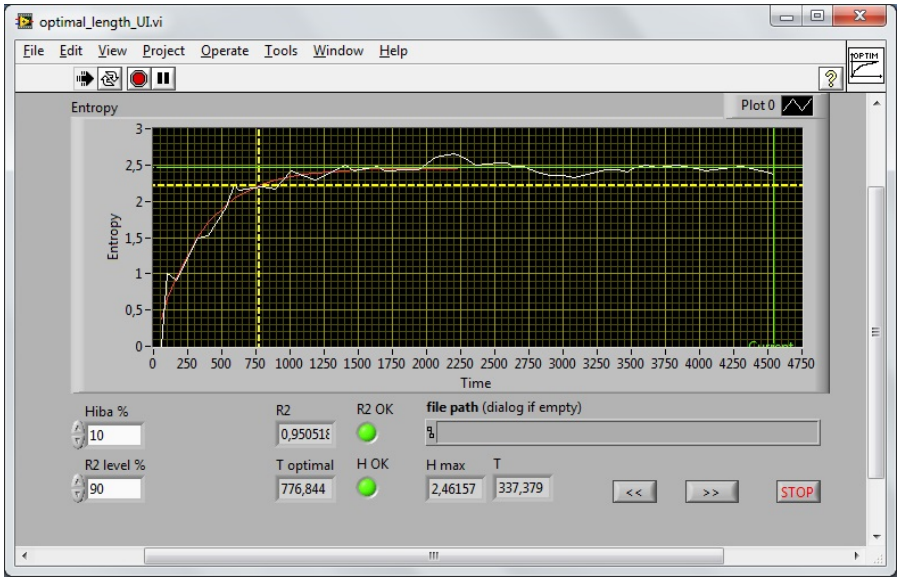

Figure 4. Exponential regression of informatical entropy

Figure 4 shows the measured entropy and the estimated value. Current R^2 is 95,05%. T is 337. 5T=1685 1/100 sec.

Continuing the measurement after this point makes more accurate result, using more resource (time, energy, …)

This application calculates entropy after the measurement. Calculating entropy online can forecast the optimal length of soil surface.

Conclusion

There are many standards for surface measurement. Tribology, road surface have ISO standards. Standards describe detailed measurement process. They have recommendation for time elapse, without knowing the measured surface.

Our method calculation based on measured surface. Calculating the exponential regression of entropy-time function, we are able to forecast when the measurement is sufficient.

References

[1] Blahunka Z., & Faust D. (2013). A művelésből származó talajfelszín egyenlőtlenség mérésének új módszere. *Mezőgazdasági Technika*, *2013*(6), 2–4.

[2] Blahunka, Z., Faust, D., Bártfai, Z., & Lefánti, R. (2011). Mobile robot soil surface monitoring. In L. Magó, Z. Kurják, & I. Szabó (Eds.), (p. 104). Gödöllő: SZIE Gépészmérnöki Kar.

[3] Coutinho, M. G. (2013). *Guide to Dynamic Simulations of Rigid Bodies and Particle Systems*. Springer.

[4] Seber, G. A. F., & Wild, C. J. (2005). *Nonlinear Regression*. John Wiley & Sons.

[5] Shannon, C. E., & Weaver, W. (1949). *The mathematical theory of communication*. University of Illinois Press.

[6] Wang, J. H. (2006). *Intelligent MEMS INS/GPS integration for land vehicle navigation* (Vol. 67). Retrieved from http://www.ucalgary.ca/engo_webdocs/YG/06.20246.Jau-Hsiung%20Wang.pdf

Stress Optimization Process of Bevel Gearbox Housing with Six Axes

Ervin PINTÉR, László KÁTAI, István SZABÓ
Department of Machine Construction, Institute for Mechanics and Machinery

Abstract

With technological development more and more complex computer systems are essential. In some fields of applications such as agriculture creating a complex bevel gearbox is crucial. The developed gearbox designed with six axis. One axle is driven and it drives the other five axes through bevel gears.
Few agriculture company are interested in application of such kind of gearbox. Generally these companies deal with corn drying tower with new auger and conveyor system development. One electro-motor drive input axis of gearbox, and the other five axel drive every augers and conveyors.

Multi-axis bevel gearbox planning is a complex task. Complexity consists of on one hand the fact that models widely used for steel material cannot be directly adapted for cast aluminum and on the other hand location of the place of stress concentration of cast houses.

Applying of FEA software could be the solution of the complexity. Mission of our design project is to examine the behavior of the new generation gearbox house in different load conditions. The primary objective was to optimize the geometry. As a first step the basic prototypes, simulations were carried out. The static test loads simulations have shown the stress concentration points that are critical so that optimum geometry has been achieved.

With the redesigning of these points gear housing prototypes have been successfully prepared taking account of casting aluminum criteria.
Examination of stresses nearby bearing forces and screws has been laid emphasis on. This is a critical point of the FEA software, even so - because of the special attention - the size of the washer has been optimized the way that the maximum stress became appropriate. Determination of adaptor hole geometry was another important result. This could be made with such kind of die casting process which tolerates stress without final manufacturing.

Keywords

gearbox housing, FEA, optimization

1. Introduction

Development of the sciences, society and all fields of the industry has been accelerated in the 21st century. Industry needs are constantly changing and expanding. In the past 25 years engineering sciences and industry have been

extremely developed. New methods, equipments and software appeared in engineering [1].

In some fields of applications such as agriculture creating a complex bevel gearbox is crucial. The developed gearbox designed with six axis. One axle is driven and it drives the other five axes through bevel gears. Few agriculture company are interested in application of such kind of gearbox. Generally these companies deal with corn drying tower with new auger and conveyor system development. One electro-motor drive input axis of gearbox, and the other five axel drive every augers and conveyors.

2. Optimization process

2.1. Gearbox development process

In the first step the input parameters have been determined. The gear box could drive five axis. The input 37 kW power is given by an eight-pole electric motor work on 750 rpm. The required speed ratio was 1:1 by the bevel gear train. The required gearbox has to be light, rigid and available for aluminum die casting.

A study has been worked out but the appropriate gearbox could not have been found in industry. Design process has been started. You can read more about design process in [2], and 3D CAD model can be seen on Figure 1. After design process FEA examinations has been started.

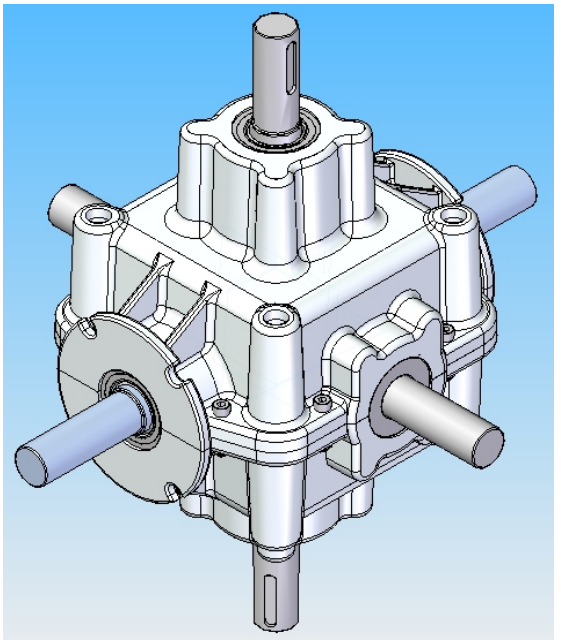

Figure 1. 3D CAD model of gearbox

2.2. Material selection

We used aluminum alloy by gearbox casing. Aluminum has more advantages. It is light, does not rust and can usually be used unpainted. In comparism with steel, mechanical properties of the aluminum are weaker. Otherwise the stronger alloys could be comparable with strength of steel but are less ductile [3].

Al 7075-T6 aluminum alloy has been selected which is mostly used for thin-walled and complex mold castings. This material has fine castability properties, excellent mold filling capacity can be achieved. This type of aluminum alloy is less liable to cracking. Vibration and pressure castings have surpassing corrosion resistance.

2.3. Defining input parameters and boundary condition

Gearbox analyzing and optimizing have been worked out with finite element method software. The applied software was ANSYS.

The gearbox housing must be rigid in order to carry the loads with slight deformation. The gearbox divided into two halves, and they are connected with bolted joint. Stress in gearbox housing caused by bolt preload forces and bearing forces. The condition of stable bond is the application of preload force. Gearbox casing parts are being loaded through washer. Stress state in cover halves are being influenced by the screw size and its preload force value.

Optimization process has been started with defining criteria. Manufacturability and mechanical properties of aluminum alloy were the first to be taken into consideration. The criteria were the followings:

- We required to minimize the applied aluminum alloy weight per gearbox case. Casing has to be reduced with 14 kg.
- We required to reduce stress under 155 MPa.
- We required to reduce deformation under 0,025 mm.

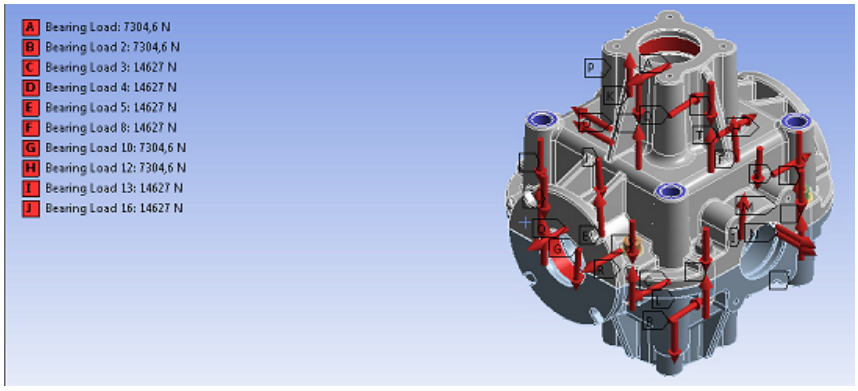

Figure 2. Boundary conditions

After coarse analyzing, weak points could be determined. We started this study with importing gearbox geometry into Ansys software. Next step was to

create connections between parts and coarse mesh method was applied. Furthermore bolt preload forces and bearing forces were defined. Boundary conditions were defined with finite element analysis. The load force resulted from bevel gear train. The bevel gear train generate axial and radial forces. By these forces gearbox housing are being loaded through bearing. Boundary conditions are shown on Figure 2.

2.4. FEA examination and optimization

We ran analysis. The result of analysis was inappropriate. The highest stress value exceeded the value of criteria. Therefore, we increased wall thickness. The very think wall resulted optimal stress value, but the deformation was too high. Therefore, we redesigned gearbox housing and we applied new feature. We designed casing with thin wall, ribs and shoulder faces. We ran new analysis.

The fourth stress analysis results are shown on Figure 3. The highest tensile stress in screw connection, its value is 213,62 MPa. This value is too high, we need smaller stress value (under 155 MPa) by this aluminum alloy (Al7075-T6) [4].

The deformation was also analyzed and the results are shown on the Figure 4. The bearings and bevel gear train required rigid gearbox casing. The resulted 0,032mm deformation value was high, we had to reduce this value. Application of ribs could reduce deformation, but the optimum value required thicker wall size.

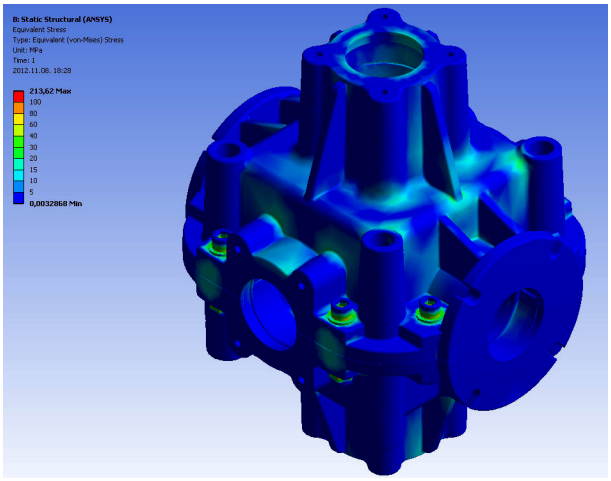

Figure3. Stress analysis result by the forth test procedure

The presented FEM process has resulted optimal gearbox casing geometry. Thin wall thickness with stronger ribs could reduce stress in gearbox casing, as it is shown on Figure5. Castability and equal stress state in gearbox casing were taken into consideration during geometry modification process. Skewness of wall and fillets should have been sufficiently large.

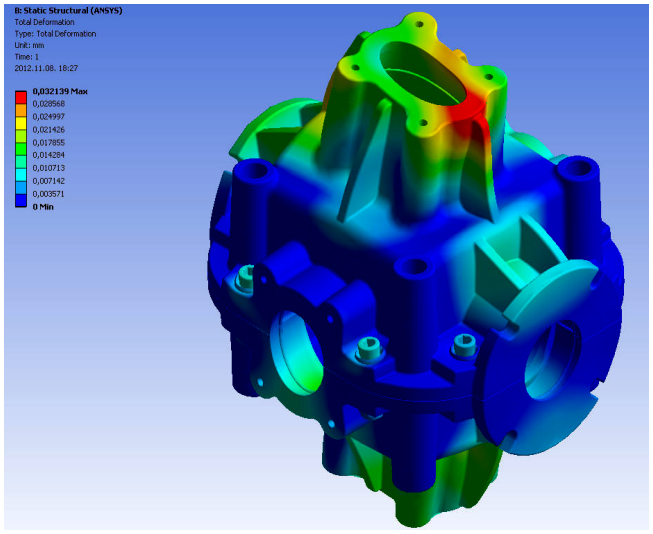

Figure 4. Deformation analysis result by the forth test procedure

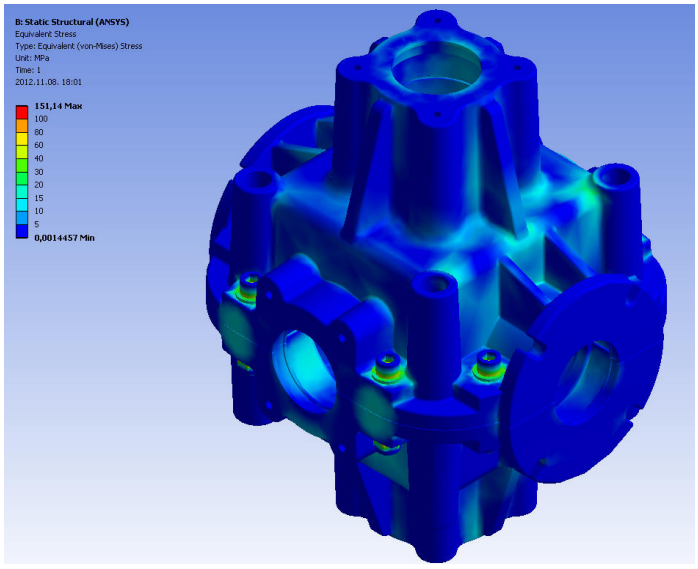

Figure 5. Final stress analysis result

Generated stress under FEM analysis of the final geometrical construction was under 60MPa in gearbox casing. The biggest stress - 151MPa - has been observed in screws.

By the deformation of gearbox casing an angular error of axis and bearings has been occured. The bearings can carry only defined angular error. The large value of error reduces bearing lifetime. Angular error could cause other problem in gearbox operation.

Angular error could create irregular connection between bevel gear teeth, and it also reduces bevel gear train lifetime. A repeated geometrical modification of the gearbox housing has reduced deformation value. Maximum deformation was 0,023mm shown on Figure 6.

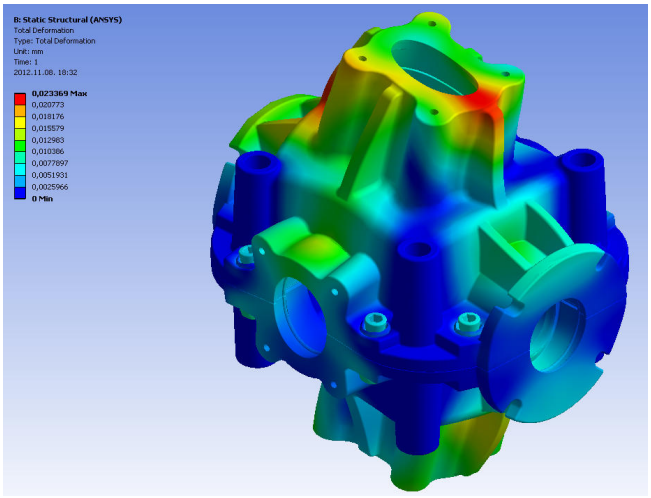

Figure 6. Final deformation analysis result

Conclusion

In the field of using light bevel gear train the improved gearbox should be a possible solution. The developed gearbox should be used on low PRM until 37 kW power.

Appropriate gearbox construction has been improved with optimization process. First coarse finite element analysis with Ansys software has been applied. In the next step optimal wall thickness has been created with applying ribs and choosing appropriate screw size. Finally optimal rib thickness has been defined.

Acknowledgement

The authors would like to acknowledge the IT assistance support of Zoltán Gergely.

References

[1] Szendrő P.: Gépelem, Mezőgazda Kiadó, Budapest, 2007. ISBN: 978-963-286-371-9

[2] Pintér E. – Kátai L. – Szabó I. – Szabó E.: Development of bevel gearbox with six axes, Gép, LXIII. évfolyam, 2012. 12. szám, p. 99-102. ISSN 0016-8572
[3] J. Dwight: Aluminum design and construction, E & FN Spon, 1999
[4] Horvát Á., Csík Z., Jacob S., Patric N., Andó M.: Developement of brake caliper for rally-car, Sustainable Construction and Design, vol. 3, issue 3, pp. 191, 2012

Institute for Mathematics and Informatics

Professor Dr. Sándor MOLNÁR
Director of the Institute

Dear Reader,

The Institute of Mathematics and Informatics consists of the following distinguished departments: the Department of Mathematics (head: Prof. Dr. Zoltán Sebestyén) and the Department of Informatics (head: Prof. Dr. Sándor Molnár). The External Department of Applied Informatics (head: Prof. Dr. Andras Edelmayer) is located at the Computer and Automation Research Institute of the Hungarian Academy of Sciences (MTA SZTAKI). Our research activities in 2014 were as follows.

Department of Mathematics
In the past year period a four-year research project on "Dynamic modelling of stage-structured multi-species population systems", funded by the Hungarian Scientific Research Fund (OTKA), have been successfully closed with 27 scientific articles mostly published in leading international journals, co-authored in international cooperation, with a cumulated impact factor over 30. The main results concern the methodological development of biological pest control.

Department of Informatics:
The Department has focused its research efforts primarily on linear systems theory. Energy and environment modeling remains a field of interest, sustainability in macroeconomic models is one of the new topics under investigation. Besides a PhD thesis being finalised on the application of artificial neural networks in geostatistical processes, the other relevant focus of activities is applied research in the fields of embedded measurement, control and communication systems, signal processing, detecting and control algorithms.

External Department of Applied Informatics
The Department focuses on system and control theory application, fault detection, distributed networking, advanced filtering methods, signals and systems theory. Another field of research is intelligent metering and transportation vehicle fleet guidance under traffic conditions. Some additional topics are the representations of signals and systems using orthogonal rational bases.

Dr. Sándor MOLNÁR
Director

Water chemistry analysis in the sediment of the Baradla cave using geomathematical methods, Aggtelek, NE Hungary

Edit BORBÁS[1], József KOVÁCS[2],
István Gábor HATVANI[2],
Anita Sleiszné CSÁBRÁGI[1],
Sándor MOLNÁR[1]
[1]Department of Informatics,
Institute of Mathematics and Informatics,
[2]Department of Physical and Applied Geology,
Eötvös Loránd University

Abstract

Water was observed in the sediment of the Baradla Cave, located in Northeast Hungary. In order to investigate its characteristics wells were drilled. Hydrochemical samples were taken directly from the wells and from the cave stream on several occasions between November 2009 and April 2010. In February 2010 there was a chance to observe how the chemical composition of the waters of the creeks and the sediments altered during the snow melt. Several chemical parameters of the samples were analyzed. Based on the results of the hydrochemical analyses cluster analysis was applied to define the relationship between the sampling points. A Discriminant analysis was conducted to verify the classification. As a result of the classification, the water of the observation wells in the sediment proved to be separated from the water of the cave's creek and the springs on the surface. Research shows that there is no permanent connection between the water in the cave sediment and the water of the cave creek in the cave water system.

Keywords

Baradla cave, water in the sediment, separated water system, cluster analysis

1. Introduction

The Baradla Cave is located in Northeast Hungary, in the Aggtelek National Park (Figure 1). The cave, Aggtelek and its surroundings were listed as a part of the World Cultural and Natural Heritage by UNESCO in 1995. The Baradla Cave has been protected by the Ramsar Convention since 2001.

The Baradla-Domica Cave System has a Hungarian (21 km) and a Slovakian part (6 km). The Hungarian part is the Baradla Cave itself and the Slovakian part

is the Domica Cave. There are natural entrances in Hungary, near the village of Aggtelek, while the Slovakian natural entrances are very close to the village of Domica village; this made it possible for prehistoric people to utilize the cave. Tourism started in the 1760s in the Aggtelek section. Research and excavations began in 1801. The most significant researcher was Imre Vass, who excavated the greater part of the main branch of the cave between 1821 and 1825. He documented the excavation, and his book (published in 1831) still forms the basis of research into the Baradla Cave [Vass, 1831]. The hydrological research of the cave system was begun by Hubert Kessler in the early 20th century. He recognized that there are deeper routes under the cave, which he named as the Lower Cave [Kessler, 1938]. László Jakucs started to study the cave in the 1950s [Jakucs, 1951]. In 1955 there was a turning point in the history of the recognition of the cave when, after a flood, the cave, which was supposed to consist of one cave, turned out to consist actually of two separated caves. In the same year scientists were able to pass through the spring mouth into the cave, which was almost completely filled with water. This cave is now known as the Short Lower Cave. In the early 1980s a 1 km long section was explored. At the end of the 20th century a 150m long section of Long Lower Cave was explored and studied. Numerous water tracing experiments completed in the 1970-1980's allowed the hydrological separation and length determination of these two lower caves.

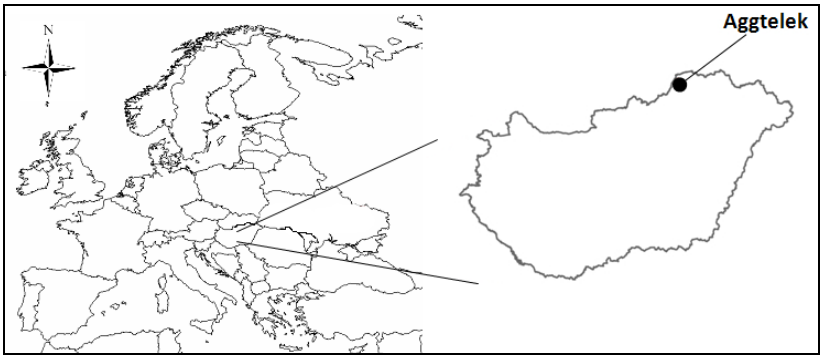

Figure 1. Location of the studied cave

In 2002 a research team studied the several meter thick cave sediment. During the sampling (carried out by manual drilling) in the cave-sediment, water was observed. With casing and filtering, the drills were able to monitor water level. As a result, the water in the cave-sediment was also observable and able to be compared over a long time scale. In 2006, water level recording begun in the observation well (Olympos well) (Figure 2). Due to the spring snow melt the water level rose 2 meters in 4 days, indicating a connection between the water in the cave sediment and the weather processes above ground **[**Berényi et al., 2006].

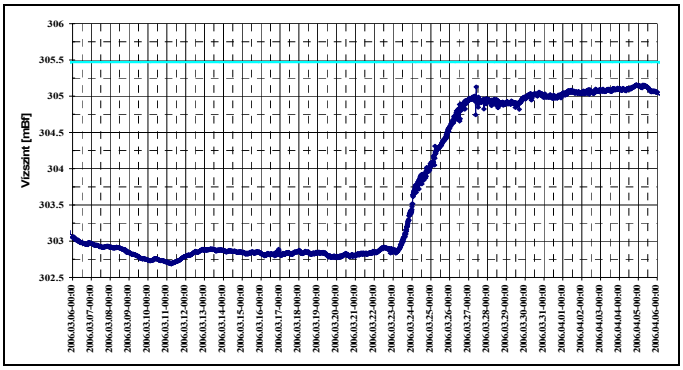

Figure 2. The effect of spring snow break on the water level of the Olympos well in 2006 (Berényi et al. 2006) (the straight line shows the level of the terrain, mBf=meters above Baltic Sea level)

The chemical parameters of the water in the cave-sediment, creek and springs were studied spatially and temporally using multi variant statistical methods. These methods were cluster analysis and multidimensional scaling.

2. Geological and Hydrological description of the cave

The Baradla Cave is located in the South part of the Gömör-Torna Karst. The main body of the mountain consists of marine sedimentary limestone from the Triassic Period. The mountain consists of karst partly overlaid by Pannonian sediment and partly uncovered karst. The mountain was tectonically active for a long time; therefore, the bedrock is intensely crumbly, which played a major role in the formation of the cave [Gyuricza et al., 2003].

The evolution of the cave started in the mindel-riss interglacial stage [Gyuricza-Sásdi, 2009]. Based on the examination of the stalactites in the cave, the main branch is at least 150 000 years old. Its size had not changed since the last interglacial stage [Zámbó et al., 2002]. Several periods can be identified in the evolution (Figure 3). First, water in the tectonic fissures expanded the cavern by mixture corrosion. The cave was filled to the roof with sediment brought here by the water. These sediments were carried by water from the surface, and contain mostly sand, gravel and silt. Later, the runoff from the creeks increased and started to erode vertically and load the sediment off from the passages. This filling-erosion cycle might have repeated several times. Nowadays, sediment deposition can be observed [Berényi et al., 2006].

The area of the cave system's watershed exceeds 34 km^2. Beside the infiltration, rainwater reaches the cave through surface sink-holes located in the covered karst. These sink-holes are associated with the cave's side branches. Thanks to the sink-holes and the infiltration from the surface, water recharge into the cave is almost constant. However, flowing water cannot be observed usually in the cave because of the cave sink-holes in the main branch, which lead

to the Lower Cave. The water of the cave system reaches the surface through the Jósva spring, which is, with its two spring mouths, the largest karst spring in the area. One of the spring mouths is the Táró spring, which brings the Short Lower Cave's water to the surface, and the other is the Medence spring, which brings the Long Lower cave's water to the surface. The average discharge of the Jósva spring is over 14,000 m^3 a day.

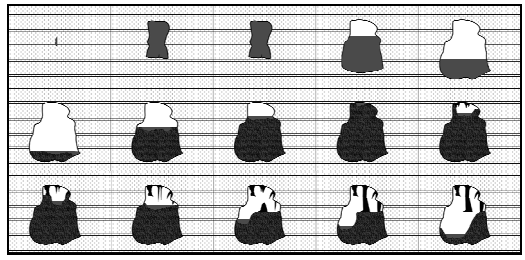

Figure 3. The evolution of the cave (Berényi et al. 2006) showing how it was filled up with sediment and how the sediment was transported from the cave by the floods of the creeks

3. Composition of the sediment

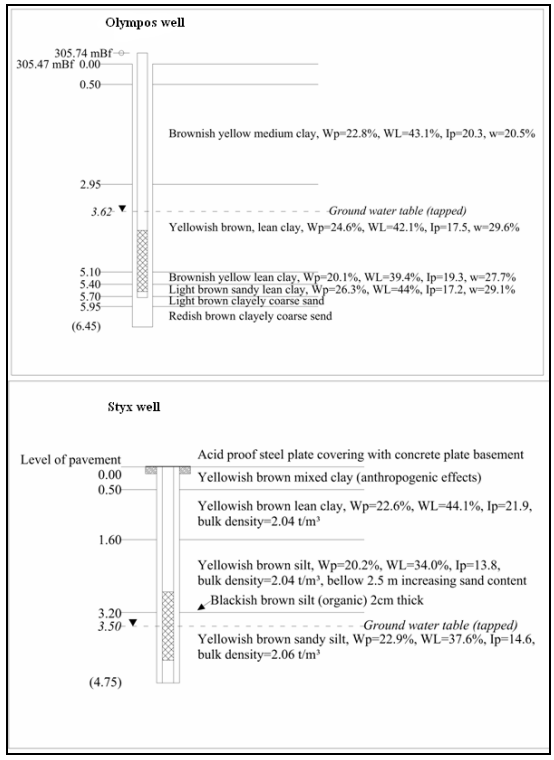

Figure 4. Sediment characteristics of the Olympos well and the Styx well (Berényi et al. 2008) (mBf=meters above Baltic Sea level)

Samples from the observation wells (Olympos well, Styx well) – sunk into the cave-sediment – were processed using particle size distribution and X-ray diffraction. In the Olympos observation well, based on pumping test results, the permeability coefficient was estimated at 10^{-6} m/s. According to Freeze and Cherry [1979], this aquifer value indicates silty sand. Based on the granulometric composition measurements the main mineral component of the sediment in the Baradla Cave is quartz, with only minor quantities of other minerals present. The character of the sediment indicates a not too distant metamorphic denudation area [Berényi et al., 2006]. Figure 4 shows the sediment characteristics of the observation wells.

4. Measurement methods

4.1. Sampling locations

Between November 2009 and April 2010 water samples were taken ten times from six areas.

From the surface we took samples from the Jósva spring, which brings the cave system's water to the surface (the Táró and Medence springs). And we had four other sampling locations inside the cave (Figure 5).

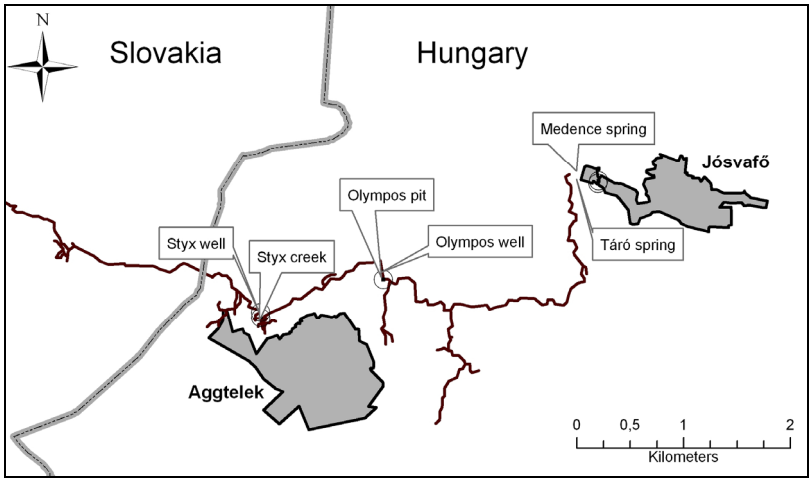

Figure 5. Location of the sampling points in the cave

The samples in the cave were taken from the creek and also from the drilled wells from the following locations:

– The Styx well (Figure 6): a constructed observation well in a side branch leading to the Styx creek. This area is in a section of the cave near the village of Aggtelek. The depth of the well is 4.75 m (Figure 4). Water is not continuously present; it periodically dries up.

Figure 6. Styx well closed and open

- The Styx creek: this is the main watercourse of Baradla Cave and arrives from Slovakia. An active watercourse can be observed in this section of the cave most of the year. The distance between the Styx creek and the Styx well is 30 m. Despite the short distance, the creek's effect on the water level in the well could not be proven. The reason for this is the low permeability coefficient.
- The Olympos well: this is 2.2 km from the Aggtelek entrance; its depth is 6.45m (Figure 4).
- The Olympos pit: this is 2 m from the observation well. It was dug in the second half of the 1980s for geological sampling purposes. Water appeared in the pit a few years after it was dug; this water is presumably the leaking water accumulated on the sediment surface. In order to observe the change of water level, a gauge was deployed during the drilling. During the sampling, the water level was constantly monitored.

4.2. Hydrochemical analyses

Laboratory examinations of the water samples were conducted according to the Hungarian standards for the following parameters: water temperature (^{0}C), electrical conductivity (mS cm^{-1}), Ca^{2+}, Mg^{2+}, Na^+, K^+, HCO_3^-, SO_4^{2-}, NO_3^-, Total Dissolved Solids-TDS (mg L^{-1}), pH. The Ca^{2+}, Mg^{2+} and HCO_3^- content was determined according to the Titrimetric Method; the SO_4^{2-} and NO_3^- content was determined with the Spectrometric Method; and the Na^+ and K^+ content was determined using the Flame Photometric Method.

5. Results and discussion

Having analyzed the 56 samples, the descriptive statistics of the measured parameters were counted for all the sampling points, the median can be seen in Table 1.

Table 1. Median values of the chemical parameters.

Sample name	Temperature (^{0}C)	Conductivity (mS cm^{-1})	Ca^{2+} (mg L^{-1})	Mg^{2+} (mg L^{-1})	Na^{+} (mg L^{-1})	K^{+} (mg L^{-1})	HCO_3^- (mg L^{-1})	SO_4^{2-} (mg L^{-1})	NO_3^- (mg L^{-1})	pH
Medence spring	12.0	630	116.2	12.2	1.2	0.9	376.4	35.7	4.1	7.2
Olympos pit	9.0	524	106.2	5.5	0.9	0.3	324.5	24.9	1.3	8.1
Olympos well	9.5	425	80.2	16.3	0.9	0.5	236.9	29.2	4.6	7.9
Styx creek	9.0	665	125.7	9.5	1.3	0.6	389.4	48.4	3.8	7.8
Styx well	10.0	474	86.4	7.3	0.7	1.1	240.1	54.7	3.2	7.8
Táró spring	9.8	609	118.2	7.3	1.2	0.5	363.4	34.4	3.8	7.8

The conductivity values in the observation wells sunk in the cave-sediment are significantly lower than the ones at the other measurement locations due to the lower Ca^{2+} and HCO_3^- content. Regarding the other parameters, significant differences cannot be observed between the leaking water in the sediment, the cave creek, and the springs.

Previous studies had already evinced that the main components of the water of the Baradla cave are calcium, bicarbonate and magnesium [Izápy-Maucha 2002]. As expected, based on the average values of the hydrochemical parameters, the water of the cave is considered to be in the calcium-magnesium-bicarbonate hydrochemical facies [Back, 1966] (Table 1, Figure 7). Differences cannot be observed between the sampling locations, considering the joint effect of the parameters in the Piper diagram (Figure 7).

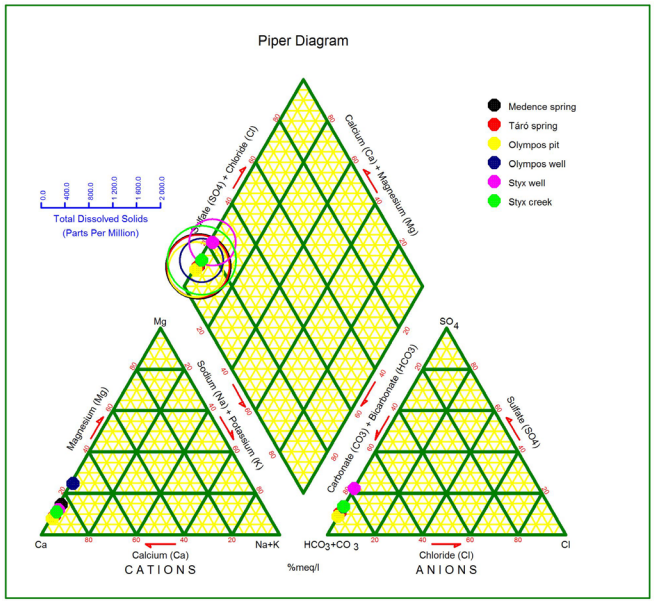

Figure 7. Piper diagram of the sampling locations

Considering the temporal variability of the parameters measured at the sampling locations, significant changes were noticed in the chemical characteristics of the water samples in February 2010, when there was a remarkable snow melt in the cave's watershed area. Previously similar changes were noticed in the water of Béke cave near to Baradla cave when a flood occurred in the area [Telbisz et al., 1999].

Due to the melt water, the TDS value decreased primarily in the cave creek and the springs (Figure 8), and after the effect of melt waters had passed the TDS values rose to the level at which they were before the flood. In the case of the cave-sediment sampling locations the TDS values did not change or the changes were not considerable.

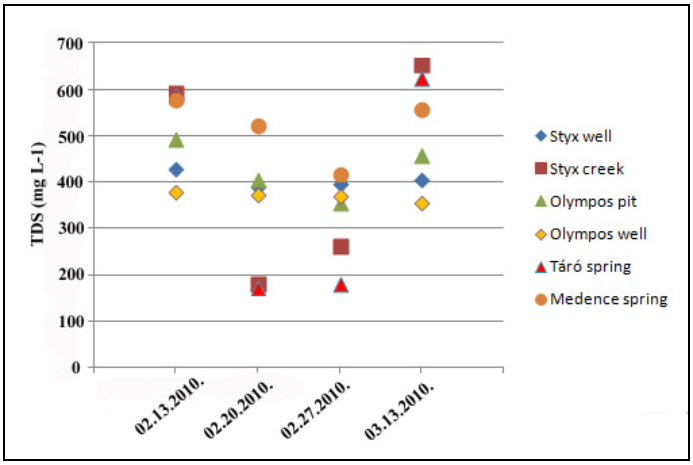

Figure 8. Total Dissolved Solids' values of the samples after snow melt in February 2010

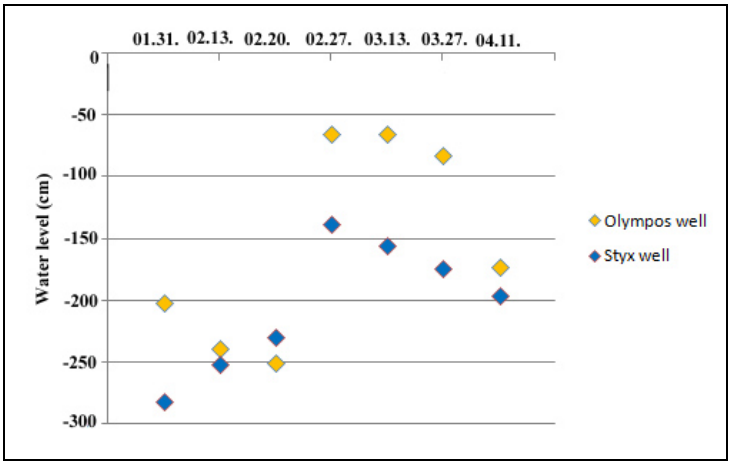

Figure 9. Groundwater levels in the observation wells between January 31, 2010 and April 11, 2010

The biggest difference (close to 70%) was observed in the data set of the Styx creek and Táró spring. In the Styx creek the TDS was 595 mg L^{-1} before the flood (February 13, 2010), and one week later (February 20, 2010) this value had decreased to 182 mg L^{-1}. In the case of the Táró spring, the values were the following: 587 mg L^{-1} (before the flood), and 174 mg L^{-1} (after the flood).

The snow melt had a significant effect on the water level of the observation wells in the cave (Figure 9). The water level rose by 1-1.5 m and decreased more slowly in comparison (over a couple weeks) to the normal level.

The analysis of the TDS from all sampling locations for the total measured period clearly shows that the TDS in the observation wells is originally lower than in the cave's other observed locations (the Táró and Medence springs, the Styx creek) (Table 1). Comparing the data (Table 1, Figures 8 and 9) we drew the conclusion that the melt water had the greatest effect on the configuration of the water's chemical characteristics in the observation wells.

6. Statistical methods

The results of the hydrochemical analyses allowed us to compare the sampling locations over all measured parameters. We used hierarchical cluster analysis. Its result is a dendrogram where the analyzed objects are on the horizontal axis, and the linkage distance is on the vertical axis. The result needs to be checked by hypothesis testing, for this Discriminant analysis was used.

Cluster analysis was applied to the characteristic parameters of the 6 sampling locations for every sampling point in time. In both cases, Discriminant analysis was used to check the classification. The results of these two applications were 100% and 95%.

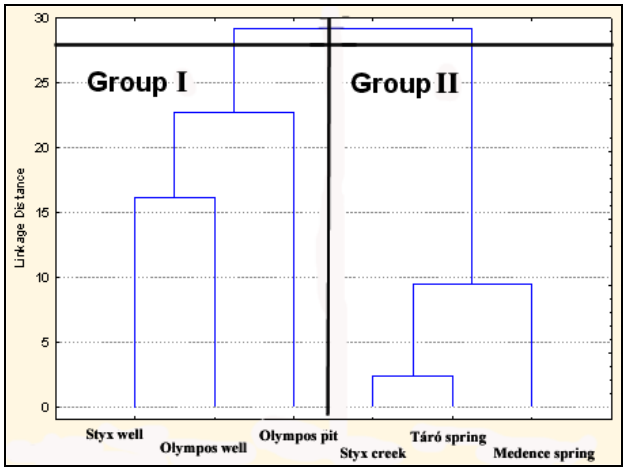

Figure 10. Dendrogram of the characteristic parameters of the sampling locations

In the first case, two clusters were noticed at a Linkage Distance of 28 (Figure 10). Group I contains three sampling points, the two observation wells (the Styx and Olympos wells) and the Olympos pit. Group II contains the Styx creek, and the Táró and Medence springs. This result means that the chemical characteristics of water in the sediment are different from those of the cave creek).

In the second case, two groups were identified at a Linkage Distance of 150 (Figure 11). Group 1 contains the samples taken from the three sampling locations settled in the sediment (as in Figure 10) and the samples taken from the springs and creek when their waters had been diluted by floods, while Group 2 contains the samples from the springs and creek, just as in Figure 8.

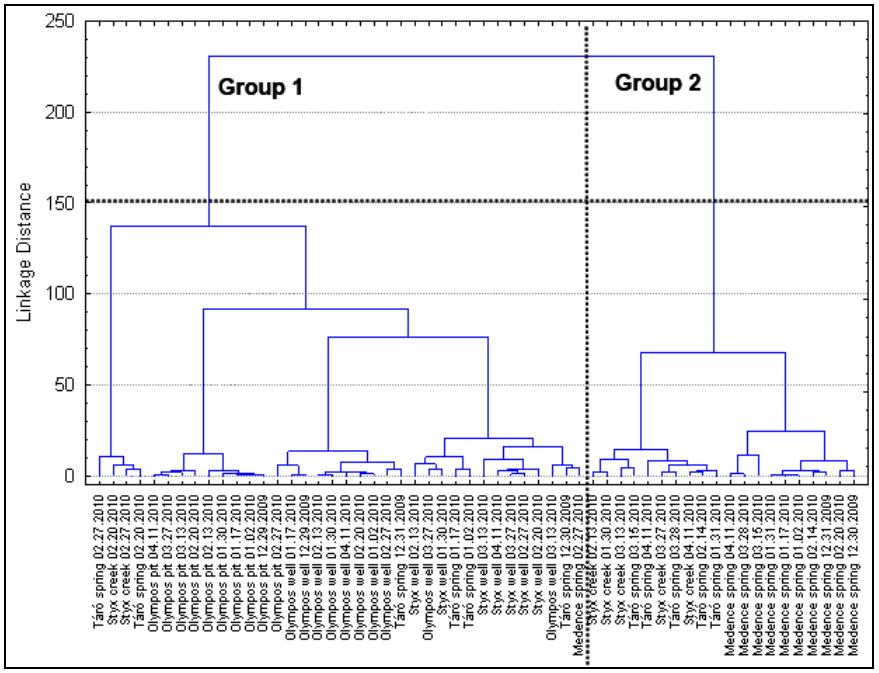

Figure 11. Dendrogram of each sampling in time

The descriptive statistics of these two groups were plotted on box-and-whisker diagrams. The bottom of the box represents the lower quartiles (the 25th percentile) and the top the upper quartiles (the 75th percentile). Half of the data is located in the box. The band in the box represents the median (the 50th percentile). Any data not included between the whiskers is plotted as an outlier with small circle or star [Norusis, 1993].

Group 1 indicates a lower concentration for all parameters except pH. Chemical characteristics of the water in the cave-sediment indicate lower concentration and permanency (Figure 12). This water leaks into the sediment during melting, and retains its characteristics during the stay.

Conclusion

Water was observed in the sediment of Baradla Cave located in Northeast Hungary. In order to observe its characteristics wells were sunk into the sediment. Hydrochemical analyses were conducted on samples taken directly from the wells and from cave creek and springs on several occasions.

Water samples could be classified into calcium-magnesium-bicarbonate hydrochemical facies, as had been expected. The hydrochemical analyses were begun in November 2009 and finished in April 2010. As a result, there was an opportunity to observe if and how the chemical contents of the creek and sediment water changed during the snowmelt. The water level values in the wells increased after one week, while the TDS of the ground springs and cave creek decreased. In the samples obtained from the observation wells, this change was not noticeable. The observation wells in the cave-sediment are filled with water whenever a flood occurs and their chemical characteristics do not change even after the flood. Comparing the observation wells to other cave observation locations it is observed that the TDS values are originally low due to dilute melt water, and the fact that the main ingredient of the cave sediment is quartz. Therefore dissolution is minimal in the stone-water interaction.

Karst dissolution is the main process that determines the chemical characteristics of cave creek and springs. During floods it can change significantly (the floodwater dilutes it to a high degree). And after the flood has receded the chemical content settles back to its previous state.

Research shows that there is no permanent connection between the water in the cave sediment and the water of the cave creek in the cave water system.

References

[1] Back, W. (1966): Hydrochemical facies and ground-water flow patterns in northern part of Atlantic Coastal Plain, U.S. Geol. Surv. Prof. Paper 498-A., 42 p.

[2] Berényi Üveges, I., Berényi Üveges, J. and Vid, G. (2006): Adalékok a Baradla-barlang fejlődésének elméletéhez üledék vizsgálatok alapján: Karszt és Barlang, p. 33-40.

[3] Berényi Üveges, J., Vid, G., and Berényi Üveges I. (2008): Sediments and groundwater in the Baradla and Béke caves, Hungary: 4th European Speleological Congress, Vercors, France.

[4] Freeze, R.A., and Cherry, J.A. (1979): Groundwater: Prentice Hall. Engwood Cliffs. New Jersey, 29 p.

[5] Gyuricza, Gy., Piros, O., Szilágyi, F., and Salamon, G. (2003): Baradla-barlangrendszer, *in* Székely, K., Magyarország fokozottan védett barlangjai, Budapest, p. 26-36.

[6] Gyuricza Gy., Sásdi L. (2009): A Baradla-barlangrendszer kialakulásának kérdései a tágabb környezet földtani fejlődésének tükrében: Földtani Közlöny 139/1, p. 83-92.

[7] Izápy, G., and Maucha, L. (2002): Az Aggteleki-hegység karszthidrológiai vizsgálata a jósvafői Kutatóállomáson. – A karsztvízkutatás Magyarországon – bükki karsztvízkutatás legújabb eredményei c. konferencia kiadványa. Felszín alatti Vizekért Alapítvány – VITUKI. Budapest.

[8] Jakucs, L. (1951): Vízföldtani vizsgálatok a Gömöri-karszton: Földtani Közlöny, v. 81, p. 442-445.

[9] Kessler, H. (1938): Az Aggteleki-barlangrendszer hidrográfiája: Földrajzi Közlöny, v. 66, p. 1-30.

[10] Norusis, M.J. (1993): SPSS for WindowsTM: Professional StatisticsTM. Release 6.0, SPSS Inc. USA, 385 p.

[11] Telbisz, T., Vigassy, T., and Zámbó, L. (1999): Variances of karst corrosion on the basis of differences in the solution of Ca- and Mg-carbonates - in: Bárány-Kevei, I. - Gunn, J. (edt): Essays in the Ecology and Conservation of Karst. - Acta Geographica 36 (Spec. Issue), Szeged, pp.193-200.

[12] Vass, I. (1831): Az Agteleki barlang leírása fekte területével. talprajzolatával és hosszába való átvágásával. két táblán, Pesten nyomtatta Landerer.

[13] Zámbó L., Ford, D., and Telbisz T. (2002): Baradla-barlangi cseppkő kor-adatok a késő-negyedidőszaki klímaingadozások tükrében, Földtani Közlöny, 132 / Különszám, pp. 231-238.

Extended oligopoly models and their asymptotical behavior

Ferenc SZIDAROVSZKY[1], Sándor MOLNÁR[2], Márk MOLNÁR[3]
[1]Systems and Industrial Engineering Department, The University of Arizona,
[2]Sándor Molnár, Department of Informatics, Institute of Mathematics and Informatics,
[3]Márk Molnár, Institute of Economics, Szent István University,

Abstract

We will investigate the different extensions of the Cournot oligopoly model including models with intertemporal demand interaction, including production adjustment cost, pollution treatment cost sharing, and cost interaction. The local asymptotic stability of the steady state is examined in all cases and the stability conditions are compared to the classical Cournot model.

Keywords

Cournot oligopoly model, production cost, pollution treatment cost, cost interaction

1. Introduction

Cournot oligopolies, their different variants, extensions and generalizations play an important role in the literature of mathematical economics. The early results up to the mid 70s are summarized in Okuguchi (1976), and their multi-product extensions with application studies are discussed in Okuguchi and Szidarovszky (1999). In the earliest studies the existence and uniqueness of the Nash-equilibrium of static oligopolies was the central issue, and later the attention has been turned to the asymptotical properties of the dynamic extensions. Puu and Sushko (2002) give a comprehensive summary of the most important more recent findings. All models discussed in the literature so far, are based on certain simplifying assumptions, which made the simple, analytic examination possible.

In this paper we will drop some of the simplifying assumptions of earlier models and will focus on more sophisticated models. In particular, we will consider models with intertemporal demand interaction, production adjustment costs, pollution treatment cost sharing and also with cost interaction. The simplified versions of some of the models to be discussed in this paper have been introduced earlier in Okuguchi and Szidarovszky (1999) as well as in the forthcoming book of Bischi et al. (2006). This paper develops as follows. Oligopolies with intertemperal demand interaction will be discussed in Section 2 followed by models with production adjustment costs. Section 4 will focus on oligopolies with pollution treatment cost sharing, and Section 5 will discuss the

case of cost interaction among the firms. Conclusions will be drawn in the last section of the paper.

2. Oligopolies with Intertemporal Demand

In this section we will examine the effect of intertemporal demand interaction. In the case of durable goods the demand at any time period depends on the price and the demands of earlier periods. Even in the case of nondurable goods taste or habit formation has effect on future demands.

Let N be the number of firms producing a single item. Let x_k be the output of firm k and $C_k(x_k)$ its cost. Market saturation, habit formation, etc. of earlier time periods are condensed into a variable Q which is assumed to follow the dynamic rule

$$Q(t+1) = H\left(\sum_{k=1}^{N} x_k(t), Q(t)\right), \tag{2.1}$$

where H is a real valued function on $\left[0, \sum_{k=1}^{N} L_k\right] \times R$ with L_k being the capacity limit of firm k.

The price function f is assumed to depend on both the total output of the industry and the current value of parameter Q. So the profit of firm k can be given as

$$\prod_k = x_k f(x_k + S_k, Q) - C_k(x_k), \tag{2.2}$$

where $S_k = \sum_{l \neq k} x_l$ is the output of the rest of the industry.

In this section we assume that functions f and $C_k (1 \leq k \leq N)$ are twice continuously differentiable, and

$$f'_x < 0;$$
$$f'_x + x_k f''_{xx} < 0;$$
$$f'_x - C''_k < 0$$

for all k and feasible values of x_k, S_k and Q.

Under these conditions Π_k is strictly concave in x_k, so with fixed values of S_k and Q there is a unique best response of firm k, since the feasible set for x_k is the compact set $[0, L_k]$. It can be given as follows:

$$R_k(S_k,Q)=\begin{cases}0 & \text{if} \quad f(S_k,Q)-C_k'(0)\le 0\\ L_k & \text{if} \quad L_k f'(L_k+S_k,Q)+f(L_k+S_k,Q)-C_k'(L_k)\ge 0\\ x_k^* & \text{otherwise,}\end{cases} \tag{2.3}$$

where x_k^* is the unique solution of equation

$$f(x_k+S_k,Q)+x_k f_x'(x_k+S_k,Q)-C_k'(x_k)=0 \tag{2.4}$$

in interval $(0, L_k)$. In the first two cases of (2) the partial derivatives of R_k are zeros, except the boundary points. Implicit differentiation shows that in the third case

$$r_k=\frac{\partial R_k}{\partial S_k}=-\frac{f_x'+x_k+f_{xx}''}{2f_x'+x_k f_{xx}''-C_k''} \quad \text{and} \quad \bar{r}_k=\frac{\partial R_k}{\partial Q}=-\frac{f_Q'+x_k f_{xQ}''}{2f_x'+x_k f_{xx}''-C_k''}. \tag{2.5}$$

Assumptions (B) and (C) imply that

$$-1<r_k<0 \tag{2.6}$$

as it is usual in the theory of discrete concave oligopolies. In addition, assume that

$$f_Q'+x_k f_{xQ}''\le 0$$

for all feasible values of x_k, S_k and Q. Then

$$\bar{r}_k\le 0. \tag{2.7}$$

Let $a_k>0$ denote the speed of adjustment of firm k and assume that the firms change their outputs in the direction towards their best responses. This dynamism can be mathematically described by the discrete system

$$x_k(t+1) = x_k(t+a_k)\left(R_k\left(\sum_{l \neq k} x_l(t), Q(t) \right) - x_k(t) \right) \quad (1 \leq k \leq N) \tag{2.8}$$

$$Q(t+1) = H\left(\sum_{k=1}^{N} x_k(t), Q(t) \right). \tag{2.9}$$

A vector $(\bar{x}, \ldots, \bar{x}_N, \overline{Q})$ is a steady state of this system if and only if for all k,

$$\bar{x}_k = R_k\left(\sum_{l \neq k} \bar{x}_l, \overline{Q} \right)$$

and

$$\overline{Q} = H\left(\sum_{k=1}^{N} \bar{x}_k, \overline{Q} \right).$$

The local asymptotical stability of this system can be examined by linearization. The Jacobian of the system at the steady state can be written as follows:

$$\mathbf{J} = \begin{pmatrix} 1-a_1 & a_1 r_1 & \ldots & a_1 r_1 & a_1 \bar{r}_1 \\ a_2 r_2 & 1-a_2 & \ldots & a_2 r_2 & a_2 \bar{r}_2 \\ \vdots & \vdots & & \vdots & \vdots \\ a_N r_N & a_N r_N & \ldots & 1-a_N & a_N \bar{r}_N \\ h & h & \ldots & h & \bar{h} \end{pmatrix},$$

where h and $\bar{h}$ denote the partial derivatives of H at the steady state. The steady state is locally asymptotically stable if all eigenvalues of $\mathbf{J}$ are inside the unit circle. For the sake of simplicity assume symmetric firms, then $a_1 = \ldots = a_N = a$, $r_1 = \ldots = r_N = r$, and $\bar{r}_1 = \ldots = \bar{r}_N, = \bar{r}$. Then the eigenvector equation of $\mathbf{J}$ has the special form

$$(1-a)u_k + ar \sum_{l \neq k} u_l + a\bar{r}v = \lambda u_k \quad (1 \leq k \leq N) \tag{2.10}$$

$$h \sum_{k=1}^{N} u_k + \bar{h} v = \lambda v. \tag{2.11}$$

Let $U = \sum_{k=1}^{N} u_k$, then equation (2.10) can be rewritten as

$$arU + a\bar{r}v + (1 - a - ar - \lambda)u_k = 0. \tag{2.12}$$

Assume first that $\lambda = 1 - a - ar$, then this eigenvalue is inside the unit circle if

$$a < \frac{2}{1+r}. \tag{2.13}$$

Otherwise $u_1 \ldots = u_N = u$, and simplifies as

$$\begin{aligned} &(1 - a(N-1)ar - \lambda)u + a\bar{r}v = 0 \\ &hNu + (\bar{h} - \lambda)v = 0. \end{aligned} \tag{2.14}$$

Nontrivial solution exists if and only if

$$\mathrm{Det}\begin{pmatrix} 1 - a(1 + (1-N)r) - \lambda & a\bar{r} \\ hN & \bar{h} - \lambda \end{pmatrix} = 0.$$

This is a quadratic equation:

$$\lambda^2 + \lambda(-1 - \bar{h} + az) + (h - \bar{h}Na\bar{r} - a\bar{h}z) = 0, \tag{2.15}$$

where we use the simplifying notation $z = 1 + (1-N)r$. Notice that (2.6) implies that $l < z < N$. The roots of the quadratic equation are inside the unit circle if and only if

$$\bar{h}(1 - az) - hNa\bar{r} < 1 \tag{2.16}$$

$$-1 - \bar{h} + az + \bar{h}(1 - az) - hNa\bar{r} + 1 > 0 \tag{2.17}$$

$$1 + \bar{h} - az + \bar{h}(1 - az) - hNa\bar{r} + 1 > 0. \tag{2.18}$$

These relations can be rewritten as

$$a[\bar{h}z + hN\bar{r}] > \bar{h} - 1 \tag{2.19}$$

$$a[z(1-\bar{h})-hN\bar{r}]>0 \tag{2.20}$$

and

$$a[z(1+\bar{h})+hN\bar{r}]<2(1+h). \tag{2.21}$$

It is reasonable to assume that $-1<\bar{h}<1$ and $h>0$. Then we have the following cases

(i) If $\bar{h}z+hN\bar{r}<0$, then (2.19) holds, if

$$a<\frac{\bar{h}-1}{\bar{h}z+hN\bar{r}}. \tag{2.22}$$

Notice that relation (2.20) always holds, since the multiplier of a in the left hand side is positive. If $z(1+\bar{h})+hN\bar{r}\le 0$, then (2.21) also holds for all $a>0$, otherwise it holds if

$$a<\frac{2(1+h)}{z(1+\bar{h})+hN\bar{r}}. \tag{2.23}$$

So in this case the steady state is locally asymptotically stable if a is sufficiently small.

(ii) If $\bar{h}z+hN\bar{r}>0$, then (2.19) is always valid. Since $z(1-\bar{h})-hN\bar{r}>0$, inequality (2.20) is also true for all $a>0$. If $z(1+\bar{h})+hN\bar{r}\le 0$, then (2.21) is also satisfied, otherwise it holds if (2.23) holds.

So in this case the steady state is either always locally asymptotically stable, or it is when the value if a is sufficiently small.

In comparison to the classical case without intertemporal demand interaction notice that in that case

$$f'_Q=f''_{xQ}=h=\bar{h}=\bar{r}=0,$$

so from (2.15) the eigenvalues are $\lambda_1=0$ and $\lambda_2=1+\bar{h}-az=$ $=1-a(1+(1-N)r)$. The first eigenvalue is always inside the unit circle, and the second is there if and only if

$$1<\frac{2}{1+(1-N)r}=\frac{2}{z}. \tag{2.24}$$

Since this inequality is stronger than (2.13), this is the stability condition for the classical case. Simple algebra shows that

$$\frac{2}{z} \leq \frac{2(1+\bar{h})}{z(1+\bar{h})+hN\bar{r}}$$

and equality occurs if and only if $\bar{r}=0$. Therefore in this sense, intertemporal demand interaction makes the system more stable, since the stability region for a becomes larger.

3. Oligopolies with Production Adjustment Cost

In this section we consider again an N-firm single-product oligopoly, when the price depends on only the total production of the industry. However, the firms face additional cost if they increase their production levels compared to their outputs in the previous time period. Let $t+1 \geq 1$ be a time period, then the profit of firm k can be written as

$$\prod_k = x_k f(x_k + S_k) - C_k(x_k) - A_k(x_k - x_k(t)), \tag{3.1}$$

where $S_k = \sum_{l \neq k} x_l$ is the output of the rest of the industry as before and we assume that the output trajectories are nondecreasing. Assume that functions f, C_k and A_k are twice continuously differentiable, furthermore,

$$\begin{array}{ll} \text{(E)} & f' < 0, C_k' \geq 0,\ A_k' \geq 0 \\ \text{(F)} & f' + x_k f'' < 0 \\ \text{(G)} & f' - C_k'' < 0,\ A_k > 0 \end{array};$$

for all k and feasible values of x_k, $x_k(t)$ and S_k.

Under these conditions Π_k is strictly concave in x_k, and in the case of finite capacity limits of all firms, there is a unique best response of firm k, which will be now denoted by $R_k(S_k, x_k(t))$. It can be defined similarly to (2.3), and by implicit differentiation it is easy to see that

$$r_k = \frac{\partial R_k}{\partial S_k} = -\frac{f' + x_k f''}{2f' + x_k f'' - C_k'' - A_k''} \tag{3.2}$$

and

$$\bar{r}_k = \frac{\partial R_k}{\partial x_k(t)} = -\frac{A_k''}{2f' + x_k f'' - C_k'' - A_k''}. \tag{3.3}$$

Assumptions (E)-(G) imply that

$$1 < r_k < 0 \le \bar{r}_k < 1 \tag{3.4}$$

and

$$-1 < r_k - \bar{r}_k \tag{3.5}$$

for all k. In this case the dynamic system (2.8)-(2.9) is modified as follows:

$$x_k(t+1) = x_k(t) + a_k\left(R_k\left(\sum_{l \neq k} x_l(t), x_k(t) \right) - x_k(t) \right) \tag{3.6}$$

for $k = 1, 2, \ldots, N$. A vector $(\bar{x}_1, \ldots, \bar{x}_N)$ is a steady state of this system if and only if for all k,

$$\bar{x}_k = R_k\left(\sum_{l \neq k} x_l, x_k \right).$$

The Jacobian of system ( ) now has the special structure

$$\mathbf{J} = \begin{pmatrix} 1 - a_1(1 - \bar{r}_1) & a_1 r_1 & \cdots & a_1 r_1 \\ a_2 r_2 & 1 - a_2(1 - \bar{r}_2) & \cdots & a_2 r_2 \\ \vdots & \vdots & & \vdots \\ a_N r_N & a_N r_N & \cdots & 1 - a_N(1 - \bar{r}_N) \end{pmatrix}.$$

For the sake of simplicity we consider only symmetric firms, when $a_1 = \ldots = a_N = a$, $r_1 = \ldots = r_N = r$ and $\bar{r}_1 = \ldots = \bar{r}_N = \bar{r}$. Then the eigenvector equation has the special form

$$(1 - a(1 - \bar{r}))u_k + ar \sum_{l \neq k} u_l = \lambda u_k. \tag{3.7}$$

Let $U = \sum_{k=1}^{N} u_k$ as before, then

$$arU + (1 - a(1 - \bar{r}) - ar - \lambda)u_k = 0. \tag{3.8}$$

Assume first that $\lambda = 1 - a(1 - \bar{r}) - ar$, then this eigenvalue is inside the unit circle if

$$a(r - \bar{r} + 1) < 2,$$

and since the multiplier of a is positive (by relation (3.5)), it holds if a is sufficiently small:

$$a < \frac{2}{r - \bar{r} + 1}. \tag{3.9}$$

Otherwise $u_1 = \ldots = u_N = u$, and (3.8) has the special form:

$$(1 - a(1 - \bar{r}) + (N - 1)ar - \lambda)u = 0,$$

and nontrivial solution exits if and only if

$$\lambda = 1 - a(1 - \bar{r} - (N - 1)r).$$

Notice that the multiplier of a is always positive, since $1 - \bar{r} - (N - 1)r = (1 + r - \bar{r}) - Nr$ with both terms being positive. So λ is inside the unit circle if

$$a < \frac{2}{1 + r - \bar{r} - Nr}, \tag{3.10}$$

so if the value of a is sufficiently small. Notice that since $r < 0$, (3.10) is more restrictive than (3.9), so inequality (3.10) is the stability condition. Notice also that in the absence of production adjustment cost $\bar{r} = 0$, in that case the stability condition is relation (2.24), and since $\bar{r} \geq 0$, (3.10) is less restrictive than (2.24) unless $\bar{r} = 0$. That is, production adjustment costs usually make the system more stable.

4. Oligopolies with Pollution Treatment Cost Sharing

Pollution emerges in many industries as the result of the manufacturing process. In this section we will examine N-firm single-product oligopolies with the

additional assumption that the firms treat jointly the pollution and share the treatment cost in proportion to their share in the total output. Therefore the profit of firm k is

$$\prod_k = x_k f(x_k + S_k) - C_k(x_k) - x_k \frac{T(x_k + S_k)}{x_k + S_k} \tag{4.1}$$

where f is the price function, C_k is the cost function of firm k as before, and T is the total pollution treatment cost function. By introducing the notation

$$G(x_k + S_k) = \frac{T(x_k + S_k)}{x_k + S_k} \text{ and } F(x_k + S_k) = f(x_k + S_k) + G(x_k + S_k) \tag{4.2}$$

we have

$$\prod_k = x_k F(x_k + S_k) - C_k(x_k), \tag{4.3}$$

where Π_k has the form of the payoff functions of classical oligopolies in which f is replaced by F.

By assuming that functions $f, G, C_k (1 \le k \le N)$ are twice continuously differentiable ($G(0)$ is taken as the finite limit of this function at zero), from we see that

$$r_k = \frac{\partial R_k}{\partial S_k} = -\frac{F'_x + x_k F''_{xx}}{2F'_x + x_k F''_{xx} - C''_k}, \tag{4.4}$$

where R_k (S_k) is the best response of firm k. The corresponding dynamic system and its steady state can be presented similarly to the previously discussed cases. Assume that

$$\begin{array}{ll} \text{(H)} & F'_x < 0 \\ \text{(I)} & F' + x_k F''_{xx} < 0 \\ \text{(J)} & F'_x - C''_k < 0 \end{array};$$

for all k and feasible values of x_k and S_k, then clearly

$$-1 < r_k < 0, \tag{4.5}$$

and the stability condition is inequality (2.24). Notice that the stability region for a becomes larger when *r* increases. Therefore pollution treatment cost sharing makes the system more stable if

$$-\frac{f'_x + x_k f''_{xx}}{2f'_x + x_k f''_{xx} - C''_k} < \frac{f'_x + G'_k + x_k f''_{xx} + x_k G''_{kk}}{2f'_x + 2G'_k + x_k f''_{xx} + x_k G''_{kk} - C''_k}$$

which is the case, when

$$x(G'f'' - f'G'') + C''(G' + xG'') > 0, \tag{4.6}$$

where we assume symmetric firms again. The conditions given earlier do not imply this relation, so it depends on the particular choice of the functions involved in this model.

5. Oligopolies with Cost Interaction

Here we assume that the firms hire manpower, purchase supplies and materials from the same market, so the cost of each firm depends on its own production level as well as on the total production of the rest of the industry. This cost interaction has not been considered in earlier models. So the profit of firm k is as follows:

$$\prod_k = x_k f(x_k + S_k) - C_k(x_k, S_k), \tag{5.1}$$

where f, S_k are as before, and C_k is the modified cost function of firm k.

The corresponding dynamic system and its steady state can be presented similarly to the previously discussed cases.
With fixed value of $S_{k,}$ we have

$$\frac{\partial \prod_k}{\partial x_k} = -f(x_k + S_k) + x_k f'(x_k + S_k) - C'_{kx}(x_k, S_k) \tag{5.2}$$

and

$$\frac{\partial^2 \prod_k}{\partial x_k^2} = 2f'(x_k + S_k) + x_k f''(x_k + S_k) - C''_{kxx}(x_k, S_k).$$

So if we assume that

$$\text{(K)} \quad f' < 0 \ ;$$
$$\text{(L)} \quad f' + x_k f'' < 0 \ ;$$
$$\text{(M)} \quad f' - C''_{kxx} < 0$$

for all k and feasible values of x_k and S_k, then Π_k is strictly concave in x_k, and if all firms have finite capacity limits, then there is a unique best response R_k (S_k) of each firm *k*. By implicit differentiation

$$r_k = \frac{\partial R_k}{\partial S_k} = -\frac{f' + x_k f'' - C''_{kxx}}{2f' + x_k f'' - C''_{kxx}}, \tag{5.3}$$

where the denominator is always negative. Assuming again symmetric firms, from the previous sections we know that cost interaction makes the system more stable if the value of r increases. This is the case, when $C''_{XS} < 0$.

We finally note that the payoff functions (5.1) reduce to (4.1) by the special selection

$$C_k(x_k, S_k) = C_k(x_k) + x_k \frac{T(x_k + S_k)}{x_k + S_k} \ .$$

Conclusions

In this paper four extensions of the classical Cournot model were introduced and their local asymptotical stability was examined.

In the first case we assumed the presence of intertemporal demand interaction in the market as the result of market saturation, taste or habit formation etc. In the second case we assumed that any increase in the output during any time period results in an additional cost. In the third case the firms treat pollution jointly and share the cleaning cost in proportion to their share in the total output. In the fourth case we assumed that the cost of each firm depends on the firm's own output as well as on the output of the rest of the industry.

For the sake of simplicity we considered only symmetric firms and presented the stability conditions in term of the common speed of adjustment of the firms. In all cases the condition requires its value to be sufficiently small. This stability region increases by intertemporal demand interaction in the market as well as by the presence of production adjustment costs. Conditions were derived in the other two cases to guarantee the increase of the stability region. These conditions depend on the particular choice of the cost and price functions.

In the discussions of this paper we assumed symmetric firms for mathematical convenience only. The general case can be investigated in a similar manner based on the methodology being applied in Bischi et al. (2006).

References

[1] Bischi, G I., C. Chiarella, M. Kopel and F. Szidarovszky (2006), Nonlinear
[2] Oligopolies: Stability and Bifurcations, Elsevier, Amsterdam (forthcoming).
[3] Okuguchi, K. (1976), Expectations and Stability in Oligopoly Models, SpringerVerlag, Berlin/ /New York.
[4] Okuguchi, K. and E Szidarovszky (1999), The Theory of Oligopoly with Multi-Product Firms (2 *nd* edition), Springer-Verlag, Berlin/ /New York.
[5] Puu, T. and I. Sushko (eds.) (2002), Oligopoly Dynamics, Springer-Verlag, Berlin/New York.

Solutions for closed-loop hierarchical games in the management of limited resources

Richárd KICSINY[1], Zoltán VARGA[1], Antonino SCARELLI[2], Vincenzo PISCOPO[2]

[1]Department of Mathematics, Institute for Mathematics and Informatics,
[2]Department of Biological and Ecological Sciences, University of Tuscia, Italy

Abstract

In the present paper, a recent deterministic continuum-strategy two-player discrete-time dynamic hierarchical game (or Stackelberg game) with fixed finite time duration and closed-loop information structure is introduced. The game can be widely used to model problems in different applications (mainly in conflicts of consuming a limited resource, where one player, called leader, is a superior authority choosing a strategy choice first, and another player, called follower, chooses after).

To find a (hierarchical) equilibrium, two solution algorithms are given, which can be used under certain payoff convexity and different conditions with respect to the parameters of the game. The first one is a backward induction method, which is simpler to apply but, apparently, less generally usable than the second one.

Several practical examples are also given to illustrate the applicability of both methods.

Keywords

deterministic, continuum-strategy, Stackelberg game, closed-loop information

1. Introduction

Continuum-strategy deterministic hierarchical games, in which the players' strategy choices take place in a determined order (von Stackelberg, 2010), form an important and intensively developing field in game theory with comprehensive application interests (Staňková and Olsder, 2006; Staňková and De Schutter, 2011). A very current and extremely important application area of game theory and, in particular, hierarchical games (or Stackelberg games) is water resource management (Madani, 2010; Kicsiny et al., 2014a, Scarelli et al., 2013).

Two-player discrete-time dynamic hierarchical games are characterized with state equations, according to which the game evolves in time, see (Staňková and De Schutter, 2011):

$a_{t+1} = A(a_t, x_t, y_t, t) \quad (t = 1,...,T-1)$;
$T \in \mathbf{N}$: number of time steps,
$a_t \in \mathbf{R}$: state of the game at time t,
$x_t, y_t \in \mathbf{R}$: strategy of the leader and the follower, respectively, at time t,
A : function determining the next state from the current state and current strategies.

At each step, the leader chooses a strategy first then the follower.

There are three basic types of games according to the information structure: In case of open-loop structure, the players know the initial state a_1, in feedback games, they know the current state a_t and in closed-loop games, they know all states up to the current one $a_1,...,a_t$.

Since it is difficult to apply general concepts, special solution methods must be used or worked out for different cases. E.g. in (Kristály and Nagy, 2013), the existence of solutions for hierarchical games is studied on convex strategy sets in certain Riemann manifolds.

In this paper, a recently set up model of a deterministic continuum-strategy two-player discrete-time dynamic hierarchical game with fixed finite time duration and closed-loop information structure (Kicsiny et al., 2014b) is introduced. The types of the considered payoff functions can be widely used in different applications (mainly in conflicts of consuming a limited resource, where one player, called leader, is a superior authority choosing a strategy choice first, and another player, called follower, chooses after). In case of strict concavity or strict monotony on the payoff functions, with some supplementary conditions, the unique hierarchical equilibrium always exists and can be directly determined from the zeros of the corresponding derivatives (see Section 2.2 in (Kicsiny et al., 2014b)). To find an equilibrium in case of certain payoff convexity, two solution algorithms are given, which can be used under different conditions on the game parameters. The first one worked out in (Kicsiny et al., 2014b) and called Solution algorithm 1 below, is a backward induction algorithm (see e.g. (Adda and Cooper, 2003)), which is simpler to apply but, apparently, less generally usable than the second one worked out in (Kicsiny, 2014) and called Solution algorithm 2.

2. Preliminaries

For the Reader's convenience, this section contains the main concepts corresponding to hierarchical games used in this paper (see also (Kicsiny et al., 2014b)).

Hierarchical game

Let us consider the following deterministic two-player discrete-time game:

One of the players is called leader, the other is follower. From now in this paper, leader and follower are denoted with L and F, respectively. The game evolves in discrete (time) steps t ($t = 1,...,T$), with fixed time duration $T \in \mathbf{N}$. At each step, L makes her/his strategy choice $x_t \in X_t$ first, then F makes her/his choice $y_t \in Y_t$, where X_t is L's strategy set, Y_t is F's strategy set at step t.

Let the payoffs (payoff functions) be deterministic functions of the strategy choices:
L's payoff is
$X_1 \times ... \times X_T \times Y_1 \times ... \times Y_T \to \mathbf{R}$,
$(x_1,...,x_T,y_1,...,y_T) \mapsto F(x_1,...,x_T,y_1,...,y_T)$,
F's payoff is
$X_1 \times ... \times X_T \times Y_1 \times ... \times Y_T \to \mathbf{R}$,
$(x_1,...,x_T,y_1,...,y_T) \mapsto G(x_1,...,x_T,y_1,...,y_T)$.
At each step, the player to move decides as follows:
In the knowledge of the earlier strategy choices, s/he determines the later strategy choices of both players as the response to all her/his currently possible decisions, and s/he makes such a strategy choice that maximizes her/his payoff for the game from step t to step T.
This game is called deterministic continuum-strategy two-player discrete-time *hierarchical game* with fixed finite time duration. ■
Relating to the above defined type of games, let us assume the following from now:

1. $X_t = Y_t = [0,1]$ ($t = 1,...,T$), that is the strategy sets are normalized.
2. The game has complete information structure, that is the strategy sets and the players' payoff functions are of common knowledge.
3. The game has perfect information structure that is the player to move knows all strategy choices of both players so far, at each move of each step.

Hierarchical equilibrium
Hereafter, we use the following *hierarchical equilibrium* (or *equilibrium* in short) concept in the present paper for the studied hierarchical games:

Proceeding backwards from the last step of the game (from step T) to the first step, at step t ($t = 1,...,T-1$) F predicts the later strategy choices $x_{t+1}^*,\ldots,\ x_T^*$, $y_{t+1}^*,\ldots,\ y_T^*$ (which may be complicated functions of the earlier choices, e.g. of y_t) and maximizes her/his payoff G by a strategy choice $y_t^* \in \arg\max_{y_t} G(x_1,...,x_t,x_{t+1}^*,...,x_T^*,y_1,...,y_t,y_{t+1}^*,...,y_T^*)$. L predicts the later strategy choices $x_{t+1}^*,\ldots,\ x_T^*,\ y_t^*,\ldots,\ y_T^*$ (which may be complicated functions

of the earlier choices, e.g. of x_t) and maximizes her/his payoff F by a strategy choice $x_t^* \in \arg\max_{x_t} F\left(x_1,...,x_t,x_{t+1}^*,...,x_T^*,y_1,...,y_{t-1},y_t^*,y_{t+1}^*,...,y_T^*\right)$.

Assume that all sets included in the above description are nonempty. Then a strategy pair $\left(\left(x_1^*,...,x_T^*\right),\left(y_1^*,...,y_T^*\right)\right)$ containing such strategy choices, which satisfy the above concept is a (hierarchical) equilibrium of the game.
In case of $t=T$, the strategy choices with indices higher than t are of course omitted.

3. Game specification

The hierarchical game studied in this work has been proposed in (Kicsiny et al., 2014b). For the Reader's convenience, the game specification is recalled in details in this section.

The payoff functions of the players are determined by the amounts used of a given resource. At each step, the follower (F) can choose only from the remaining amount after the leader's (L's) choice. The resource amount remaining after both players' choices is added to the resource amount pre-fixed for the next step. The following terminology is used in the game:

Notation:
R: total resource reserve in the game,
$T \in \mathbf{N}$: number of steps,
$t = 1,...,T$: current step,
$x_t \in [0,1]$: proportion of the resource consumed by L from the available reserve at step t,
$(x_1,...,x_T)$: strategy of L,
$y_t \in [0,1]$: proportion of the resource consumed by F from the available reserve after the choice of the leader at step t,
$(y_1,...,y_T)$: strategy of F,
$r_t \in [0,R]$: pre-fixed resource amount reserved for step t to rationalize the consumption for the whole duration of the game, from step 1 to step T (note that $\sum_{t=1}^{T} r_t = R$),
$\pi(\rho)$: unit price of the resource corresponding to the current reserve $\rho \in [0,R]$ (assumed to be a monotonically decreasing, twice differentiable function),
γ_t: gain for F from a unit of the used resource at step t,
α: rate of the direct gain for L from a unit of the used resource at any step,

q : tax rate on the profit of F paid to L ($q \in [0,1[$).

Formal variables for the fictional step 0: x_0 :=0, y_0 :=0, r_0 :=0 (in appropriate unit).

The total payoffs are the sum of the payoffs for the separate steps:

The leader's payoff is

$$F(x_1,...,x_T,y_1,...,y_T)=\sum_{t=1}^{T} f_t(x_1,...,x_t,y_1,...,y_t) \quad , \tag{1}$$

the follower's payoff is

$$G(x_1,...,x_T,y_1,...,y_T)=\sum_{t=1}^{T} g_t(x_1,...,x_t,y_1,...,y_t) \quad , \tag{2}$$

where

$$f_t(x_1,...,x_t,y_1,...,y_t)=\left(\alpha-\pi\left[R-\sum_{i=1}^{t-1}\left(1-\prod_{k=1}^{t-i}(1-y_{t-k})(1-x_{t-k})\right)r_i\right]\right)$$
$$x_t\left(\sum_{i=1}^{t-1}\left(\prod_{k=1}^{t-i}(1-y_{t-k})(1-x_{t-k})\right)r_i+r_t\right)+q$$
$$\left(\gamma_t-\pi\left[R-\sum_{i=1}^{t-1}\left(1-\prod_{k=1}^{t-i}(1-y_{t-k})(1-x_{t-k})\right)r_i\right]\right)y_t(1-x_t)$$
$$\left(\sum_{i=1}^{t-1}\left(\prod_{k=1}^{t-i}(1-y_{t-k})(1-x_{t-k})\right)r_i+r_t\right), \tag{3}$$

$$g_t(x_1,...,x_t,y_1,...,y_t)=(1-q)\left(\gamma_t-\pi\left[R-\sum_{i=1}^{t-1}\left(1-\prod_{k=1}^{t-i}(1-y_{t-k})(1-x_{t-k})\right)r_i\right]\right)$$
$$y_t(1-x_t)\left(\sum_{i=1}^{t-1}\left(\prod_{k=1}^{t-i}(1-y_{t-k})(1-x_{t-k})\right)r_i+r_t\right). \tag{4}$$

4. Theoretical results

Solution algorithm 1 (based on Kicsiny et al., 2014) and Solution algorithm 2 (based on Kicsiny, 2014) are given below. Both algorithms correspond to certain payoff convexity.

Solution algorithm 1

Let us consider the game defined in Section 3 and the following inequalities:

$$\frac{\alpha - q\gamma_T}{1-q} \geq \pi\left[R - r_0 - \ldots - r_{T-1}\right], \quad \text{(C1)}$$

$$\alpha \leq \pi[R], \quad \text{(C1a)}$$

$$\alpha \geq \pi\left[R - r_0 - \ldots - r_{T-1}\right], \quad \text{(C1b)}$$

$$\frac{\alpha - q\gamma_T}{1-q} \leq \pi[R], \quad \text{(C2)}$$

$$\gamma_T \leq \pi[R], \quad \text{(C2a)}$$

$$\gamma_T \geq \pi\left[R - r_0 - \ldots - r_{T-1}\right]. \quad \text{(C2b)}$$

$$\frac{\alpha - q\gamma_t}{1-q} \geq \pi\left[R - r_0 - \ldots - r_{t-1}\right], \quad \text{(C3)}$$

$$q\gamma_{t+j} - \alpha + \pi[R](1-q) \geq 0, \quad \text{(C3a1)}$$

$$q\gamma_{t+j} - \alpha + \pi[R](1-q) \leq 0, \quad \text{(C3a2)}$$

$$\left(q\gamma_{t+j} - \alpha + \pi[R](1-q)\right)\left(r_0 + \ldots + r_{t-1} + r_t\right) + q\left(r_{t+1} + \ldots + r_{t+j}\right)$$
$$\left(\pi\left[R - r_0 - \ldots - r_{t-1} - r_t\right] - \pi\left[R - r_0 - r_{t-1}\right]\right) \geq 0, \quad \text{(C3a2/1)}$$

$$\left(q\gamma_{t+j} - \alpha + \pi\left[R - r_0 - \ldots - r_{t-1}\right](1-q)\right)r_t + q\left(r_{t+1} + \ldots + r_{t+j}\right) \leq 0,$$
$$\left(\pi\left[R - r_0 - \ldots - r_{t-1} - r_t\right] - \pi[R]\right) \quad \text{(C3b)}$$

$$\frac{\alpha - q\gamma_t}{1-q} \leq \pi[R], \quad \text{(C4)}$$

$$\gamma_{t+j} - \gamma_t \geq 0, \quad \text{(C4a1)}$$

$$\gamma_{t+j} - \gamma_t \leq 0, \quad \text{(C4a2)}$$

$$\left(\gamma_{t+j} - \gamma_t\right)\left(r_0 + \ldots + r_{t-1} + r_t\right) + \left(\pi\left[R - r_0 - \ldots - r_{t-1} - r_t\right] - \pi\left[R - r_0 - \ldots - r_{t-1}\right]\right)$$
$$\left(r_{t+1} + \ldots + r_{t-j-1} + r_{t+j}\right) \geq 0 \quad \text{(C4a2/1)}$$

$$\left(\gamma_{t+j} - \gamma_t\right)r_t + \left(\pi\left[R - r_0 - \ldots - r_{t-1} - r_t\right] - \pi[R]\right)\left(r_{t+1} + \ldots + r_{t+j-1} + r_{t+j}\right) \leq 0. \quad \text{(C4b)}$$

$$\gamma_t - \pi\left[R - r_0 - \ldots - r_{t-1}\right] \geq 0, \quad \text{(C5)}$$

$$\frac{\alpha - q\gamma_t}{1-q} \geq \pi\left[R - r_0 - \ldots - r_{t-1}\right], \quad \text{(C5a)}$$

$$\frac{\alpha - q\gamma_t}{1-q} \leq \pi[R], \quad \text{(C5b)}$$

$$\gamma_t - \pi[R] \le 0. \qquad \text{(C6)}$$

A solution (equilibrium) of the game can be determined as follows:

1. Determine the equilibrium strategy pair for step T according to the following: The equilibrium for step T $\left(x_T^*, y_T^*\right)$ is the strategy pair (0,0) if the condition pair (C1) and (C1a) hold, (1,0) if (C1) and (C1b) hold, (0,0) if (C2) and (C2a) hold and (0,1) if (C2) and (C2b) hold.
   If one of the condition pairs holds and $T \ge 2$, proceed with Step 2 of this algorithm, otherwise, stop the algorithm.
2. Check if $\frac{\partial^2 f_\tau(x_1,...,x_\tau,y_1,...,y_\tau)}{\partial x_{\tau-s}^2} \ge 0$, $\frac{\partial^2 g_\tau(x_1,...,x_\tau,y_1,...,y_\tau)}{\partial x_{\tau-s}^2} \ge 0$ and $\frac{\partial^2 g_\tau(x_1,...,x_\tau,y_1,...,y_\tau)}{\partial y_{\tau-s}^2} \ge 0$ $(\tau = 2,...,T,\ \ s = 1,...,\tau-1)$ are satisfied.
   If the conditions hold, proceed with Step 3 of this algorithm with t=T-1, otherwise, stop the algorithm.
3. If t=0, stop the algorithm, otherwise, determine the equilibrium strategy pair for step t according to the following:
   Case A
   Among the equilibrium strategy pairs for the game of steps from (t+1) to T, (x_{t+j}, y_{t+j})=(0,1) $(t = 1,...,T-t)$ is the first such strategy pair for a step which is not (0,0). In such a case, if (C3) and (C3a1) hold or if (C3) and (C3a2) and (C3a2/1) hold then the strategy pair (0,0) is an equilibrium for step t $\left(x_t^*, y_t^*\right)$. If (C3) and (C3b) hold then an equilibrium is (1,0) for step t. If (C4) and (C4a1) hold or if (C4), (C4a2) and (C4a2/1) hold then an equilibrium is (0,0) for step t. If (C4) and (C4b) hold then an equilibrium is (0,1) for step t.
   Case B
   Among the equilibrium strategy pairs for the game of steps from (t+1) to T, (x_{t+j}, y_{t+j})=(1,0) $(t = 1,...,T-t)$ is the first such strategy pair for a step which is not (0,0). In such a case, if (C5) and (C5a) hold then the strategy pair (1,0) is an equilibrium for step t $\left(x_t^*, y_t^*\right)$. If (C5) and (C5b) hold then an equilibrium is (0,1) for step t. If (C6) holds then an equilibrium is (0,0) for step t.
   If the determined equilibrium strategy pair is (0,0) for all steps in the equilibrium for the game of steps from (t+1) to T, then the equilibrium strategy pair for step t can be similarly determined as $\left(x_T^*, y_T^*\right)$ in Step 1 (substituting t for T).
   If an equilibrium strategy pair for step t can be determined according to the above conditions, an equilibrium corresponding to the steps from t to

T has been determined from the strategy pairs of the corresponding steps as $\left(\left(x_t^*,...,x_T^*\right),\left(y_t^*,...,y_T^*\right)\right)$, and proceed with Step 3 of this algorithm after decreasing t by 1, otherwise, stop the algorithm.

Solution algorithm 2

Let us consider the game defined in Section 3 and the following inequalities:

$$\alpha-\pi[R]\le q(\gamma_l-\pi[R]) \quad (l=1,...,T-1) \tag{C7a1}$$

$$\gamma_l-\pi\left[R-\sum_{n=0}^{l-1}r_n\right]>0 \quad (l=1,...,T-1) \tag{C7a2}$$

$$(\gamma_{l+m}-\pi[R])\le 0 \quad (l=1,...,T-1,\ m=1,...,T-l) \tag{C7b1}$$

$$\alpha-\pi\left[R-\sum_{n=0}^{l+m-1}r_n\right]>q\left(\gamma_{l+m}-\pi\left[R-\sum_{n=0}^{l+m-1}r_n\right]\right)$$

$$(l=1,...,T-1,\ m=1,...,T-l) \tag{C7b2}$$

$$\alpha-\pi[R]\le q(\gamma_l-\pi[R]) \quad (l=T) \tag{C8a}$$

$$\gamma_l-\pi\left[R-\sum_{n=0}^{l-1}r_n\right]>0 \quad (l=T) \tag{C8b}$$

$$q\left(\gamma_u-\pi\left[R-\sum_{n=0}^{u-1}r_n\right]\right)>\alpha-\pi\left[R-\sum_{n=0}^{u-1}r_n\right] \quad (u=1,...,l-1). \tag{C9}$$

An equilibrium can be determined in case of $T\ge 2$ as follows:

1. Check if $\frac{\partial^2 f_t(x_1,...,x_t,y_1,...,y_t)}{\partial((1-y_{t-s})(1-x_{t-s}))^2}\ge 0$ and $\frac{\partial^2 g_t(x_1,...,x_t,y_1,...,y_t)}{\partial((1-y_{t-s})(1-x_{t-s}))^2}\ge 0$ for any $x_1,y_1,...,x_T,y_T\in[0,1]$ ($t=2,...,T$, $s=1,...,t-1$) are satisfied.
   If the conditions hold, proceed with Step 2 of this algorithm, otherwise, stop the algorithm.
2. Determine the latest (in the real course of the game) step (step l, $l=1,...,T$), for which conditions (C7a1), (C7a2) and (C7b1) hold or conditions (C7a1), (C7a2) and (C7b2) hold or conditions (C8a) and (C8b) hold. The conditions for the steps should be checked proceeding backwards from step T.
   If there is such a step, proceed with Step 3 of this algorithm, otherwise, stop the algorithm.
3. Check condition (C9) for each step u ($u=1,...,l-1$) if $l\ge 2$. Choose strategy pair (0,0) for the steps for which (C9) does not hold. For the rest of the steps, both (0,0) and (0,1) still come into consideration. For step l, choose (0,1).
4. After step l, till the last but one step, choose (1,0) if $\gamma_{l+m}-\pi[\cdot]>0$

($m = 1,..., T - l - 1$) and (0,0) if $\gamma_{l+m} - \pi[\cdot] \le 0$ at the beginning of the corresponding step, provided that $l \le T - 2$. Choose (1,0) at the last step if $\alpha - \pi[\cdot] > 0$ at the beginning of the step, otherwise, choose (0,0), provided that $l \le T - 1$.

5. Then the game tree has been determined with only nodes with more than one (two) possible strategy choices according to Step 4 of this algorithm. The follower's final payoff can be calculated based on equalities (2) and (4) for each terminal node. Then a path for the follower's maximal payoff value can be directly identified (with the players' corresponding payoffs). This path also directly corresponds to an equilibrium of the game.

5. Application

Examples 1 and 2 below represent an application field namely water resource management. In this case, the resource (R, $r_t \in [0, R]$) in the game is fresh (ground)water (in m^3). The leader is the local authority/government, who manages the use of the water reserve for a given time period (for ten days) between the social sector (different services run by the local government itself) and the follower, which is an agricultural producer/sector using water for irrigation.

Every day, for the need of the social sector, the authority assigns a proportion of the water reserve available at the beginning of the day, which is the sum of the predefined daily amount and the reserve remained from the former days. Then the producer decides on the proportion of the available reserve left after the authority's decision.

The water has a given unit price increasing with decreasing actual reserve, which must be paid by both players. The authority's payoff on a day is the social gain (corresponding to α) received from satisfying, to some extent, the demand of the social sector, minus the price of the used water, plus the tax (corresponding to q) paid by the producer proportionally to her/his profit from the water use. The producer's payoff on the given day is the net profit after tax.

Example 1 (with linear water price) (Kicsiny et al., 2014a)

r_1=48 m^3, r_2=42 m^3, r_3=30 m^3, r_4=18 m^3, r_5=24 m^3, r_6=18 m^3, r_7=30 m^3, r_8=36 m^3, r_9=24 m^3, r_{10}=30 m^3 (R=300 m^3, T=10), α=3.5 EUR/m^3, q=0.3, γ_1=13.4 EUR/m^3, γ_2=13 EUR/m^3, γ_3=9 EUR/m^3, γ_4=8 EUR/m^3, γ_5=11.5 EUR/m^3, γ_6=7 EUR/m^3, γ_7=11.6 EUR/m^3, γ_8=5 EUR/m^3, γ_9=-1 EUR/m^3, γ_{10}=1.2 EUR/m^3, $\pi(\rho) = -\frac{2.9}{300}\rho + 3$ EUR/m^3.

Solution algorithm 2 can be successfully applied in this example.
The determined equilibrium for the whole game is $\left(\left(x_1^*,...,x_{10}^*\right),\left(y_1^*,...,y_{10}^*\right)\right)=\left((0,0,0,0,0,0,0,0,1,0,1),(0,1,0,0,0,0,0,1,0,0,0)\right)$, the authority's and the producer's payoffs are 835.5 EUR and 1705.6 EUR, respectively.

Example 2 (with nonlinear water price) (Kicsiny et al., 2014a)
The parameter values are the same as in Example 1 except the price function $\pi(\rho)=-\frac{3\cdot 755^4}{(\rho+755)^4}$ EUR/m^3.

Both Solution algorithms 1and 2 can be successfully applied here with the same results.
The determined equilibrium for the whole game is $\left(\left(x_1^*,...,x_{10}^*\right),\left(y_1^*,...,y_{10}^*\right)\right)=\left((0,0,0,0,0,0,0,0,1,0,1),(1,1,0,0,0,0,0,1,0,0,0)\right)$, the authority's and the producer's payoffs are 833.9 EUR and 1658.1 EUR, respectively.

Further application fields and examples can be found in (Kicsiny et al., 2014a, b; Scarelli et al., 2013; Kicsiny, 2014).

Conclusion

In the present paper, a recent deterministic continuum-strategy two-player discrete-time dynamic hierarchical game with fixed finite time duration and closed-loop information structure has been introduced. The type of the considered payoff functions are rather generally used in different applications.

Since general closed-loop problems are challenging to solve, it is important to work out specific solution methods for specific games. Two solution algorithms (called Solution algorithms 1 and 2) have been given, which can be used under certain payoff convexity.

Based on many carried out calculations (not detailed here because of limits in volume) Solution algorithm 2 proves to be quite more generally usable than Solution algorithm 1. In particular, Example 2 can be solved with both methods producing the same results, while Example 1 can be solved only with Solution algorithm 2.

Further future research may address the case of more than two players (several leaders or followers with or without priority among them, etc. (see e.g. (Szidarovszky et al., 1991; Molnár and Szidarovszky, 2011)).

Acknowledgement

The first author thanks his colleagues in the Department of Mathematics in the Faculty of Mechanical Engineering (Szent István University) for their support.

References

[1] Adda, J., Cooper, R. W. (2003). Dynamic economics: Quantitative methods and applications. MIT Press.

[2] Kicsiny, R. (2014). Closed-loop hierarchical games with convexity conditions on the payoffs for the management of limited resources. Submitted for publication.

[3] Kicsiny, R., Piscopo, V., Scarelli, A., Varga, Z. (2014a). Dynamic Stackelberg game model for water rationalization in drought emergency. Journal of Hydrology, 517, 557-565.

[4] Kicsiny, R., Varga, Z., Scarelli, A. (2014b). Backward induction algorithm for a class of closed-loop Stackelberg games. European Journal of Operational Research, 237, 1021-1036.

[5] Kristály, A., Nagy, Sz. (2013). Followers' strategy in Stackelberg equilibrium problems on curved strategy sets. Acta Polytechnica Hungarica, 10, 7, 69-80.

[6] Madani, K. (2010). Game theory and water resources. Journal of Hydrology, 381, 225-238.

[7] Molnár, S., Szidarovszky, F. (2011). Game Theory: Multiobjective Optimization, Conflict Resolution, Differential Games. Budapest: Computerbooks. (in Hungarian)

[8] Scarelli, A., Kicsiny, R., Piscopo, V., Varga, Z. (2013). A game-theoretical model for water resource management. 9th Spain-Italy-Netherlands Meeting on Game Theory (SING9 2013), Book of abstracts, 61-62.

[9] Staňková, K., Olsder, G. J. (2006). Inverse Stackelberg games versus adverse-selection principal-agent model theory.
http://www.nextgenerationinfrastructures.eu/catalog/file/462440/ISDG_06_Stankova2.pdf (2014. 10.)

[10] Staňková, K, De Schutter, B. (2011). Stackelberg equilibria for discrete-time dynamic games – Part I: Deterministic games. Proceedings of the 2011 IEEE International Conference on Networking, Sensing and Control, Delft, The Netherlands, 249-254.

[11] Szidarovszky, F., Molnár, S., Okuguchi, K. (1991). An n-person Stackelberg leader-leader model. Applied Mathematics and Computation, 46, 3, 221-232.

[12]. von Stackelberg, H. (2011). Market structure and equilibrium. Springer. (Translated by Urch, L., Hill, R., & Bazin, D.)

Institute for Process Engineering

Professor Dr. János BEKE
Director of the Institute

Dear Reader,

The Institute for Process Engineering as a dominant education and research collective at the Faculty of Mechanical Engineering – in its activity - cultivates three professional working areas: automotive technologies, energetics and measurement technologies. During our educational and scientific work we paid special respects to the following topics:

- Basic technical knowledge in aspect of engineering approach,
- Engineering thermodynamics, electrical engineering and electronics,
- Basic and applied knowledge of energy conversion, energy utilization and energy economy,
- Special technical knowledge for development of environmental industry and utilization of alternative energy sources,
- Basic and applied knowledge of automotive and off-road techniques and technologies
- Disciplines of measurement technology applied in different engineering processes,

Accordingly our tradition, the Institute for Process Engineering is eager to present some of its scientific activities concerning the year of 2014.

In last year we paid special attention on the following scientific topics

- Influences of different road profiles on the life span of the vehicles: the aim of the research was to develop a comparative method that makes possible to compare the vibration generating effects of different road profiles.
- Examination and modeling of different heat pump systems: the control of energetic systems using multiple energy sources can cause difficulties, but by means of adequate model-based design principles, higher efficiency climate systems can be operated. As a first step we set up a model experiment, during which we analyzed all the parameters that helped us to optimize the appropriate energetic control systems.
- Possibility of using alternative energy sources in the energy supply: in frame of the project TÁMOP-4.2.1.B-11/2/KMR-2011-0003, titled of „Increasing the level of education and research at the Szent Istvan University" our institute had a chance to analyze the usability of the near surface geothermic and geothermal energies as well as the kinetic energy production of typical continental drifts.

Professor Dr. János BEKE
Director

Environmental energies as alternatives in the energy supply

Péter KORZENSZKY, István PATAY, László TÓTH,
Norbert SCHREMPF, János BEKE
Department of Energetics, Institute for Process Engineering

Abstract

In the frame of the project TÁMOP-4.2.1.B-11/2/KMR-2011-0003, titled of „Increasing the level of education and research at the Szent Istvan University" the learning of renewable energies was a substation research area. The aim of this subproject was to develop the theoretical bases of utilizing the near surface geothermic and geothermal energies as well as the kinetic energy of typical continental drifts in different mechanical and technological innovations with high efficiency.

Keywords

Renewable energy, environmental energy, geothermal energy, wind energy

1. Introduction

The goal of the geothermic research is to establish an alternative energetical research and advisory network, which is based on geothermic, geothermal and wind energy while it takes into consideration the special geological, agricultural and social properties, logistical capabilities of small villages, regions when determining its research aims.

2. Geotermal energy

After the start of the project, the primary task was the study of companies for the exploitation of geothermal energy, and of existing investments, the collection and processing of the plant operating experiences. We tried to answer the questions of the the practical applicability, after the companies has been contacted. Flowcharts and supporting material were prepared, which can be used and presented in education, about the functioning and operation of the known systems. We had the chance to examine a variety of products, as a result of relationship built with heat pump manufacturer and distributor companies. The next step was to plan the measurement technique tasks to be accomplished, related to the topic of use of ambient energy.

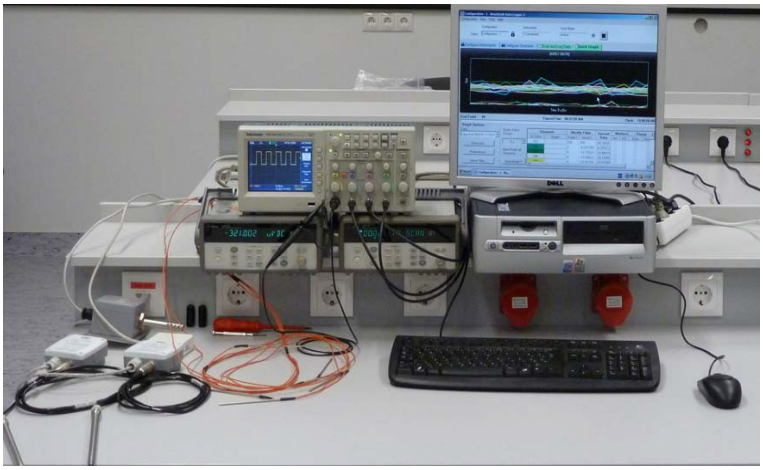

Figure 1. Measurement assembly for geothermal energy utilization

Since the beginning of the project there was a steady increase in the number of available databases. By the end of the project, studies were prepared on each sub-project areas, such as the possibilities to exploit the thermal heat by the thermal baths in Hungary, in the lights of concrete examples. The different sub- areas and the tasks performed are illustrated by some photos. The following figures show some excerpts from the documentations prepared for each measurement assembly. It is appropriate to test the individual units, sensors and equipment one by one and to test them as an assembled system, after designing a measurement loop assembly, but prior to the site installation occurs (Figure 1.)

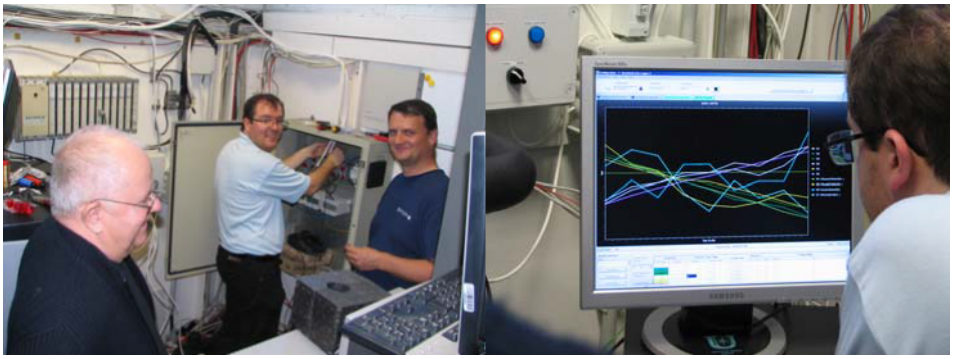

Figure 2. Measuring the use of geothermal heat

In the experiments performed, the amount of heat extracted from the ground, was one of the most important characteristics examined. The layout of the available soil probes were also considered during each measurement. To assess

the layout of the probes, and the interaction of probes, was the responsibility of an other research group.

The simultaneous measurement of many parameters illustrated in Figure 2.

The change in the measured values over time, carries valuable information, so the real time display of the values is very important. The installation of the detectors and the precise connections requires prudent and careful teamwork.

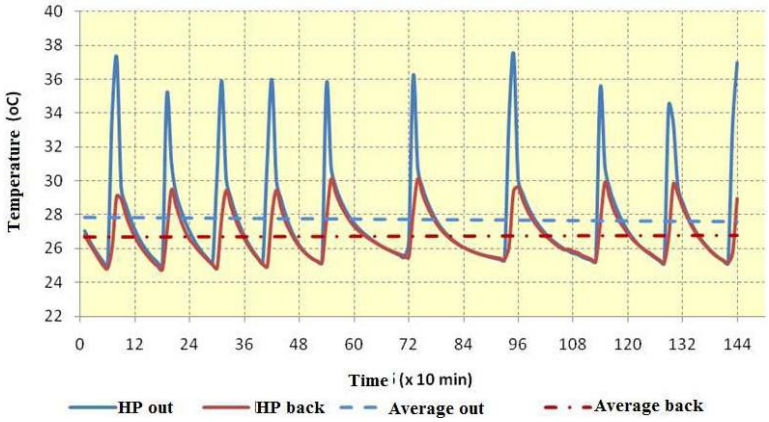

Figure 3. The buffer tank inlet and outlet water temperature during a short test cycle

The tube-in-tube heat exchanger test bench created during the research will be used for educational purposes in the future. We have performed a set of measurements according to a predetermined schedule, after instrumentation of the available equipment. As a result of the measurements, we have determined the boundaries and the circumstances of the applicability of the tools.

Figure 4. Heat pump measurement loop at Szent Istvan University, Faculty of Mechanical Engineering

The existing air-to-water heat pump measurement loop is suitable for modeling the extreme and normal operating conditions. After the instrumentation of the measurement loop, knowing the measured temperature, flow and electrical parameters, it can be easily mapped the overall, and the instantaneous efficiency of the system (Figure 4).

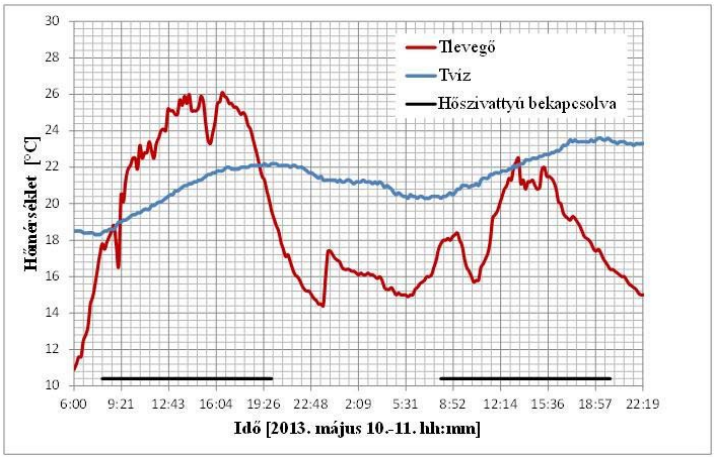

Figure 5. Changes in water temperature of the pool in case of air

Figure 5 illustrates the measurement results of a pool keeping warm while the outside air temperature reaches 10° C of differences. The expert network established by the intellectual resources, presentation tools and research laboratories of Szent István University, can serve currently unmet demands. The targeted basic research criteria which was realized as part of this project, gives the opportunity to perform a science-based innovative activity that is able to give the continuous technical research and development background which fits the residential and community needs.

3. Wind energy

There were already initiatives for the installation of wind generators and industrial usage of wind energy in Hungary in the 1960's. Experts in the energy industry considered that Hungary does not have enough wind energy potential, therefore it is not practical to use this renewable energy source. Even in present days (2014) there are belittling opinions about the usage of wind energy. Despite the fact that the already present 330 MW wind energy potential transferred 740 GWh/annum (2012) electric energy to the Hungarian energy network, achieving the fourth highest place amongst European countries with respect to the utilization of wind generators.

To determine the national wind potential, several methods were invented, researches introduced.

The best result of these was produced by the project 3A/0038/2002 NKFP, titled as „Analysis of Hungary's atmospherical renewable energy sources, mapping of present potentials and the promotion of their usage with meteorological measurements and forecasts". The wind maps resulting from this research possess an accuracy of 25 km2 on a 5*5 km roster. This data pool represents a comprehensive picture of Hungary's wind potential, although it is not suitable for the creating a preliminary prognosis for actual wind generator installations. Wind energy research tasks of the TAMOP-4.2.1.B-11/2/KMR-2011-0003 project:

1. Creation of a wind energy potential laboratory
2. Participation in model experiments
3. Computer simulation of aerodynamic experiments
4. Wind potential analysis
5. Modelling of location specific attributes
6. Modelling of the operation of grouped wind generators, analysis of flow affecting effects
7. Creation of a database for the experts' network
8. Implementation of research results into education
9. Development of education material for Hungarian and foreign courses

4. Wind energy theory and methodology

Wind's altitude dependence
Wind speed can be calculated at any given z height, if its value is given at reference altitude z_R. As per the logarithm rule:

$$\frac{v}{v_R} = \frac{\ln\left(\frac{z}{z_0}\right)}{\ln\left(\frac{z_R}{z_0}\right)} \tag{1}$$

where:
v is the required wind speed (m/s), at z height (m)
v_R is the given wind speed (m/s), ai z_R reference height (m).

WAsP (Wind Atlas Analysis and Application Program)
The sub-models of WAsP:

1) Complex terrain flow model:

$$\Delta S = \frac{u_2(\Delta z_2) - u_1(\Delta z_1)}{u_1(\Delta z_1)} \ [\%] \tag{2}$$

u_1 – undisturbed wind speed; u_2 – disturbed wind speed
Δz – height above ground level

In WAsP, the Complex terrain flow sub-model is a linear, spectral model based on the Jackson-Hunt theory, which divides an interior and an exterior layer in the wind flow.

2) Model for sheltering obstacles:

$$\frac{\Delta u(z_a)}{u(z_a)} = 9{,}75\left(\frac{h}{z_a}\right)^n \frac{h}{x}(1-P)\eta \exp\left(-0{,}67\eta^{1.5}\right) \tag{3}$$

$$\eta = \frac{z_a}{h}\left(\frac{0{,}32}{\ln(h/z_0)} \cdot \frac{x}{h}\right)^{\frac{1}{n+2}} \tag{4}$$

where n = 0,14 in WAsP

3) Roughness change model:

$$if\ c_1 h \le z \quad u(z) u' \frac{\ln(z/z_{01})}{\ln(c_1 h/z_{01})} \tag{5}$$

$$if\ c_2 \le z \le c_1 h \quad u(z) u'' + (u' - u'') \frac{\ln(z/c_2 h)}{\ln(c_1/c_2)} \tag{6}$$

$$if\ c_2 h \le z \quad u(z) = u'' \frac{\ln(z/z_{02})}{\ln(c_2 h/z_{02})} \tag{7}$$

Where:

$$u' = (u_{*1}/\kappa)\ln(c_1 h/z_{01}) \tag{8}$$

$$u'' = (u_{*2}/\kappa)\ln(c_2 h/z_{02}) \tag{9}$$

$$c_1 = \frac{1}{3};\ \ c_2 = \frac{1}{15} \tag{10}$$

The ‘BZ’ (Bessel expansion on a Zooming grid) flow model:

For the calculation of the terrain’s influence on wind speed, WAsP applies Troen’s ‘BZ’ model. This model is the experiment of Jackson and Hunt (Theory on the flow over mountains).

Wind energetics measurement methods

Tower measurement:

In the case of tower measurements, the required parameters are detected at discrete heights. In Hungary, the smallest wind energetics measuring tower reaches 60 m, while the largest boasts with a height of 125 m. The configuration of measuring towers, the selection and then installation of instruments are executed in accordance with precise standards. The base components of the system are as follows: data recorder, 2 pcs of wind speed sensors, wind direction sensor, temperature and relative humidity sensors, atmospheric pressure sensor, communicational system and power supply.

The requirements regarding the installation of the sensors are defined in standard MSZ EN 61400-12-1: Wind power plants, part 12-1: The power output measurement of electricity generating wind turbines.

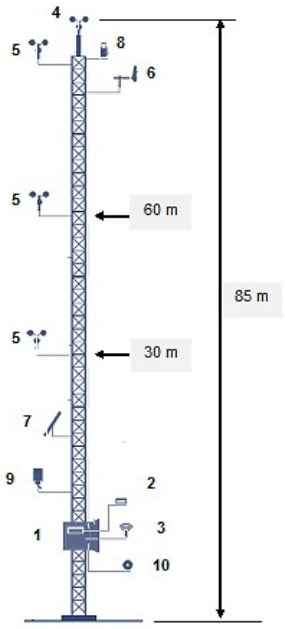

Figure 6. Wind energetics measuring system, general layout on a pillar
1-switch-box, 2-data recorder, 3-data transfer, 4-5-wind speed sensor, 6-wind direction sensor, 7-PV power supply, 8-foreign object indicating light, 9- temperature and relative humidity sensor, 10- atmospheric pressure sensor

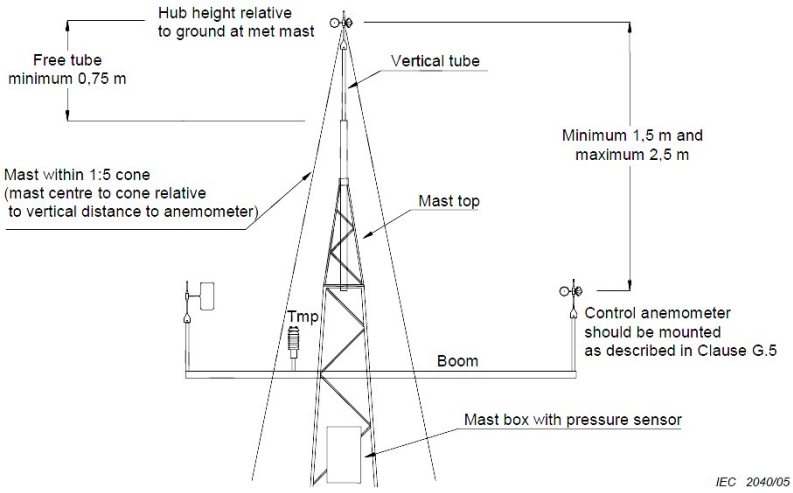

Figure 7. Example of the installation of anemometer, control anemometer, wind speed sensor and other sensors

The SODAR measurement:

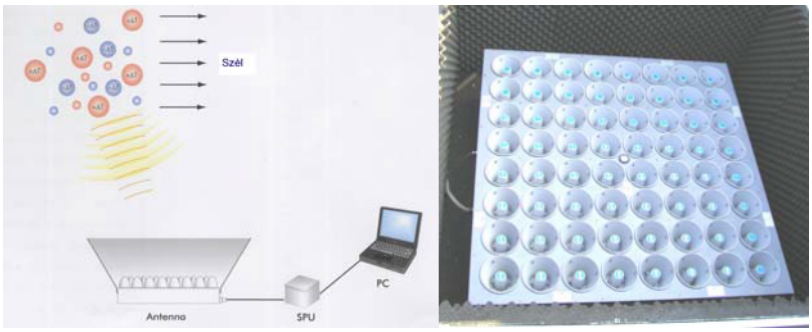

a) b)

Figure 8: SODAR in use (source: Varga et al. 2005)
a) SODAR measuring principle b) 64 Doppler radars

SODAR (SOnic Detection And Ranging), is a meteorological instrument, which measures wind speed and direction by means of sound waves. The measurement is based on the scattering of sound waves by atmospheric turbulence. The irregular alteration of micro turbulence defines the actual vertical and lateral wind component.

Locations inspected under TÁMOP-4.2.1.B-11/2/KMR-2011-0003 programme: The selection of locations was based on the geography of the terrain. Owing to this, 3 typical features were defined: plain, rise and mountainous area.

Due to the limited geographical features of Hungary, mountainous features are difficult to be analysed, so instead we have chosen one, which is basically located in the meteorological and wind zone of a mountainous terrain.

Methods and techniques used during research

Throughout the searching process, we used the procedures, methods and models from standard collection MSZ EN 61400, such as WindPro 2.7 and WAsP 9.0 wind energetics software.

The used sensors:

1 2 3 4 5

Figure 9. The sensors and data recorder in operation

Measured values: wind speed at 2 heights, 1 wind direction, 2 static air temperature, 1 relative humidity and 1 atmospheric pressure measurement.

The sampling time: 1 sec, averaging 10 minutes of data

Positioning of sensors:

- 60,68 m, 1 Thies 'First class' wind speed sensor (A),
- 50,58 m, 1 Thies „compact" wind direction sensor,
- 40,78 m 1 Thies „First class" wind speed sensor (B),
- 10 m, 1 atmospheric pressure sensor, 2 temperature sensors.

The Ammonit Meteo 32 data recorder and storage unit, together with its related systems as well as the communicational system and UPS (uninterruptible power supply) were positioned at 9 m above ground level.

During data evaluation we created data pairs, which are displayed in a time scale. We also prepared the relief and terrain cover models of the various locations. By means of the relief and terrain cover models, we were able to create the flow model from the measured data, which served as a base for defining the whole wind field.

Based on the wind field, finally we could create a prognosis on electricity supply capacity with a given wind power station type. (We extrapolated the data of 2 months to the whole year, which resulted in a great inaccuracy. However the purpose of this project was to design the method for such models, and this time frame proved to be sufficient for that.)

5. Wind energy results

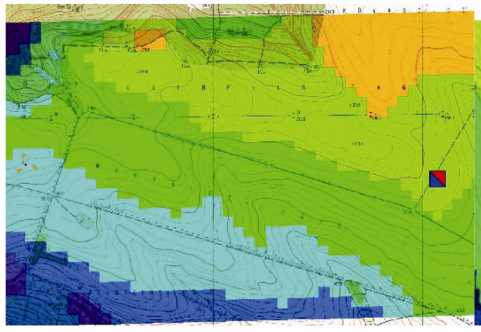

Figure 10. Electric energy production on hill terrain
(MWh/y; P=3.0MW; H=140m; D=113m)

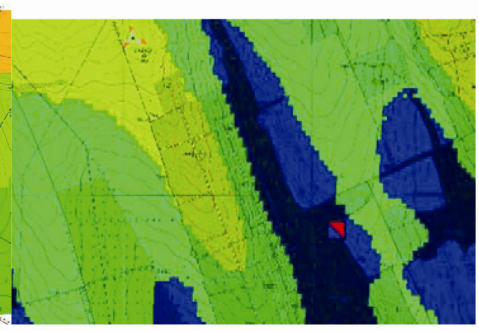

Figure 11. Electric energy production mountaineous terrain
(MWh/y; P=3.0MW; H=140m; D=113m)

On hill terrain the production of 6575-6877 MWh/annum electric energy is expectable, based on the wind generator installed on such a location with the nominal power of 3 MW, 140 m hub-height and 113 m rotor diameter (Illustration 10).

On mountaineous terrain the modelled wind generator is expected to produce 10600-10900 MWh/annum electric energy.

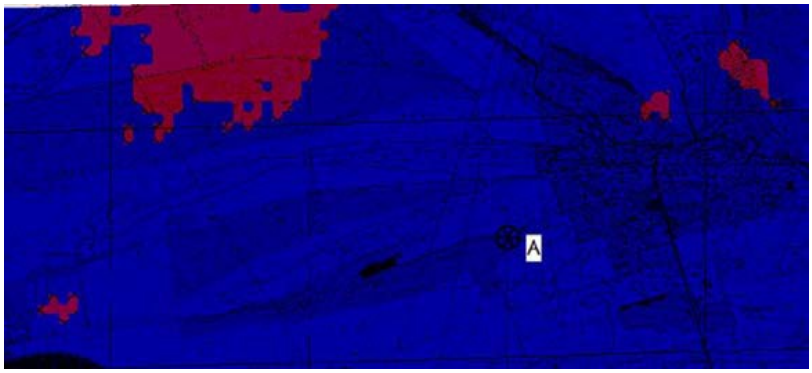

Figure 12. Electric energy production on flatlands (MWh/y; P=3.0MW; H=140m; D=113m)

On the analysed flat land, the modelled production of the wind generator is expected to be around 6900-7000 MWh/year.

5. Wind energy Conclusion

Details of the task:

I. Create wind energy potential analytical laboratory. (from existing devices). The main units of the research lab created:

- Wind tunnel, which is suitable for calibration of anemometers and to perform wind energy model tests
- Energetical wind measurement system, with 60 meter high measurement tower
- WindPRO wind energy modeling software
- Wasp wind energy modeling software

II. Hydrodynamic model experiments

- Location-specific flow factors modeling and computer simulation of the flow conditions
- Simulation of the operating conditions of cup anemometers

III. Wind Potential Analysis

- Based on site measurements, computer simulations of wind potential analysis was performed in three typical locations in Hungary

IV. Modeling of wind turbine group operations, and analysis of flow modifier effects.

- Modeling of wind turbine farms, based on the analysis of wind potentials
- Modeling the different layouts of wind turbine farms, optimized for various conditions

- We studied the energetical, and hydrodynamic impact of the surface environment changes of the simulation sites, on the wind power electricity generation

V. Creating a database for expert network.

- A database was created, which forms the basis for further simulations with the help of the measurements at locations used for the model experiments
- We have created a base methodology of measurement, analysis and evaluation system which is capable to compare energetical measurements performed at different locations at the same time

VI. Translating research findings into education, curriculum development for the Hungarian and foreign language courses of the topic.

- The research findings have been published in professional journals, national and international scientific conferences, and monographs which
- as a whole, or its parts – expand the knowledge of current basic and specialized higher education of the institution

Acknowledgement

Many thanks to TÁMOP-4.2.1.B-11/2/KMR-2011-0003, „Az oktatás és kutatás színvonalának emelése a Szent István Egyetemen" („Increasing the level of education and research at the Szent Istvan University") project.

References

[1] Beke, J.(2012): Környezet-energetikai K+F (trendek, kihívások). Szaktanárok Továbbképzése, VKSZI, Gödöllő, 2012.12.04.

[2] EMD International A/S (2014): WindPRO Modulbeschreibung, Aalborg EMD International A/S (2014): WindPRO 2.9 Handbuch, Aalborg Gasch, R. (1991): Windkraftanlagen. B.G. Teubner, Stuttgart

[3] Géczi, G. Korzenszki, P. Bense, L. (2013): Ideális körülmények a levegő-víz hőszivattyú uszodatechnikai alkalmazása során. Magyar Épületgépészet, LVII. Évfolyam, 7-8: 7-10. HU ISSN 1215 9913.

[4] G. Géczi, L. Bense, P. Korzenszky (2013): EXAMINATION OF ENERGETIC INDEXES OF AIR TO WATER HEAT PUMP. Bioenergy And Other Renewable Energy Technologies And Systems. 34th International Symposium of the Section IV of CIGR. Cracow, 2013

[5] Korzenszky P. – Géczi G. (2012): Heat pump application in food technology, Risk Factor Food Chain 2012, Topolcany, Szlovákia, 2012. szept. 19.-20., CD. Korzenszky, P. Géczi, G. (2012): HEAT PUMP APPLICATION IN FOOD TECHNOLOGY, Journal of Microbiology, Biotechnology and Food Sciences, 2012, vol 2. p:493-500. ISSN 1338-5178.

[6] N. G. et al. (1993): Wind Atlas Analysis and Application Program, Riso National Laboratory, Roskilde

[7] Schrempf, N. (2013): Szélenergetikai lehetőségek Gyergyószentmiklóson. Megújuló Energiák, Megújuló Kapcsolatok Konferencia, Gyergyószentmiklós
[8] N. Schrempf, L. Tóth (2013): Wind potential calculations on different reliefs.
[9] 3rd Synergy International Conferense, Engineering, Agriculture, Waste

Laboratory examination and modeling of air-water heat pump systems

Gábor BÉRCESI[1], Károly PETRÓCZKI[1], János BEKE[2]
[1]Department of Measurement Technologies, Institute for Process Engineering
[2]Department of Energetics, Institute for Process Engineering

Abstract

Heating and cooling of residential and communal buildings, heat water production, fish farming and pool technology are only some of the many fields where heat pump systems working with different primary energy resources can be applied successfully, economically and environmentally friendly. Because of recognition of this and the continuous growth of energy prices, application of heat pumps is expanding. These thermodynamic machines – producing heat energy from partially renewable energy sources – are using usually electrical energy for transportation of heat from a cooler to a warmer space.

Because of the high costs of an efficient, high power heat pump system that could cover the heat demand of a large building, nowadays application of combined heating and cooling systems using heat pump together with a traditional (fossil) energy source is becoming common. However control of the energetic systems using multiple energy sources can cause difficulties. But by using adequate model-based design principles, higher efficiency climate systems can be operated. As a first step of a research on the climate control system of buildings using heat pumps for heating and cooling we set up a model experiment with an air-water heat pump where we cooled and heated some water and during this process we measured all the important energetic parameters – temperatures, volume flows and electric energy consumption of the system. This allows us to set up an identified mathematical model of heat pump systems that can be applied also in a more complex system model to understand and optimize energetic control systems. This article deals with description and evaluation of these measurements.

Keywords

heat pump, model experiment, metrology, modeling

1. Introduction

Rising amount of built-in heat pump systems and growth of energy prices gives focus on improving efficiency of operation of these systems. This besides decreasing operating costs lowers their CO_2 emission (resulted by electric

energy consumption) therefore increases their environmental protectoral effect. In heating of buildings even the air source heat pumps with a COP value of 1.9 can be more cost effective than oil or even natural gas with much lower green house gas emission, and with avoiding the disadvantages like limited availability of other renewable energy sources such as solar energy utilized by solar collectors. (Forsén, 2005) Heat pumps can be successfully applied also in domestic hot water production – often next to room heating - (Aziz, et al., 2013) and pool technology, where very good COP values (almost five in average) can be reached while tempering water in intermittent operation. (Géczi, et al., 2013a) Another prosperous application is fish farming, where by heating and tempering of fish pools breeding possibility and time can be extended, therefore the productivity can be increased. (Baird, et al., 1993) According to Géczi et al. (2013b) if this heating is solved by heat pumps, even 30% cost saving and 45% CO_2 emission reduction can be achieved compared to the other possible heating solutions (electrical energy, natural gas). Heat pumps in food technology are also very useful, for example in soda water manufacturing water to be bottled can be cooled with them and the extracted heat energy in a higher temperature at the secondary side of heat pump can be used for heating of rooms or producing hot water for washing the bottles. (Korzenszky, Géczi, 2012)

Within these, applications of heat pumps with different primary and secondary fluids (e.g., air-source or ground source heat pumps) in buildings and associated facilities has a particular importance for heating and cooling purposes, often combined with a complex supplementary heating system e.g., by using a solar collector or photovoltaic system. (Tóth, et al., 2011)

At Szent István University in 2012 a new multifunctional educational building, the Knowledge Transfer Centre (TK) was opened that has a heating and cooling system using combined energy sources – ground source heat pump system as primary and natural gas boiler and air source heat pump as supplementary energy source for heating and cooling. This system was equipped with an independent, 38 channel data acquisition system and through this it became available for researches about operating conditions and control of HVAC (Heating Ventilation Air Conditioning) systems utilizing combined energy sources. (Gergely, et al., dátum nélk.) Figure 1 shows the view of the building and the hydraulic schematic of its heating and cooling system.

For control of internal temperature and other climate parameters of buildings there are well algorithms e.g., in terms of the value of set-point: program-controlled, and weather-dependent control can be mentioned. However in buildings using combined energy sources where there are several options to meet the energy needs the control can be more difficult. (Hámori, 2008) Nowadays during the control design of such systems empirical formulas and results of economical calculations are taken into account. Due to continuous change in prices and neglect of other important aspects, like the greatest possible use of renewable sources or minimizing of CO_2 emission it is not a right approach. However use of adequate design solutions allows realization of optimal control functions even by many aspects.

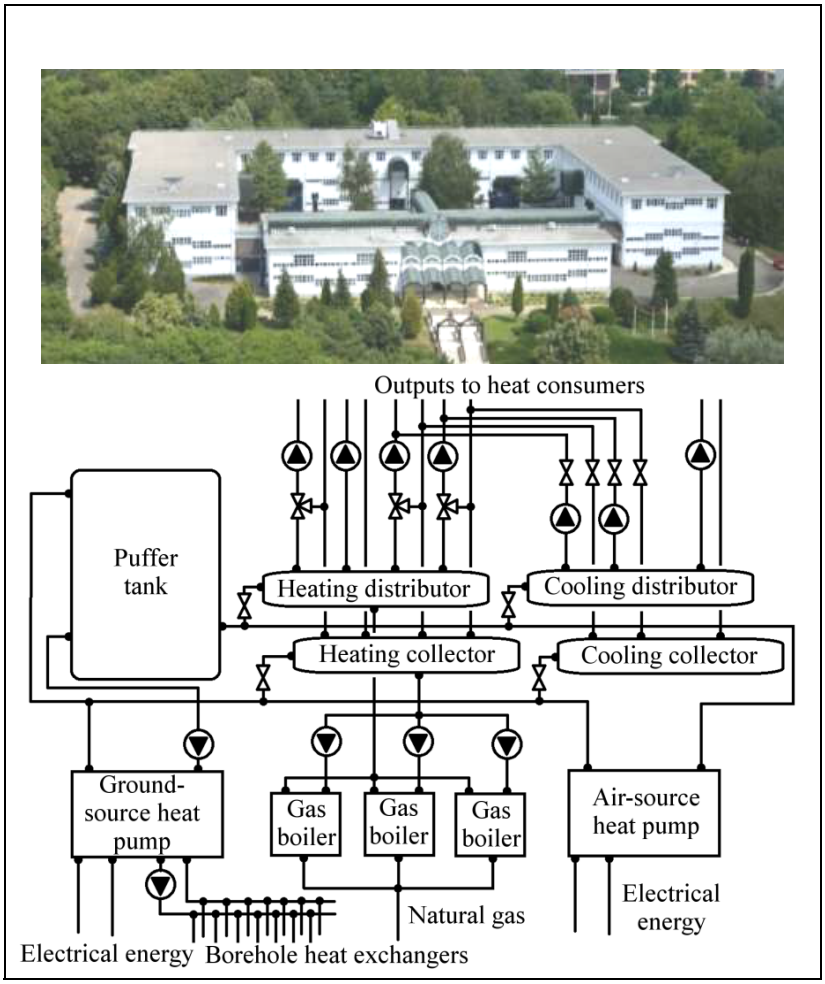

Figure 1. View of Knowledge Transfer Centre and schematics of its HVAC system

For construction of an optimal control the first step is to learn the operation and dynamical behavior of these systems with development of a control model. (Carman, et al., 2010) (Cho, et al., 2010) For this purpose an experimental measuring system was installed which allows separate examination and modeling of heat pump systems and additionally provides an opportunity for analysis of their performance in function of some environmental circumstances.

2. Materials and methods

Materials

The model experiment is based on a Microwell HP 700 type air-source air-water heat pump. There is also a pump with a nominal flow rate of 16 m^3/h, a tank

with 1 m^3 volume, pipelines, valves and measuring instruments. With the installation it is possible to set manually the volume flow through the heat pump using a bypass pipe and valves behind the pump (that provides constant flow-rate). The base of the measuring system was an Almemo 2590-9 type data acquisition system connected to PC. The measuring system was set to 20 s sampling interval. Temperature of ambient air (together with its humidity), temperatures of the input and output water of the heat pump and water in the tank is measured by four pieces of K-type (NiCr-Ni) thermocouples. Measurement of electrical energy consumption is made by an Itron SL7000 type multifunction electrical measuring unit that has an LED indicated pulse output that provides 10 000 pulses/kWh. For measurement of these pulses and detecting them with Almemo system a phototransistor based optical sensor adaptor with a TTL level converter circuit was developed. Voltage and input current was measured separately to make it possible to compute power factor of the heat pump. For measurement of volume flow an Arad WST type flow meter is used which is equipped with a Reed-switch providing one contact as 10 liters of water flows through the pipeline. Since the resolution of the frequency measurement unit of the data acquisition system was insufficient, a simple microcontroller based frequency measuring device was developed to calculate, and display the flow rate and provide a higher frequency signal proportional with flow to the data acquisition system to ensure accurate measurement. Figure 2 shows a picture of the measurement installation and figure 3 shows the hydraulic loop and measured parameters of the experimental measuring system.

Figure 2. View of the experimental measurement installation

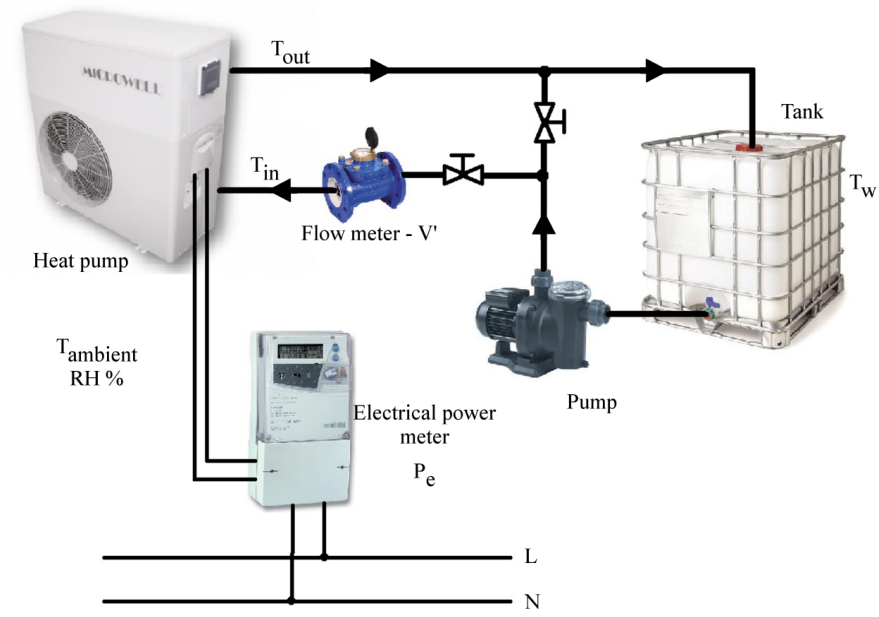

Figure 3. Connections of the measurement assembly

Methods

Heat pumps usually can be used also for heating and cooling. During the experiments the tank of water was heated from about 10°C to 45°C then it was cooled back to 10°C with the heat pump at constant flow-rate. More than 40 heating and cooling cycles were measured at different ambient temperatures from March to June in 2013 and June in 2014.

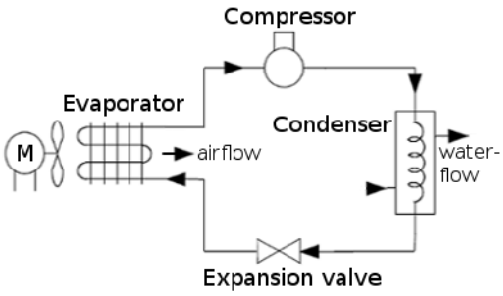

Figure 4. The structure of air-water heat pump

Air-source heat pumps like the one that we used during our examinations are utilizing the heat energy of the ambient air and heat or cool water with that. Operation of the heat pumps is based on a refrigeration cycle of

thermodynamics. In them air is blown through the evaporator heat exchanger where the low pressure working fluid is evaporating. Then the refrigerant is compressed by an electrically driven compressor unit and pressed into another heat exchanger called condenser where the heat energy in a higher temperature is transferred to water. After condensation the fluid flows through a pressure lowering expansion valve and the cycle is closed in the evaporator. Figure 4 shows the structure of air-water heat pump.

One of the most important parameters of heat pumps is coefficient of performance or COP (in some literature signed with ε) value that shows the relation of output heating or cooling power $\left(\dot{Q}_{out}\right)$ and input electric power (P_e):

$$COP = \frac{\left|\dot{Q}_{out}\right|}{P_e} \tag{1}$$

Ideal heat pumps that implement a Carnot-cycle have the highest COP value (COP_C) that depends only on the temperature of the condenser (T_C) and the temperature difference between the condenser and the evaporator (T_C-T_E): (Forsén, 2005)

$$COP_C = \frac{T_C}{T_C - T_e} \tag{2}$$

The efficiency of heat pump η_C – that can be important in case of modeling – shows relation between theoretical maximum COP_C and the calculated COP value based on the measurement data:

$$\eta_C = \frac{COP}{COP_C} \tag{3}$$

Typical value of η_C for air-water heat pumps is between 0.45 and 0.65. (Komlós, et al., 2007)

There are two common ways of modeling heat pump operation. One of them writes the thermodynamic equations of all the four states represented by four main parts of the heat pump. (Badiali, Colombo, 2010) But the simplest one deals only with the energy flows in and out of the system. Figure 5 shows the block diagram of simplified energy flow model of an air-water heat pump where T_a is the ambient air temperature (inlet and outlet) T_w is the water temperature (inlet and outlet), $\dot{m}_a$ and $\dot{m}_w$ are the mass flows of the air and water, c_a and c_w are the specific heat of the air and water, $\dot{Q}_{in}$ is the input heat flow $\dot{Q}_{out}$ is the output heat flow and P_e is the electric power.

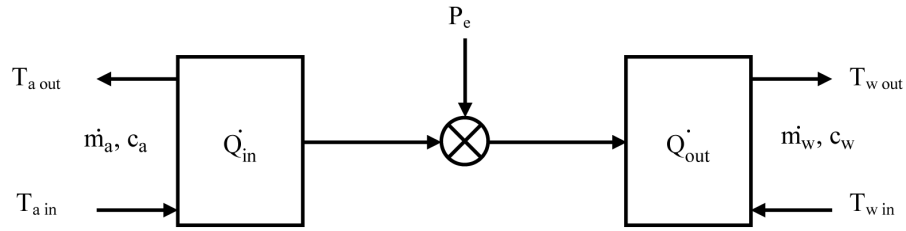

Figure 5. Diagram of simplified heat pump model

The output heat flow:

$$\dot{Q}_{out} = COP \cdot P_e \tag{4}$$

The input heat flow:

$$\dot{Q}_{in} = \dot{Q}_{out} - P_e = \left(COP - 1\right) \cdot P_e \tag{5}$$

The output temperature of air:

$$\dot{T}_{a\,out} = \frac{\dot{m}_a \cdot c_a \cdot \left(T_{a\,in} - T_{a\,out}\right) - \dot{Q}_{in}}{C_a} \tag{6}$$

where: C_a is the heat capacity of ambient air in the heat pump

The output temperature of the water:

$$\dot{T}_{w\,out} = \frac{\dot{m}_w \cdot c_w \cdot \left(T_{w\,in} - T_{w\,out}\right) - \dot{Q}_{out}}{C_w} \tag{7}$$

where: C_w is the heat capacity of heated or cooled water in the heat pump (van Schijndel, de Wit, 2003)

3. Results and discussion

After the measurements a block-oriented solution of the mathematical model described above was prepared in Matlab/Simulink software to validate it with laboratory experiments and identify parameters. Figure 6 shows the Simulink block diagram for solution of (4)-(7) system of equations.

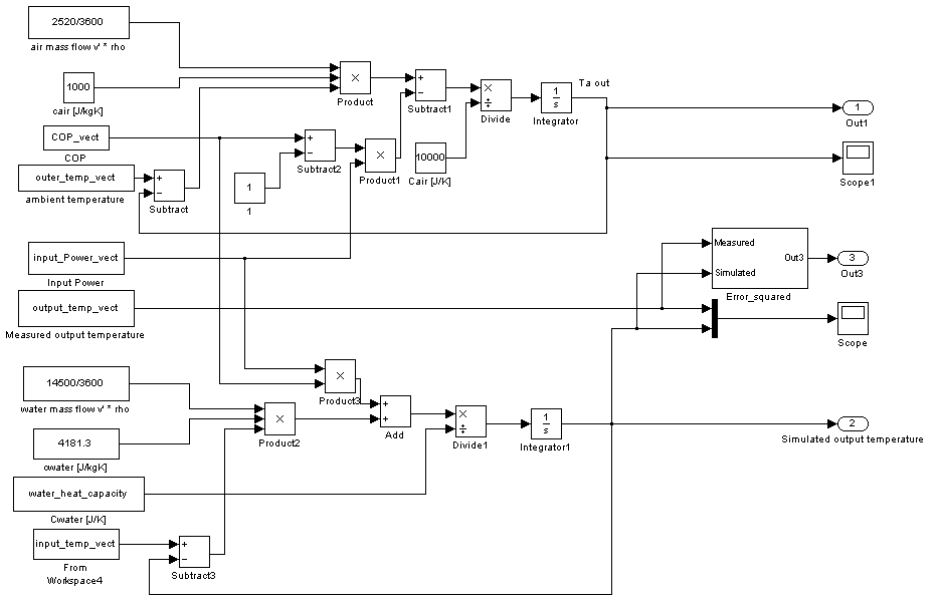

Figure 6. Simulink block diagram of heat pump model

For using the model preparation of measurement data was needed. A Matlab script for data processing was written. It reads the data stored in text file, then computes input (electric) and output power and COP values, finally generates the variables containing time series of data needed by the Simulink model.

About the physical parameters of the heat pump operation only the heat capacities (C_a and C_w) were unknown because flow of water was measured and airflow of the fan was given in operation manual. Therefore the parameter to identify was the heat capacity of water. Since output air temperature was also unknown, heat capacity of air could not be identified.

For identification method of least squares and Matlab's built-in method for minimum search were used. The result shows heat capacity of water is C_w=137 744.8 J/K, which means mass of water in the heat pump computed with c_w=4181.3 J/(kgK):

$$m_w \frac{C_w}{c_w} = \frac{137744.8}{4183.3} = 32.9\,kg \tag{8}$$

After parameter identification validation of model was done with a full heating cycle where water was heated from 14°C to 46 °C at the 14.5 m^3/h water flow and 2520 m^3/h airflow. Result of the validation is presented on Figure 7 where fit of measured and simulated (computed) value of output water temperature can be seen. The average value of absolute error between the measured and computed values is 0,018 °C that is lower than the resolution of the measuring instrument.

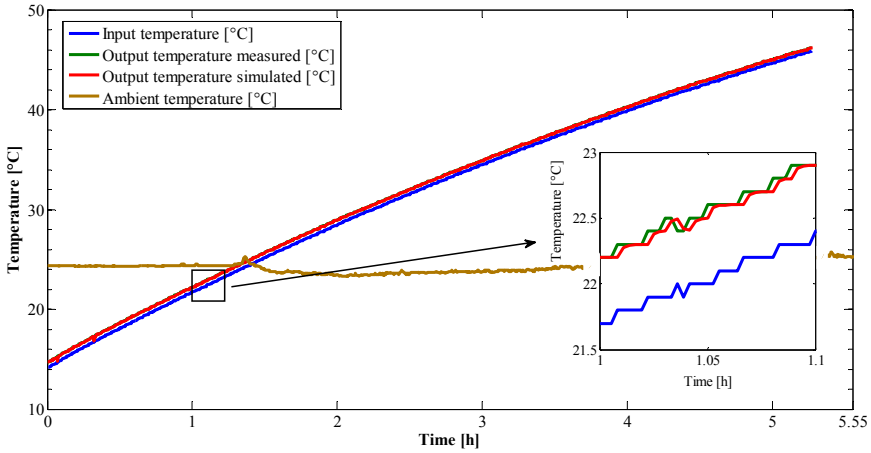

Figure 7. Result of the model validation at a heating cycle of the heat pump

Conclusions

As a result we verified that using the presented simple model, after identification, heat output and main operational characteristics of heat pumps can be determined accurately.

This model can be used to examine operation of heat pumps in extremist circumstances, like winter temperature conditions.

The general model can be applied not only for air-water heat pumps but also for other (e.g. ground-source) types. It provides enough information to use in a model for control purposes so the two heat pumps of the HVAC system presented in Introduction and Figure 1 can now be described mathematically. This brings us closer to the description of the entire system and helps development of the general method of specification and control optimization of building energetic systems.

Additionally the built up model experiment is applicable for laboratory testing and comparison of different types of low power heat pumps for residential use.

Following the investigations we supplemented the installation with a closed loop control system controlling the water temperature in tank that allows us to perform static tests also.

Another possible direction of further research using the built-up system is examining the COP and efficiency of different heat pumps as a function of ambient parameters.

References

[1] Aziz, M. A. A., Mat, S. and Sopian, K. (2013): Technology Review of Solar Assisted Heat Pump System for Hot Water Production. Latest Trends in Renewable Energy and Environmental Informatics, pp. 65 - 75.

[2] Badiali, S., Colombo, S. (2010): Dynamic modeling of mechanical heat pumps for comfort heating (MSc thesis), Stockholm, Sweden: KTH Royal Institute of Technology, 78p.
[3] Baird, C. D., Bucklin, R. A., Watson, C. A. and Chapman, F. A. (1993): Heat Pump for Heating and Cooling Water for Aquacultural Production. University of Florida - Circular 1096, pp. 1 - 4.
[4] Carman, S., Barbu, M., Minzu, V., Badea, N., Ceanga, E. (2010): Modeling and control of an autonomous energetic system obtained through trigeneration. Bal. Inst. Polit. Iaşi, 56-60 (4), pp. 61-72
[5] Cho, H., Luck, R., Eksioglu, S. D., Chamra, L. M. (2010): Cost-optimized real-time operation of CHP systems. Energy and Buildings, 41(4), pp. 445-451
[6] Forsén, M. (2005): Heat Pumps Technology and Environmental Impact, Stockholm, Sweden: Swedish Heat Pump Association, 120 p.
[7] Géczi, G., Korzenszky, P., Bense, L. (2013): Ideális körülmények a levegő-víz hőszivattyú uszodatechnikai alkalmazása során. Magyar Épületgépészet 62 (7-8), pp. 1 - 4
[8] Géczi, G., Korzenszky, P., Tamás, Sz., Bense, L., Urbányi, B. (2013): Possibility of air-to-water heat pump application in the intensive recirculationg fish farming system, ANIMAL WELFARE - ETOLÓGIA ÉS TARTÁSTECHNOLÓGIA 3(9), pp. 139-146
[9] Gergely, Z., Tóth, L., Petróczki, K. and Bércesi, G. (2013): Renewable Energy Assisted Air Conditioning System Instrumentation. HUNGARIAN AGRICULTURAL ENGINEERING 25, pp. 13 - 16
[10] Hámori, S. (2008): Épületgépészeti irányítástechnika. Debrecen, 119 p.
[11] Komlós, F., Fodor, Z., Kapros, Z, Vajda, J., Vaszil, L. (2007): Hőszivattyúzás. Budapest: Energia Központ Kht., 78 p.
[12] Korzenszky, P. and Géczi, G. (2012): Heat Pump Application in Food Technology. Journal of Microbiology, Biotechnology and Food Sciences 2 (2), pp. 493 - 500.
[13] Maaien, H. N. and Vissers, D. R. (2011): Sustainable Building and Service Modeling. Eindhoven, Netherlands: University of Technology, Eindhoven, 20p.
[14] Tóth, L., Slihte, S., Ádám, B., Petróczki, K., Korzenszky, P., Gergely, Z. (2011): Solar Assisted Ground Source Heat Pump System, HUNGARIAN AGRICULTURAL ENGINEERING 23, pp. 57 - 61
[15] van Schijndel, A. W. M. and de Wit, M. H. (2003): Advanced simulation of building systems and control with simulink. Eindhoven, Netherlands, Eighth Inernational IBPSA Conference, University of Technology, Eindhoven, pp. 1185 - 1192

Analysis of interaction of towed vehicles and road profile

László GURMAI, Péter KISS
Department of Automotive Technology, Institute of Process Engineering

Abstract

The qualities of the different road profiles highly influence the life span of the vehicles using them. The more uneven a stretch of road is, the greater the damaging effect. The aim of the research was to develop a comparative method that makes possible to compare the vibration generating effects of different road profiles. Using the comparative method a testing system was developed that is suitable to conduct accelerated fatigue tests that generate failures occurring under real working conditions.

Keywords

power spectral density, fatigue test, root mean square, vehicle damaging effects of road profiles

1. Introduction

In many cases fatigue tests of terrain vehicles resulted in malfunctions which were different from failures appearing in real terrain conditions. This can be due to the fact that the testing methods used so far have not been accurate enough in modeling the forces acting on vehicles under real conditions. In order to identify the damaging forces acting on terrain towed vehicles, first a comparative method of general use need to be developed. The use of this method opens up a possibility to develop a Fatigue Testing Method that is closer to real life forces.
During the research, a number of issues emerged, where the solution required carrying out series of measurements. One of these questions was how to compare the destructive effects of two different stochastic road profiles, and how to compare the extent of the damaging effects of two fatigue tests. According to the research objective I search answers to these questions.

2. Vehicle-Ground Relationship

The examination of the behavior of off-road vehicles, including towed vehicles belongs within the field of the theory of off-road vehicles. Of the four models of rolling wheel-track relations, the „deforming wheel on deforming surface”

model was identified as the most effective approach for examining forces acting on off-road towed vehicles according to Kiss and Laib (1999).
Terrain towed vehicles are exposed to stochastically distributed forces. These forces derive from both the random motion of the towed vehicle and from the roughness of the terrain profile, as Gedeon (1993) and Abarbanel (1996) have formulated it.

Excited by the towing vehicle and by unforeseeable factors (G_x) resulting from terrain profile the vehicle starts vibrating, which results in forces damaging its structure. The question of the thus resulting vibration was studied by Nguyen (2011) during field tests. Thus, the vehicle damaging forces depend on the degree of excitation and the vehicle structure, that is, on the transfer function (H (f)). Based on Sitkei (1986)'s description the extent of response function (G_y) measured on the vehicle depends the vehicle speed, weight, and the mechanical properties of the terrain profile. The vehicle-ground relationship is illustrated in the following figure 1, where the stochastic excitation of a linear oscillating system with a single degree of freedom and its transmission and response functions are shown.

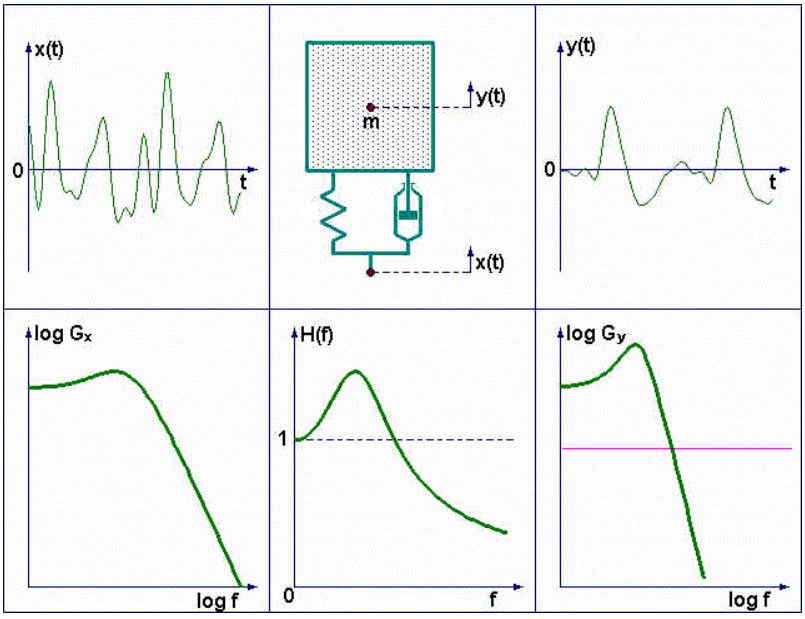

Figure 1. Excitation of a linear oscillating system with a single degree of freedom

In case of a vehicle and a road profile, the relationship is much more complex, since each wheel of the vehicle gets a separate excitation from the ground, and in case of towed vehicles the towing vehicle is exciting the examined structure. So it is appropriate to handle the power spectral density function of the vehicle terrain profile and the transmission characteristics in a matrix. The response

function ($\overline{\overline{G}}_{yy}(f)$) of the vehicle given to the spectral density function of the road profile ($\overline{\overline{G}}_{xx}(f)$) can be described by the following equation in matrix form:

$$\overline{\overline{G}}_{yy}(f) = \overline{\overline{H}}_{xy}(f)\overline{\overline{G}}_{xx}(f)\overline{\overline{H}}^{T}_{yx}(f) \tag{1}$$

where:

$\overline{\overline{G}}_{yy}(f)$: is the power spectral density matrix of the excited oscillating system [m^2s];

$\overline{\overline{H}}_{xy}(f)$: is the transmission frequency function matrix of the oscillating system [-];

$\overline{\overline{G}}_{xx}(f)$: is the power spectral density matrix of the terrain profile [m^2s].

Due to the complexity of the described relation it is appropriate to determine the calculations using computer simulations.

According to Márialigeti's study (1994) about terrain profiles it can be stated that in general in case of profiles registered in a sufficiently large number of samples, the values obtained are of stationary and ergodic characteristics, so they can be described as stochastic statistics process. Terrain profiles showing stochastic nature can be made comparable based on a power spectral density function (PSD) and the size and distribution of their micro-and macro barriers. About the application of PSD functions in engineering practice in the book of Bendat et al. (1980) an adequate description can be found.

The stochastic distribution of the terrain profiles can be characterized with the help of a power spectral density function (G (n) using random variables. The PSD functions are formally identical to the Fourier transform of the correlation which can be defined by the equation:

$$G(n) = \lim_{L\to\infty}\frac{1}{2L}\left(\int_{-L}^{L}\left(\left|\xi(x)e^{-jnx}\right|\right)dx\right)^2 \tag{2}$$

where:

L: sampling length [m]; $\xi(x)$: random variable of the road profile in vertical direction [m]

With the determination of the PSD function of the road profiles, the power spectral density of each wavelength value becomes comparable. However, this is not sufficient to compare the vibrations generating effect of two profiles of identical length. A new method had to be developed for the comparison of vehicles damaging effect of different road profiles, using the power density functions.

3. Material and Methods

To achieve the objective, the realization of the following tasks was required. The first step was to determine the mechanical and vibrational properties of the observed vehicle which makes the system, or in other terms, the transfer function determinable. After that with a series of measurements the extent of the devastating impact of the different stochastic and built obstacle systems could be determined, which is described by the response function of the structure given as a reaction to the excitation.

Measurement of the terrain's effects was carried out on a single axle, semi suspended structure, i.e. the header trailer. The trailer without overrun brakes, built to transport headers is mostly used on agricultural dirt tracks under normal operational conditions. A particular feature of the structure is that it contains no separate shock absorbers apart from its rubber tyres. The load of the trailer for the measurements was a purpose-built dummy header (Figure 2.) which - in terms of its mass and center of gravity - is equivalent to an 8 row corn header. Thanks to the construction of the structure, it is also suitable for modeling various load conditions by loading or unloading concrete blocks used as auxiliary weights.

Figure 2. SHERPA BG3 type trailer and CONSPEED 8 row DUMMY header

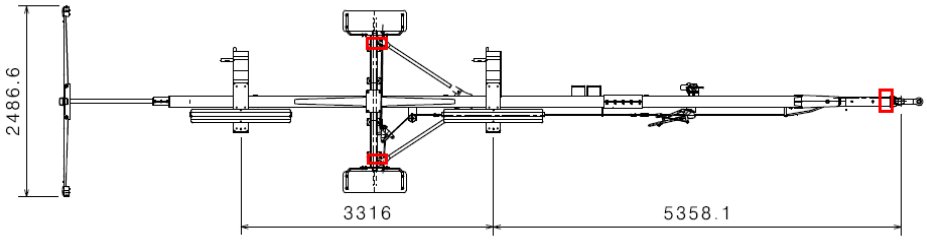

Figure 3: Single axle header trailer acceleration sensor measurement points

Acceleration sensors were placed on the trailer at the locations indicated in Figure 3. to measure the dynamic effects it is subjected to. The instruments sensed the vibrations of the trailer via piezoelectric means and forwarded the signals detected to the measurement data collection unit.

The measurement sequence is made up of four distinct phases. Measurement of the trailer's ability to overcome terrain obstructions, the coordinates of the trailer's centre of gravity and its vibrational characteristics took place in the first phase. The vehicle's own frequency as well as the spring characteristics of the tyres were also determined.

The second series of measurements focused on obtaining measurement data in realistic operational scenarios on five different types of roads. The first towing measurement sequence took place on a good quality paved road, followed by a bad quality paved road selected for this purpose. The other towing measurements were taken on three agricultural dirt tracks of varying soil types. Separate measurements were taken on sandy, clay-based and coarse gravel roads. The road profile was also recorded for every road section tested.

In the third phase of the measurements the two different accelerated fatigue tests were compared. One of the test methods was fatigue testing on the roller test bench and the other was the circular test track.

In the fourth phase of the measurement series, combinations of artificial obstacles were tested. The aim of this sequence of measurements was to test the effects of the various artificial terrain obstacles.

4. Measurement Devices

Upon measuring the vibration acceleration of the vehicle towed on terrain, PCB Piezotronics triaxial MEMS DC 200 mv/g 10 g acceleration sensors were used. Data were then collected using a Höttinger Spider 8 type data collection unit. The road profiles were registered using levelling devices functioning by the principle of communicating vessels, with the help of which the profile data were collected in increments of 100 mm. The soil's mechanical parameters were determined using a Farnell penetrometer and a GEONOR H60 hand-held shear vane tester.

The vibration accelerations registered during towing were evaluated using the DIAdem programme. The Origin programme was used for the further analysis of the data and the evaluation of the parametric equations. The determination of the power spectral density (PSD) of the road profiles was carried out using the ProVAL programme. The ADAMS programme was used to create the dynamic model of the trailer and to simulate the movements.

5. Results

The method, developed for the comparison of vehicle damaging effects of stochastic road profiles, can be determined with the use of power spectral density

functions based on profile data of micro obstacles. In Figure 4. the power spectral density is presented, based on the values of different types of road profiles.

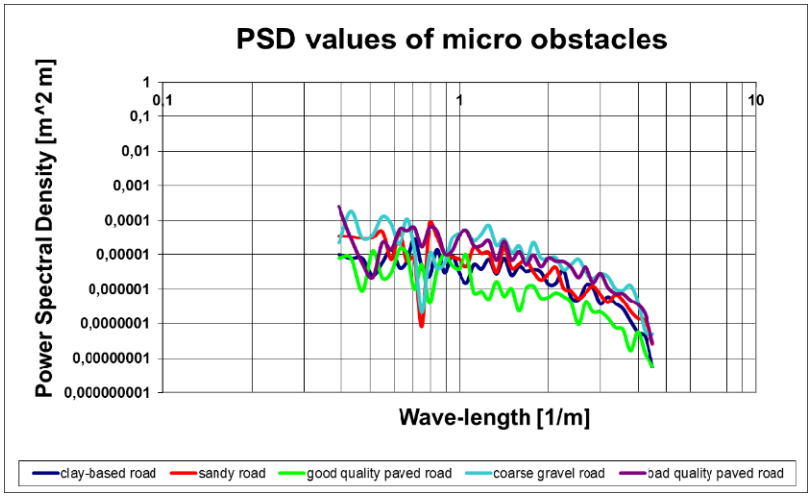

Figure 4. PSD curve of the micro obstacle system of off-road road types

Pursuant to the use of power spectral density (PSD), with the help of a so called space-time conversion, the vehicle exciting frequency spectrum of the road profile can be defined. By the determination of the area under the PSD function curve (TG), the frequency excitation effect of road profiles, in case of road profiles of the same length value, should be comparable. Using this method, the frequency excitation effects of road profiles can be clearly characterized and grouped. Figure 5. shows the previously presented PSD curves.

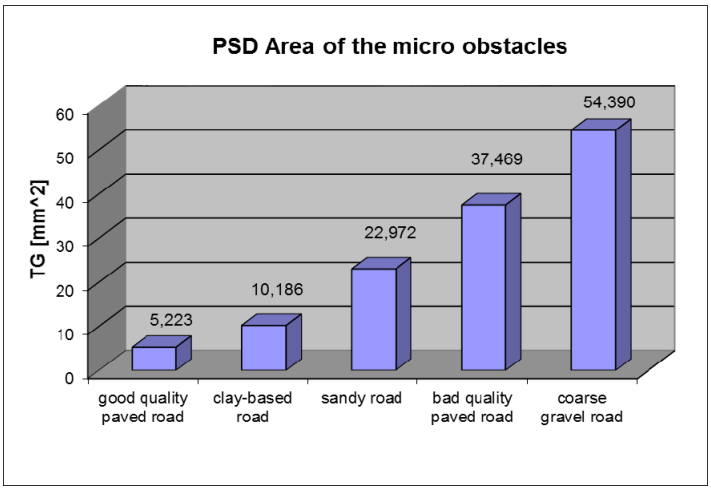

Figure 5. Areas of the PSD curve of the micro obstacle system of off-road road types

The figure clearly shows that good quality asphalt road has the least, while the gravel pebble road the greatest vehicle disruptive effect.

Our results, based on the profile data, are proved and checked by a series of measurements on a towed test vehicle. On the tested road profiles and at different towing speeds, The vibrations of the passing test vehicle were registered, which values are proportional to the vehicle devastating effect. Based on the root mean square values of the acceleration values, the different types of road were ranked and are demonstrated in Figure 6.

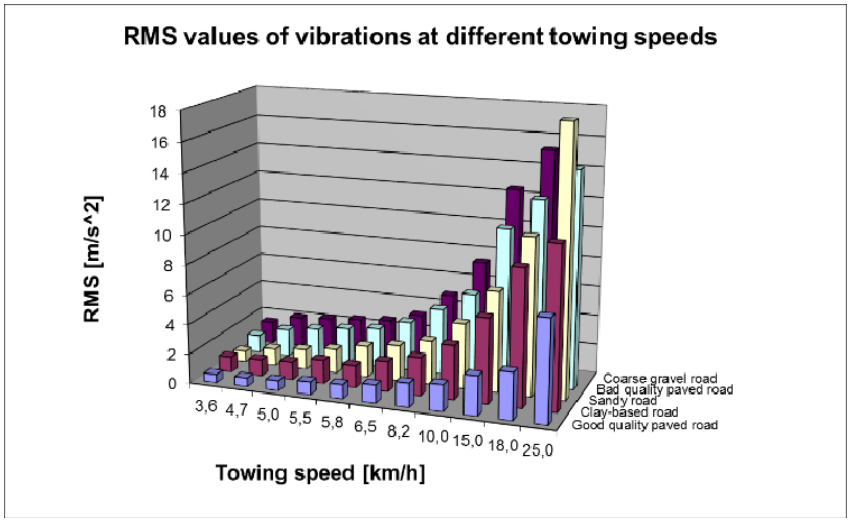

Figure 6. RMS values of the vibrations of off-road road types at different towing speeds

Comparing the two diagrams it is clearly shown that in both cases, independently of the towing speed, the same road type sequence has emerged. This means that the method used for the comparative analysis of terrain profiles is suitable.

6. Determining the transfer function of the towed vehicle

The response function of a towed vehicle for excitation depends on the vibrational behavior of the vehicle. The dynamic model of a vehicle includes the weight, centre of gravity, the number and kind of flexibility and shock-absorbing elements of the structure. To determine these values measurements were required. To determine the characteristic angular frequency and the parameters that influence it, the tire spring characteristics of the vehicle had to be examined at different tire pressures. After that the damped period of oscillation of the structure had to be measured on the basis of different loads and different spring characteristic settings. In Figure 7. characteristic angular frequency features are

shown characteristic for the test vehicle in case of different axle loads and spring characteristics.

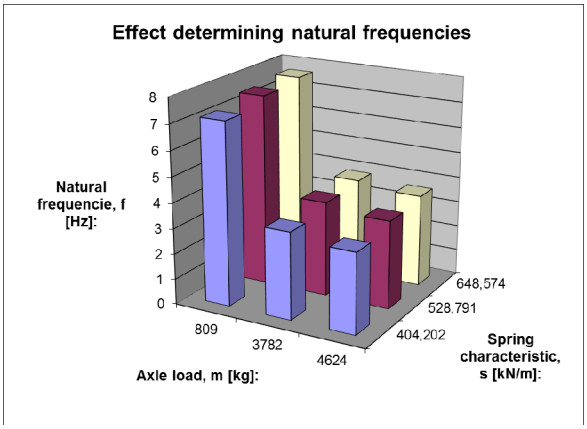

Figure 7. A comparison of the effects on the natural frequencies of the towed vehicle

Using the dynamics characteristics and the geometry data of the towed vehicle the dynamic computer model of the test vehicle was made. As a result of the motion simulation with the model, the transmission factor characteristic of the structure could be determined, for different excitation frequencies. Based on the resulting transmission factor values, characteristic angular frequency, characteristics of the structure was determined. A typical transfer function of the towed vehicle is shown in Figure 8.

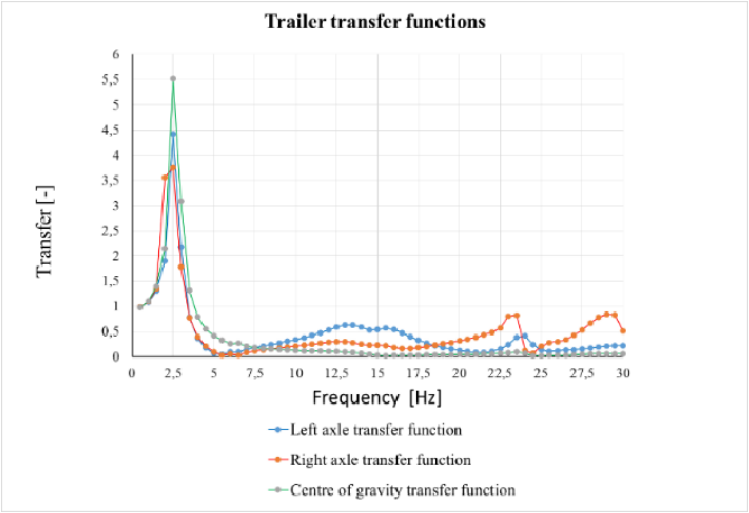

Figure 8. Transfer function between the profile excitation and the center of gravity of the towed vehicle

7. Methods for measuring destructive effects

Based on vibration amplitude values measured on vehicles, a method has been developed for comparing the destructive effects of artificial (deterministic) and off-road (stochastic) road types. With the use of this method, the vibration excitation effect of various types of road can be compared based on the root mean square value (RMS) of vibrations registered on the test vehicle. The method can be applied under one condition, that is, by measuring the excitation effect; values of all profiles must be recorded with the same test vehicle.
Figure 9. clearly shows how the RMS values of the vertical vibrations measured on the vehicle vary in case of different road types due to the increasing towing speed of the vehicle-

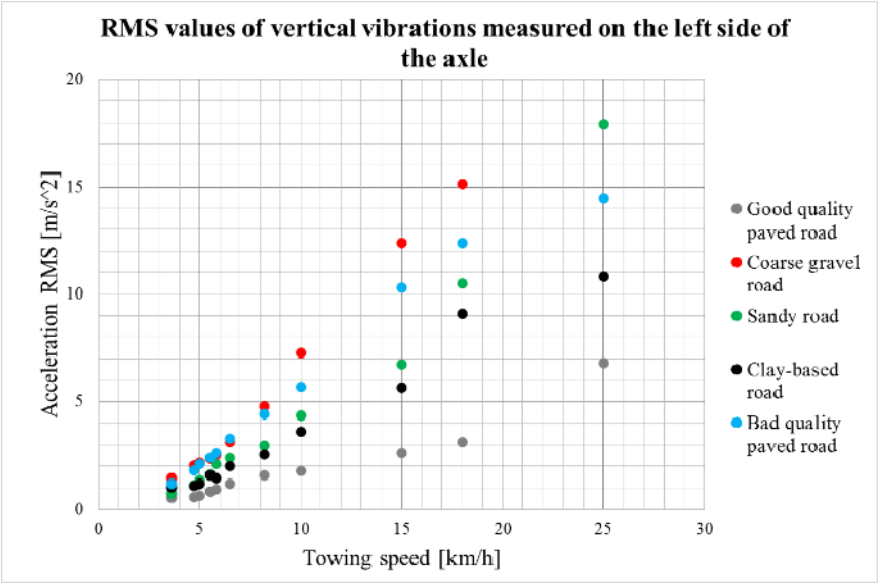

Figure 9. RMS values of vertical vibrations measured on the left side of the axle

Vibration values resulting from terrain profiles had to be examined in the frequency amplitude range as well. Using the FFT (Fast Fourier Transformation), the response function of the system can be determined. The spectral analysis of the values measured on a pebble-gravel road is shown in Figure 10.

Based on the chart it can be stated that the curves belonging to different towing speeds envelop each other and in spite of the increasing amplitude, the characteristic frequency ranges of the system are not changed. It suggests that the destructive effects of road profiles on vehicles can primarily be compared on the basis of vibration amplitudes, more accurately on their RMS values.

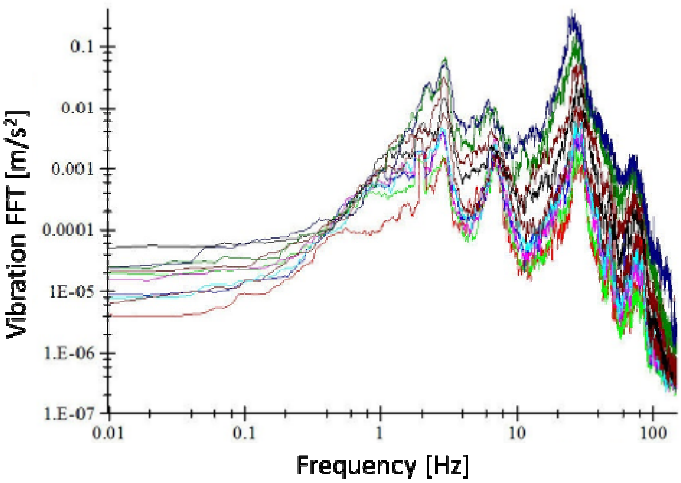

Figure 10. FFT analysis of the vertical vibrations measured on the left side of the axle on a pebble-gravel road by varying towing speeds

8. Development of fatigue test methods of vehicles

Figure 11. Obstacle Calibration Measurement in Törökszentmiklós, at the site of CLAAS Hungaria Kft.

Based on our knowledge of the comparative method of terrain profiles, a procedure was created, applicable for fatigue tests which ensures that the tested structures are, in all cases, loaded according to the appropriate load collective appropriate for the vehicles. In the case of the methods previously used for the validation of vehicles the vehicle damaging effect caused by the excitatory effect due to the same terrain obstacles. During the tests, the excitation of the road profile is the same in all cases, but the loads on the vehicles are different due to the transmission factors specific to the vehicle structure. In that unfavorable case when the natural frequency range of the vehicle is close to that of the standardized frequency of excitation, the structure is to bear much larger loads then the one fatigued on a road profile, having its own natural frequency in a different range. The developed fatigue test method, which is based on vibration

values measured under the actual operating conditions (Figure 11.), is suitable to overcome this problem. The substance of the method is that an obstacle system must be built that causes similar vibration results as those measured under actual field conditions. With that provision, extreme vibrations caused by excitations near the natural frequencies can be avoided.

Conclusion

In summary, several series of measurements were conducted during this research, where the results contain solution for both in the Theory of Off-Road Vehicles and for the validation of vehicles. A general method was developed for the comparability of stochastic road profiles based on the destructive effects of a micro obstacle system for vehicles. In addition, a new method has been introduced to compare the vehicle excitation effect of artificial terrain obstacle systems. Finally, the development of an examination procedure for fatigue test of vehicles has been implemented.

Based on the developed methods, in practice, more reliable, more adequate fatigue test systems can be created based on the loads under normal operating conditions. As a result, the examined structures will be more precisely dimensionable due to the corresponding load levels. Based on fatigue tests according to the new procedure, less off-road vehicles are expected to be produced that are under-or over-dimensioned due to improper validation procedures.

References

[1] Abarbanel, H.D.I. (1996): Analysis of Observed Chaotic Data, *Springer*, New York

[2] Bendat, J.S., Piersol, A.G. (1980): Engineering Applications of Correlation and Spectral Analysis Wiley-Interscience, New York.

[3] Gedeon J. (1993): On some basic problems of stochastic modelling. *Periodica Polytechnika Transportation Engineering*, 21 (1) pp. 89-100

[4] Kiss, P. Laib L. (1999): (In Hungarian: Terepjáró járművek mozgásának vizsgálata deformálódó talajon) Examination of Movement of Off-road Vehicles on Deformable terrain. *Járművek* 46. évfolyam, 4. szám pp. 32-38

[5] Márialigeti, J. (1994): (In Hunarian: Géptervezés) Machine Design I.. Budapesti Műszaki és Gazdaságtudományi Egyetem, Budapest, Terhelés-analízi fejezet

[6] Nguyen V. N., Inaba, S. (2011): Effects of tire inflation pressure and tractor velocity on dynamic wheel load and rear axle vibrations, Saga University, Japan, Journal of Terramechanics pp. 48 3-16

[7] Sitkei Gy. (1986): (In Hungarian: Mezőgazdasági és erdészeti járművek modellezése) Modeling Agricultural and Forestry Vehicles, Budapest: Akadémiai Kiadó.

Institute for Environmental Engineering Systems

Professor Dr. István FARKAS
Director of the Institute

Dear Reader,

The Institute for Environmental Engineering Systems consists of two departments as Department of Environmental and Building Engineering and Department of Physics and Process Control.

Form the results of the current research activity the following topics are selected out to publish in the recent issues of the Journal:

Application possibilities of mono- and polycrystalline silicon technologies:

- This research has been carried out with the Brazilian partners. It aims at to sizing the grid-connected PV systems for five important cities in Brazil which cover the 5 regions. Two different PV technologies, mono- and polycrystalline silicon were applied. For the sizing the Sunny Design online software was used. The monocrystalline silicon modules showed the highest efficiency of energy production.

Spectral dependence of different PV module technologies:

- In this paper the seasonal change of difference in the power of the PV subsystems were discussed along with its possible reasons. It has been observed that the radiation spectrum is changing during the day, and it depends on the clouds as well. A linear correlation has been found between the rate of the specific energy production of the polycrystalline and amorphous silicon subsystems, and the rate of the shortwave visible range in the irradiation.

Fractal analysis of air bubbles in frozen waters:

- In this study examination and comparison of the physical properties of the water samples (spring, well, tap and rain) from Gödöllő area are analysed. During the freezing of the water samples, the air bubbles from the water trapped in the ice. The formed patterns are unique, but observed source-specific characteristics.

Relevance of Riccati's equation in general symmetry theory of propagation phenomena:

- In this paper it has been studied the presence and crucial role of the Riccati-type differential equation is indicated in the cases of wave-, turbulence- and convection-diffusion processes. Novel-type solution formula is proposed for simultaneous convection and diffusion processes taking place in porous media.

Professor Dr. István FARKAS
Director

Relevance of the Riccati's differential equation in general symmetry theory of propagation phenomena in macroscopic dissipative continua

Csaba MÉSZÁROS[1], István FARKAS[1], Klaus GOTTSCHALK[2], Ágnes BÁLINT[3]
[1]Department of Physics and Process Control,
Institute for Environmental Engineering Systems,
[2]Leibniz-Institut für Agrartechnik (ATB)
Dept. of Post- Harvest Technology, Potsdam-Bornim, Germany
[3]Institute of Environmental Engineering, Óbuda University,Budapest,

Abstract

The presence and crucial role of the Riccati-type differential equation is indicated in the cases of wave-, turbulence- and convection-diffusion processes. Novel-type solution formula is proposed for simultaneous convection and diffusion processes taking place in porous media. Finally, the integrating factor functions of the Riccati-type ordinary differential equation are derived for all the cases of importance discussed previously.

Keywords

convection, convection-diffusion, turbulence, Riccati-type ordinary differential equation, incommensurate systems

1. Introduction

In this introductory part we would like to point out relevance of the Riccati-type ordinary differential equation (ODE) in certain well-elaborated areas of fluid dynamics, where it is present for decades, but some of its basic symmetry properties have not been applied in detail. In their detailed study about basic structural properties of one-dimensional chains (including structural changes and collective excitations in chains of molecules), [Sagdeev et al., 1988] concluded, that such one-dimensional systems are useful at studies of stationary turbulence phenomena, too. The concept of broken symmetries at creations of turbulent flow and Rayleigh-Bénard instabilities [Tribelskii, 1997] has also been known for decades, including the application of Lie-type point group-symmetries applied in approximate sense [Zhang and Qu, 2006]. The incommensurate character is relevant for both turbulent flow (whose different harmonics have generally incommensurate frequencies [Landau and Lifshitz, 2000]) and modulated crystals, with two-, or more translationally invariant subsystems, having incommensurate elementary periods, too e.g. [Izyumov and Syromyatnikov, 2013], [Vuković et al.,

1996], [Kirschner and Mészáros, 2001]. Besides, it was possible [Gyarmati, 1970] to derive – among others - the Navier-Stokes equation on the base of the so-called Governing Principle of Dissipative Processes (GPDP), which even nowadays represents one of the most frequently applied general variational principles related to thermodynamics of macroscopic dissipative continua e.g. [Martyushev and Seleznev, 2006], [Merker and Krüger, 2013]. Paricularly, a detailed modelling of the basic Bénard convection problem was also realized by use of this principle [Singh, 1976], despite of the fact, that its underlying mathematical structure expressed essentially by the entropy production function could have been refined further by use of the representation theory of continuous groups [Mészáros et al., 2014]. It is also known from the basic variational calculus e.g. [Gelfand and Fomin, 1963], [Blanchard and Brüning, 1982] that by second variation of a given functional connected to sufficient condition of the existence of extrema, a Riccati-type ODE can be derived (or a more general variant of its, given in matrix form). The second variation has not been applied in the case of GPDP, despite of the fact, that Riccati´s ODE appears very frequently at different problems in continuum mechanics, as it is illustrated below.

2. Detailed examples

Surface waves

The elastic surface waves (i.e. Rayleigh-type waves) may be represented by solutions of a wave equation. Let u be a component of the longitudinal or transversal deformation vector and c_l is the relevant longitudinal or transversal velocity. If we use a usual rectangular coordinate-system and assume, that the continuous elastic medium fills the infinite half-space $z < 0$, the travelling waves propagating into x-direction can be given by the expression

$$u = f(z) \cdot e^{i(kx - \omega t)}, \tag{1}$$

whose insertion into wave equation gives [Landau and Lifshitz, 1999] directly:

$$\frac{d^2 f}{dz^2} = \left(k^2 - \frac{\omega^2}{c_l^2} \right) f. \tag{2}$$

Another well-known example from continuum mechanics [Landau and Lifshitz, 2000] is related to propagation of gravity waves on the free fluid surfaces. They form is (the meaning of symbols is analogous to those used at the calculation procedure leading to (2)):

$$\frac{d^2 f}{dz^2} - k^2 f = 0, \tag{3}$$

i.e. (2) and (3) are linearized Riccati-type ODEs (the linearization method is described briefly in the first part of the Appendix, too).

Turbulent flow

In the present sub-section the relevance of the Riccati's ODE for describing of some basic features of the turbulent flow will be demonstrated within frame of the classical Landau-Hopf theory [Landau and Lifshitz, 2000], [Hopf, 1948]. Accordingly, if we apply the original Navier-Sokes' equations:

$$\frac{\partial \vec{v}}{\partial t} + (\vec{v} \cdot \nabla)\vec{v} = -\frac{\nabla p}{\rho} + \frac{\eta}{\rho}\nabla^2 \vec{v}, \nabla \cdot \vec{v} = 0, \tag{4}$$

by a suitable decomposition of the velocity function we may write directly: $\vec{\mathrm{v}}(\vec{\mathrm{r}},\mathrm{t}) = \vec{\mathrm{v}}_0(\vec{\mathrm{r}}) + \vec{\mathrm{v}}_1(\vec{\mathrm{r}},\mathrm{t})$ ($\vec{\mathrm{v}}_0(\vec{\mathrm{r}})$ is the stationary velocity field function, $\vec{\mathrm{v}}_1(\vec{\mathrm{r}},\mathrm{t})$ is the nonstationary velocity contribution, whose higher order terms may be neglected; analogous decomposition is valid for the pressure *p*, too). The general solution form of the nonstationary component is $\vec{\mathrm{v}}_1(\vec{\mathrm{r}},\mathrm{t}) = \vec{\mathrm{f}}(\vec{\mathrm{r}}) \cdot \mathrm{A}(\mathrm{t}) \equiv \vec{\mathrm{f}}(\vec{\mathrm{r}}) \cdot \mathrm{e}^{\gamma_1 \mathrm{t}} \cdot \mathrm{e}^{-\mathrm{i}\omega_1 \mathrm{t}}$, where the absolute value of the amplitude function obeys the following - type ODE [Landau and Lifshitz, 2000]:

$$\frac{\mathrm{d}}{\mathrm{dt}}|\mathrm{A}|^2 = 2\gamma_1|\mathrm{A}|^2 - \alpha|\mathrm{A}|^4, \tag{5}$$

with the constant α, which may take both positive and negative values. Although it is rarely emphasized, this ODE is also of Riccati-type in its "initial", nonlinear form with $|A|^2 (\equiv y)$ as a function to be determined and in the case of this basic-type description of appearance of the turbulent flow, the time is the independent variable instead of spatial coordinate like in (2) and (3). It is a crucial fact, that frequencies $\omega_j \ (j = 1,2,...)$ belonging to different harmonics are generally *incommensurate*. This basic, initial description has also served as a root for further well-known, refined models of turbulence (e.g. Ruelle-Takens scenario) formulated mathematically as instability of quasi-periodic motions on the 3D-torus [Landau and Lifshitz, 2000].

Simultaneous convection-diffusion processes through porous media

Since mathematical modeling of convection-diffusion processes is of importance from the point of view of both fundamental researches and solving of engineering problems, too [Pascal, 1996], [Kirschner et al., 2004], [Kirschner et al., 2007], [Mészáros and Bálint, 2011] developing of new and more accurate models of this problem represents a permanent task, whose complexity is reflected in the nonlinear character of the ODEs and partial differential equations (PDEs) to be solved. The basic PDE for the convection-diffusion problem is e.g. [Elwakil et al., 2004]:

$$\frac{\partial c}{\partial t} - \nabla \cdot \left(D(c) \nabla c \right) + \frac{dK}{dc} \cdot \frac{\partial c}{\partial z} = 0, \tag{6}$$

where $c = c(\vec{r}, t)$ denotes the concentration distribution function to be determined, $D = D(c, T, ...)$ is the usually: thermodynamic state-dependent diffusion coefficient and $K = K(c)$ is the concentration-dependent hydraulic conductivity coefficient and z-axis corresponds to the direction of the gravitational acceleration. The solutions of PDEs of type (6) may be sometimes even of solitonic type [Elwakil et al., 2004]. Solitons (for a detailed and accurate presentation of this topic see e.g. [Conte and Musette, 2008]) may exist due to balance between dispersion effects, which try to expand the initial localized wave packet, and the effects formally characterized by nonlinearities trying to localize it. By a detailed analysis of these opposite effects, Fan [Fan, 2000] proposed a general method for solving the relevant nonlinear PDEs. Accordingly, the linear term of highest order must be balanced with the nonlinear terms in the initial PDE to be solved. Then, if we represent the solutions by use of D'Alembert-type independent variables: $\zeta = x - v \cdot t (v = const.) \Rightarrow c = c(\zeta)$, in the case of convection-diffusion problems, their general form will be:

$$\begin{aligned} & c(\zeta) = a_0 + \sum_{i=1}^{q} \left(a_i \omega^i + b_i \omega^{-i} \right), \omega = \omega(\zeta), \\ & a_0, a_i, b_i = \text{const.}, (1 \le i \le q), \end{aligned} \tag{7}$$

where $q \in \Re^+$ and the component solution functions obey the Riccati-type ODE $\frac{d\omega}{d\zeta} = \kappa + \omega^2$ with „κ" as a parameter depending on the actual experimental conditions.

3. A unified treatment of the fundamental problem using some basic properties of Riccati's ODE

Firstly, we recall here some basic invariance properties of the Riccati-type ODE $y' + f(x) y^2 + g(x) y + h(x) = 0$. As it is well-known on the base of the classical literature of the topic e.g. [Mitrinović, 1939, 1949], if a particular solution $y_1(x)$ of the equation is known, it's relevant general solution can be given as

$$y(x) = y_1(x) + \frac{1}{u(x)} = \frac{CF(x) + G(x)}{CH(x) + K(x)}, C = const. \tag{8}$$

and this solution form is invariant with respect to the homographic-type (or: Möbius-) symmetry transformation (see also the Appendix from this point of view). Here, and in the forthcoming sub-section we will treat "x" as a general notation for independent variables, whose particular representatives may be identified all those used previously. Then, in order to solve the Riccati – ODE (related to (7)) the following form of its will be applied:

$$\omega' - \omega^2 - \sum_{m} a_m(p)\zeta^m = 0, \tag{9}$$

i.e. we intend to develop a refined modelling method, since the genuine convection - diffusion processes through porous media (e.g. through soil columns) are always sensitive to the underlying percolative-fractal character of matter at mesoscopic level. Therefore, we use here the linearized variant of the Riccati's ODE by specifying $h(\zeta) = \sum_{m} a_m(p) \cdot \zeta^m$, where the coefficients are of stochastic character, i.e. in $a_n = a_n(p)$ the independent variable *„p"* will be defined as the actual percolation probability. For the sake of simplicity we will assume firstly, that there is only one „dominant term" in this expression, i.e.:

$$\omega' - \omega^2 - a_n(p) \cdot \zeta^n = 0. \tag{10}$$

In this case, the solution is (we used the MAPLE computer algebra system [MAPLE, 2005]):

$$\begin{aligned}\omega = & \frac{C\left[\phi(\zeta)\cdot J_{\frac{n+3}{n+2}}\left(\frac{2\phi(\zeta)}{n+2}\right) - J_{\frac{1}{n+2}}\left(\frac{2\phi(\zeta)}{n+2}\right)\right]}{\zeta\left[CJ_{\frac{1}{n+2}}\left(\frac{2\phi(\zeta)}{n+2}\right) + N_{\frac{1}{n+2}}\left(\frac{2\phi(\zeta)}{n+2}\right)\right]} + \\ & + \frac{C\left[\phi(\zeta)\cdot N_{\frac{n+3}{n+2}}\left(\frac{2\phi(\zeta)}{n+2}\right) - N_{\frac{1}{n+2}}\left(\frac{2\phi(\zeta)}{n+2}\right)\right]}{\zeta\left[CJ_{\frac{1}{n+2}}\left(\frac{2\phi(\zeta)}{n+2}\right) + N_{\frac{1}{n+2}}\left(\frac{2\phi(\zeta)}{n+2}\right)\right]},\end{aligned} \tag{11}$$

(i.e. the general form characteristic for the projective linear groups [Deitmar and Echterhoff, 2009] can also be directly recognized in the case of this solution form, too) where:

$$\phi(\zeta) \equiv \sqrt{a_n(p)} \cdot \zeta^{\frac{n}{2}+1}, \tag{12}$$

C is an integration constant, while $J_k(\zeta)$ and $N_k(\zeta)$ both denote the Bessel-functions of k-th order, which are of the first kind, and second kind respectively. It is obvious, that the basic invariance property (A1-A3) of the Riccati ODE is reflected in the form of the solution (11), too. Then, by linearizing the ODE (10), we have to solve the following second order ODE:

$$\frac{d^2\omega}{d\zeta^2} - a_n(p)\cdot\zeta^n\cdot\omega(\zeta) = 0 \qquad (13)$$

The solution of this ODE can be obtained directly (again, we used the MAPLE 10 system), and its final form is more concise compared to (11)):

$$\omega(\zeta) = C_1\sqrt{\zeta}\cdot J_{\frac{1}{n+2}}\left(\frac{2\sqrt{-a_n(p)}\cdot\zeta^{\frac{n}{2}+1}}{n+2}\right) + C_2\sqrt{\zeta}\cdot N_{\frac{1}{n+2}}\left(\frac{2\sqrt{-a_n(p)}\zeta^{\frac{n}{2}+1}}{n+2}\right) \qquad (14)$$

($C_1, C_2 = \text{const.}$), i.e. the final result is explained by Bessel-functions of the order $\frac{1}{n+2}$ (which are again of the first- and second kind, respectively), and presented graphically on Fig.1.:

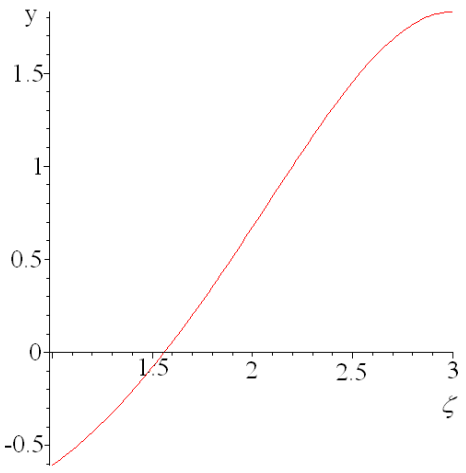

Figure 1. Solution expressed by (14) for n = 2 (in relative units)

Despite of its different convexity character, this solution is not in contradiction to the basic tanh-type solution proposed in [Fan, 2000], but represents its more general and refined variant.

Calculation of the integrating factor functions

Similarly, the technique of integrating factors [Ince, 1956] applied to the Riccati's ODE may also be used for effective general treatment of the problems discussed above. In this case, we are faced with following system of first-order ODE's [Mitrinović, 1986]. Accordingly, the function

$$(x,y)\mapsto \frac{1}{g_0(x)+g_1(x)y+g_2(x)y^2}, \tag{15}$$

will be integrating factor of $y'+a_0(x)+a_1(x)y+a_2(x)y^2=0,$ if the relevant functions obey the following conditions:

$$\begin{aligned}
&\frac{dg_0(x)}{dx}=a_0(x)g_1(x)-a_1(x)g_0(x),\\
&\frac{dg_1(x)}{dx}=2\left[a_0(x)g_2(x)-a_2(x)g_0(x)\right],\\
&\frac{dg_2(x)}{dx}=a_1(x)g_2(x)-a_2(x)g_1(x).
\end{aligned} \tag{16}$$

(It must be emphasized at this point, that in the well-organized collection of problems [Mitrinović, 1986], the formulae (15-16) are represented rather as a new open research topic instead of a simple exercise from the domain of classical theory of ODEs.) The case, we are studying corresponds to $v'+v^2=a(x)\leftrightarrow y'+y^2+a_0(x)=0$ from the first part of the Appendix (i.e. $v(x)\leftrightarrow y(x);a(x)\equiv -a_0(x)$) and the previous ODE system (16) takes the following, simplified form:

$$\begin{aligned}
&\frac{dg_0(x)}{dx}+\Omega g_1(x)=0,\\
&\frac{dg_1(x)}{dx}+2g_0(x)+2\Omega g_2(x)=0,\\
&\frac{dg_2(x)}{dx}+g_1(x)=0,
\end{aligned} \tag{17}$$

where $\Omega\in\left\{\left(k^2-\frac{\omega^2}{c^2}\right),k^2,...\right\}$ in agreement with the content of Eqs. (2) and (3). Due to its linear character and relative simplicity, the system (17) can be solved directly, and its solution (if we suppose, that the solution functions are given in the following standard forms as: $g_0(x)=\lambda e^{rt}, g_1(x)=\mu e^{rt}, g_2(x)=\nu e^{rt}$) results in the integrating factor function in the form of:

$$\frac{1}{\sum_{i=1}^{3} A_i\left(\lambda_i+\mu_i y+\nu_i y^2\right)\cdot e^{\kappa_i x}},\left(\kappa_1=0,\kappa_{2,3}=\pm 2\sqrt{\Omega}x\right), \tag{18}$$

where all coefficients (A_i, λ_i, μ_i, ν_i; (i=1,2,3)) are assumed to have constant values. Similarly, if we consider the more general case related to eq. (9), we directly arrive at the following ODE system:

$$\begin{aligned}
&\frac{dg_0(x)}{dx}+\Omega(p,x)g_1(x)=0,\\
&\frac{dg_1(x)}{dx}+2g_0(x)+2\Omega(p,x)g_2(x)=0,\\
&\frac{dg_2(x)}{dx}+g_1(x)=0,
\end{aligned} \tag{19}$$

where the possible stochastic state-dependence of the given convection-diffusion process has also been taken into account in the sense of the eq. (9) (i.e. we have a generalization $\Omega=\text{const.}\rightarrow\Omega=\Omega(p,x)$ and due to previously mentioned percolative-fractal character of transport processes through porous media, *"p"* cannot be directly used here as a simple parameter). Therefore, in this more realistic case we are faced with solving of a nonlinear ODE system. After multiplying the first ODE from (23) by 2 and the third one from the same system by ($-2\Omega(p,x)$) and by summation and integration of them, we arrive at

$$g_0(x)+\Omega(p,x)g_2(x)=C_1(p), \tag{20}$$

(i.e. the integration constants will be assumed here to depend on actual values of the percolation probability, too). Then, from (20) and the second ODE of (19) we have:

$$g_1(x)=-C_1(p)x-C_2(p), \tag{21}$$

by use of which the remaining two functions can also be obtained as:

$$\begin{aligned}
&g_0(x)=C_1(p)\int x\cdot\Omega(p,x)dx+C_2(p)\int\Omega(p,x)dx,\\
&g_2(x)=\frac{C_1(p)}{2}x^2+C_2(p)x+C_3(p).
\end{aligned} \tag{22}$$

Therefore, the relevant final form of the integrating factor function will be:

$$\frac{1}{C_1(p)\int x\Omega dx+C_2(p)\int\Omega dx+C_1(p)x^2y\left(\frac{y}{2}-1\right)+C_2(p)y(xy-1)+C_3(p)} \tag{23}$$

Finally, we would like to emphasize here, that for complete solving of the Riccati-type ODEs for both linear (18) and nonlinear (23) cases, some well-established methods from the classical theory of ODEs [Goursat, 1923] might also be applied, where a general technique of total differential equations for the case of rational functions had been elaborated in detail.

Conclusion

In the present work an attempt is given for a general symmetry treatment of the surface wave taking place in dissipative continua, convection-diffusion and turbulent flow phenomena from a unique point of view. It is demonstrated, that further detailed applications of the Riccati-type equations should play a crucial role in the future symmetry analyses of these very general type dissipative structures. Some of the newest research results about influence of helicity on rotational turbulent flows e.g. [Lesieur, 2008], [Immazio and Minnini, 2013] may also justify this concept and lead to further more detailed symmetry analyses of such phenomena on the base of applications of the general theory of projective representations of quasi-one-dimensional systems.

Acknowledgement

The authors acknowledge the support of the MÖB/DAAD Foundation No. 55731 (2014).

Appendix

Linearization

The simplified variant $v' + v^2 = a(x)$ of the Riccati-type ODE as a typical nonlinear differential equation, (whose general form is $y' + f(x)y^2 + g(x)y + h(x) = 0$), can be obtained from a second-order ODE $y''(x) - a(x)y(x) = 0$ (i.e. from a linear ODE) by integral transformation $y(x) = e^{\int v(x)dx}$.

Invariance with respect to the homography group transformations

As it is known, in general case the Riccati-type ODE, if we know a particular solution $y_1(x)$ of its, it is possible to represent the general solution as

$$y(x) = y_1(x) + \frac{1}{y_B(x)} \equiv \frac{CF(x) + G(x)}{CH(x) + K(x)}, C = \text{const.}, \qquad (A1)$$

where $y_B = y_B(x)$ denotes a general solution of a Bernoulli-type ODE (to which the initial Riccati - type ODE may be reduced via use of the particular solution

$y_1(x)$), and the solution is directly prescribed by functions F(x), G(x), H(x), K(x) in order to exploit the fundamental invariance properties of solution of the Riccati – ODE subsequently. The solution form (A1) is suitable for detailed studies of the basic invariance properties of solutions of the Riccati-type ODEs, because by applying a general transformation of the unknown function in the form of

$$y = \frac{Q(x)z + R(x)}{S(x)z + T(x)}, \quad (QT - RS \neq 0), \tag{A2}$$

(defining the Möbius group, too, e.g. [Mészáros et al., 2011] (in sense, that the latter is a subgroup of the former, more general group), widely studied at conformal mappings of the open unit disk onto itself - e.g. [Marvel et al., 2009], where it was also demonstrated, that the Riccati's ODE emerge from the infinitesimal generators of this group) leads again to a Riccati-type ODE in the form of:

$$z'(x) + F(x)z^2 + G(x)z(x) + H(x) = 0, \tag{A3}$$

Then, following the method founded in [Mitrinović, 1939], if in the transformation formula (A2) we use

$$Q(x) = \frac{1}{f(x)}, R(x) = \frac{f'(x) - f(x)g(x)}{2f^2(x)}, S(x) = 0, T(x) = 1, \tag{A4}$$

(A4) will take the form of:

$$z'(x) + z^2 = \Phi(x), \tag{A5}$$

where:

$$\Phi(x) = -\left(\frac{f' - fg}{f^2}\right)' - f \cdot \left(\frac{f' - fg}{f^2}\right)^2 - g \cdot \left(\frac{f' - fg}{f^2}\right) - h, \tag{A6}$$

and this is the *canonical form* of the Riccati-type ODE.

References

[1] Sagdeev, R. Z., Usikov D. A., Zaslavsky G. M. (1988) Nonlinear Physics (From the Pendulum to Turbulence and Chaos) (Contemporary Concepts in Physics Vol. 4.). Harwood Academic Publishers Chur-London-Paris-New York-Melbourne

[2] Tribelskii, M. I. (1997) Short-wavelength instability and transition to chaos in distributed systems with additional symmetry. Physics – Uspekhi **40** 159
[3] Zhang Shun-Li and Qu Chang-Zheng (2006) Approximate Generalized Conditional Symmetries for the Perturbed Nonlinear Convection-Diffusion Equations *Chin. Phys. Lett.* **23** 527
[4] Landau, L. D. and Lifshitz, E. M. (2000) Fluid Mechanics 2nd Ed., Oxford-Boston-Johannesburg: Butterworth-Heinemann
[5] Izyumov, Yu. A. and Syromyatnikov, V. N. (2013) Phase Transitions and Crystal Symmetry, Kluwer Academic Publishers, Dordrecht-Boston-London
[6] Vuković, T., Milošević, I. and Damnjanović, M. (1996) Molien functions and commensurability of the helicoidal ordering *Phys. Lett.* A **216** 307
[7] Kirschner, I. and Mészáros, Cs. (2001) Symmetry analysis of static soliton structures and elementary excitations in incommensurately modulated crystals *J. Phys.: Cond. Matt.* **13** 5399
[8] Gyarmati, I. (1970) Non-Equilibrium Thermodynamics (Field Theory and Variational Principles), Berlin-Heidelberg-New York: Springer-Verlag
[9] Martyushev, L. M. and Seleznev, V. D. (2006) Maximum entropy production principle in physics, chemistry and biology *Phys. Rep.* **426** 1
[10] Merker, J. and Krüger, M. (2013) On a variational principle in thermodynamics *Cont. Mech. Thermodyn.* **25** 779
[11] Singh, P. (1976) The application of the Governing Principle of Dissipative Processes to Bénard convection. Int. J. Heat Mass Trans. **19** 581
[12] Mészáros, Cs., Kirschner, I. and Bálint, Á. (2014) Relevance of the time-quasi-polynomials in the classic linear thermodynamic theory of coupled transport processes *Cont. Mech. Thermodyn.* **26** 447
[13] Gelfand, I. M. and Fomin, S. V. (1963) Calculus of Variations Englewood Cliffs, New Jersey: Prentice Hall Inc.
[14] Blanchard, Ph. and Brüning, E. (1982) Direkte Methoden der Variationsrechnung (Ein Lehrbuch), Wien: Springer-Verlag GmbH
[15] Landau, L. D. and Lifshitz, E. M. (1999) Theory of Elasticity 3rd Ed. (by E. M. Lifshitz, A. M. Kosevich, L. P. Pitaevskii), Butterworth-Heinemann, Oxford-Boston-Johannesburg-Melbourne-New Delhi-Singapore
[16] Hopf, E (1948) A mathematical example displaying features of turbulence *Commun. on Pure and Appl. Math.* **1** 303
[17] Pascal, J. P. (1996) Effects of nonlinear diffusion in a two-phase system *Physica* A **223** 99
[18] Kirschner, I., Mészáros, Cs., Bálint, Á., Gottschalk, K. and Farkas, I. (2004) Surface changes of temperature and matter due to coupled transport processes through porous media *J. Phys. A: Math. Gen.* **37** 1193
[19] Kirschner, I., Bálint, Á., Csikja, R., Gyarmati, B., Balogh, A. and Mészáros, Cs. (2007) An approximate symbolic solution for convective instability flows in vertical cylindrical tubes *J. Phys. A.: Math. Theor.* **40** 9361
[20] Mészáros, Cs. and Bálint, Á. (2011) Transient transport processes in deformable porous media *Chin. Phys.* B **20** 110507

[21] Elwakil, S. A., El-Labany, S. K., Zahran, M. A. and Sabry, R. (2004) Exact traveling wave solutions for a diffusion-convection equation in two and three spatial dimensions *Comp. Phys. Comm.* **158** 113
[22] Conte, R. and Musette, M. (2008) The Painlevé Handbook. Springer Science + Business Media B.V.: Dordrecht, The Netherlands and Bristol, UK: Canopus Publishing Limited. XXIV
[23] Fan, E. (2000) Extended tanh-function method and its applications to nonlinear equations *Phys. Lett.* A **277** 212
[24] Mitrinović, D. S. (1939) Théorème sur l'équation de Riccati *C.R. Acad. Sci. Paris* **208** 156
[25] Mitrinović, D. S. (1949) Sur une equation differentielle lineaire du second ordre transformable en elle - même *C.R. Acad. Sci. Paris* **228** 118
[26] MAPLE 10, 2005 A Symbolic Computation System; Waterloo Maple Inc.
[27] Deitmar, A. and Echterhoff, S. (2009) Principles of Harmonic Analysis Springer Science + Business Media LLC
[28] Ince, E. L. (1956) *Ordinary differential equations* New York: Dover Publications Inc.
[29] Mitrinović, D. S. (in cooperation with Vasić, P M) (1986) *Differential Equations, Collection of Exercises and Problems (Diferencijalne jednačine, Zbornik zadataka i problema* – in Serbian*)*, Naučna Knjiga, Belgrade
[30] Goursat, E. (1923) Sur l´integration des differentielles totales rationelles *Nouv. Ann. Math.* (5) **2** 81
[31] Lesieur, M. (2008) *Turbulence in Fluids*, 4th Ed. (Springer Science + Business Media B.V.)
[32] Imazio, R. P. and Minnini, P. D. (2013) Passive scalar cascades in rotating helical and non-helical flows *Phys. Script.* **T155** 014037
[33] Mészáros, Cs., Gottschalk, K., Farkas, I., Gyarmati, B. and Bálint, Á (2011) Surface waves at convection-diffusion processes through porous media *Mech. Eng. Lett.* **6** 95
[34] Marvel, S. A., Mirollo, R. E. and Strogatz, S. H. (2009) Identical Phase Oscillators with global Coupling evolve by Möbius Group Action *Chaos* **19** pp. 043104 – 1-11

Spectral dependence of different PV module technologies

István SERES, Ivett KOCSÁNY and István FARKAS
Department of Physics and Process Control,
Institute for Environmental Systems

Abstract

In this paper the study of the energy production of a 10 kWp photovoltaic system is presented. The system – installed in the autumn of 2005 – consists of two type of photovoltaic modules, polycrystalline and amorphous silicon ones. As the two different types are reacting in different way to the environmental changes, the share of the subsystems from the energy production is changing in time. From the long time data analysis a seasonal change can be observed. Beside the temperature dependence of the modules it justifies the different spectral behaviour behind the process. In the paper the correlation between the solar spectrum and the electric power rate change is to be presented.

Keywords

solar energy, photovoltaic, polycrystalline, amorphous silicon, measurements

1. Introduction

A 10 kWp photovoltaic system was set up at the top of one student hostel building of the Szent István University by the Department of Physics and Process Control in 2005. During about the 9 years of operation sufficient amount of data were collected for the analysis of the energy production of the system, and for the comparison of the operation of the two different installed PV technologies (amorphous silicon and polycrystalline). A few years before a spectrometer were used only for some weeks to study the spectral dependence of the PV units. Obviously, the limited time interval of the spectra measurements made limitation during the analysis, as well. Recently, there was an opportunity to install a standard spectrometer so the spectral measurements were started again.

2. The PV system

On the campus of the Szent István University, Gödöllő, Hungary a 10 kWp photovoltaic system was constructed. The system was installed (on 8th October, 2005) on the flat roof of a student hostel building of the campus. The azimuth angle is 5° to East and the tilt angle is 30°, which is a good yearly average value

for the site. The system has three different subsystems, two identical parts of 3,1 kWp from amorphous silicon DS40 modules (Dunasolar Ltd.), and a 3,5 kW part of ASE100 modules from polycrystalline (RWE Solar Gmbh) technology. Every subsystem uses a separate inverter (Sunpower SP3100/600 and SP2800/550), through which the produced energy is converted to the 230 V, 50 Hz electrical grid (Seres et al., 2009). The picture of the system is shown in Fig. 1.

Figure 1. The picture of the studied PV system

3. Measurements carried out

For monitoring the system, basic environmental (irradiation, temperature, etc.) and electric quantities (DC and AC voltage, power, phase angle, etc.) are measured by a computer based data acquisition system and the AC electric data through an electric meter, as well. The data introduced in this paper are originated from the above mentioned measurements.

The measurements were performed by the USB2000+ VIS-NIR-ES spectrometer, made by the Ocean Optics company, installed on the spot, on a solar collector in shading less position. The system consists of a light collecting dome, a 10 m long optical cable and the spectrometer unit which is connected to a computer through an USB port. The installation can be seen in Fig. 2.

Figure 2. Positioning the light collecting dome

The spectrometer is a single-slit unit where the incoming light is separated to different wavelength by diffraction on a 50 μm diameter optical slit (Ocean Optics, 2010). In Fig. 3, the optical slit is indicated by "2" at the light entrance.

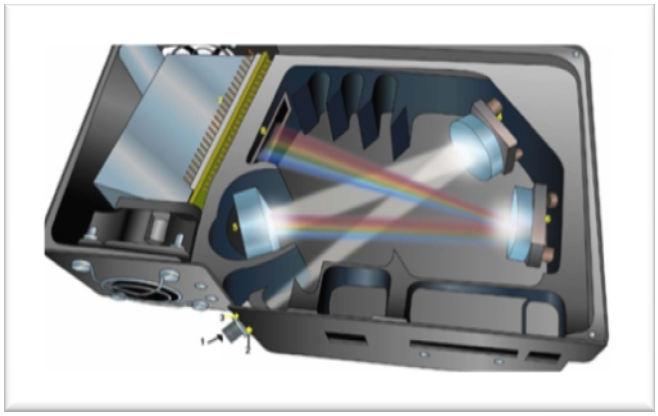

Figure 3. Working principle of the used spectrometer

The optical slit separates the incoming light by wavelength, and a serial of light sensitive sensors detects the number of the photons hitting the sensor element during an adjustable time period. The data are transferred to the computer, where the analyzer software prepares a graph or a data file about the spectral distribution. Two software were used for measuring an analyzing the data, the Overture and the Oceanview software (Ocean Optics, 2011). In Fig. 4 the screenshot of the Overture software can be seen.

Figure 4. The number of the photons in different wavelengths during 5 ms

For the energy and power analysis the power distribution as a function of the wavelength should be known. In order to get it from the number of photons, the energy carried by a photon has to be used. It is known from the Planck theory, i.e. the energy of a single photon can be written as:

$$\varepsilon = h f, \tag{1}$$

where h is the Planck constant and f is the frequency of the photon. However, in our case it would be better to express the energy by the wavelength, as these data are directly coming from the spectrometer. Knowing that the frequency can be calculated as the light speed over the wavelength, the photon energy can be got as:

$$\varepsilon = h f = h \frac{c}{\lambda} \tag{2}$$

In this way the power of the light in the given wavelength range is:

$$P = \frac{E}{t} = \frac{N\varepsilon}{t} = \frac{N}{t}\frac{hc}{\lambda} \tag{3}$$

where N is the number of the incident photons during time. Using this formula the wavelength distribution of the photon number can be converted into power versus wavelength graph, as it can be seen in the next graph (Fig. 5).

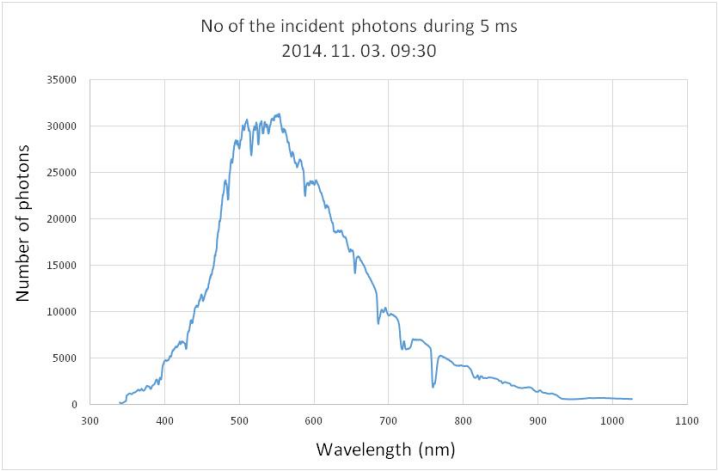

Figure 5. The number of the incident photons during 5 ms

After converting the photon number to power with the given formula, the shape of the graph will slightly change as for lower wavelength the photon energy is higher, which can be seen in the Fig. 6).

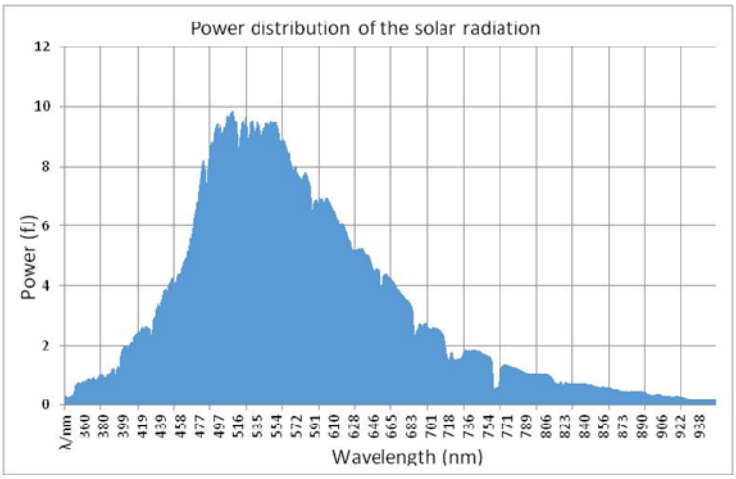

Figure 6. Spectral power distribution of the incident light

4. Analysis of the power data of the PV system

The polycrystalline (ASE) and amorphous silicon modules (DS) energy production is measured independently from each other which gives a solid basic for the analysis and comparison of the different PV technologies.

Looking at the power distribution of the subsystems in a given day (Fig. 7) it can be observed that the power of the ASE subsystem is about 30% higher than the DS subsystems.

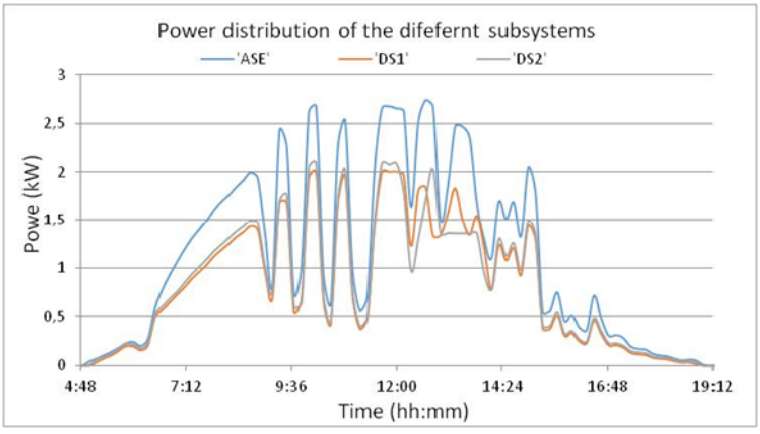

Figure 7. Power distribution of the subsystems in a given day

It is partly originated from the fact, that the installed nominal power of the ASE modules is 3,4 kWp, compared for the installed nominal power of 3,1 kWp

for each of the two DS subsystems. To be able to compare the different technologies independently from the installed power, the so called specific power will be used later on. The specific power (P_{spec}) is defined as the actual power of the subsystem divided by its nominal power i.e. it is the actual power of a 1 kWp installed unit of the given technology.

$$P_{spec} = \frac{P_{actual}}{P_{nominal}} \left(\frac{kW}{kWp} \right) \tag{4}$$

From the specific power distribution for the same period (Fig. 8) a smaller difference can be read out, however the difference still exists.

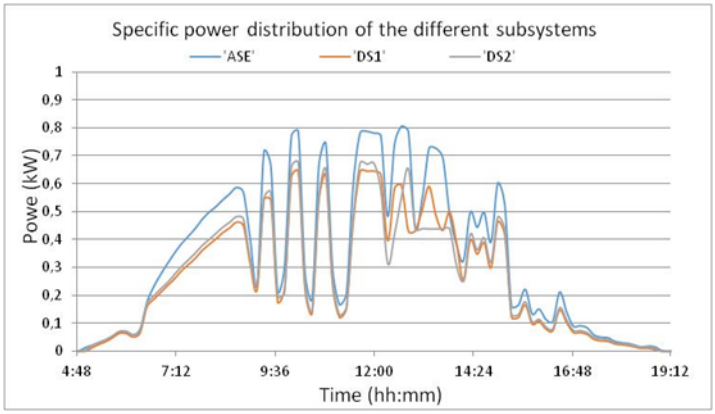

Figure 8. Specific power distribution of the subsystems in a given day

Surely, this difference can be seen during a longer time period, as well, as it is shown in the Fig. 9 from the rate of the energy production of the ASE and DS subsystems (Green et al., 2012).

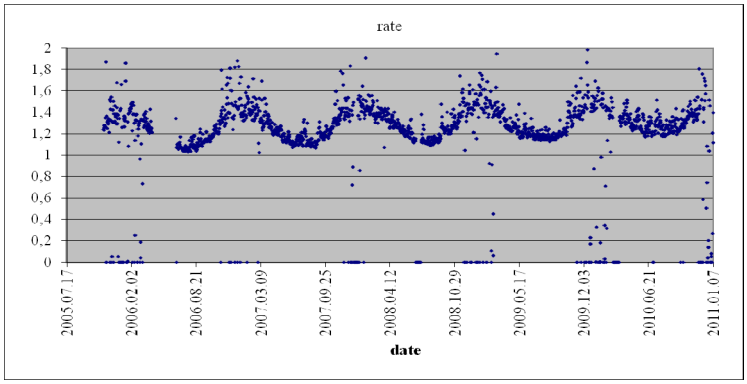

Figure 9. Rate of the energy production of the ASE and DS subsystems

This tendency along with the seasonal periodic change can also be seen from the latest energy data for the last year (Fig. 10).

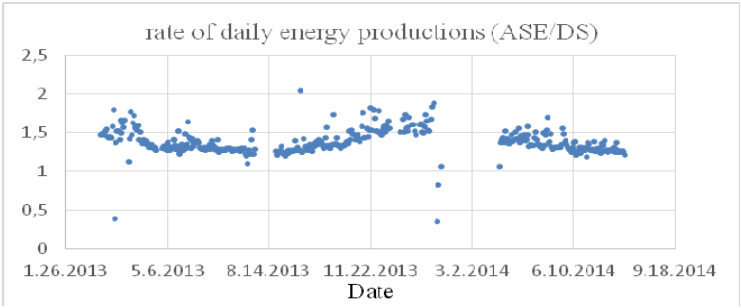

Figure 10. Rate of specific energy production of ASE and DS subsystems

5. The specific power and the spectrum

From the figure it can be seen that specific energy production is changing differently during the year, and it has a seasonal effect, which is higher in winter and lower during summer period. Behind the effect two main factors can be thought, i.e. the different temperature dependency and the different spectral sensitivity of the modules. A long time spectral measurement series was started to measure the spectrum of the solar radiation in coincidence with the power data in order to check the correlation between them. However, at this moment long time spectral data available for a shorter period, but the comparison of the daily change of the spectra to the rate of the specific energy production shows some results. In the Fig. 11 the specific energy production is compared to the total power, where we it can be seen definite difference in the shape of the fitting functions.

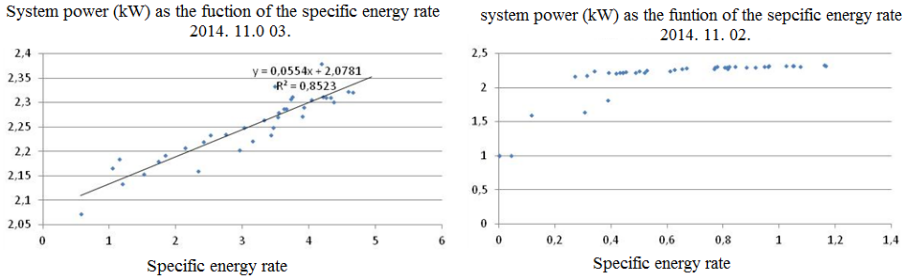

Figure 11. The specific energy production for a sunny and cloudy day

From the different behaviour of the specific power functions under similar thermal conditions (the average ambient temperature was between 5 and 10 degrees Celsius), the spectral dependence can be concluded. In an earlier work the rate of the infrared range in the incoming radiation was investigated, now the

high frequency range was studied. We suspected that in the mentioned period the energy income in the shortwave range of the visible light was changing, and this caused different change in the energy productions of the different technology modules. The result can be seen in the next Fig. 12.

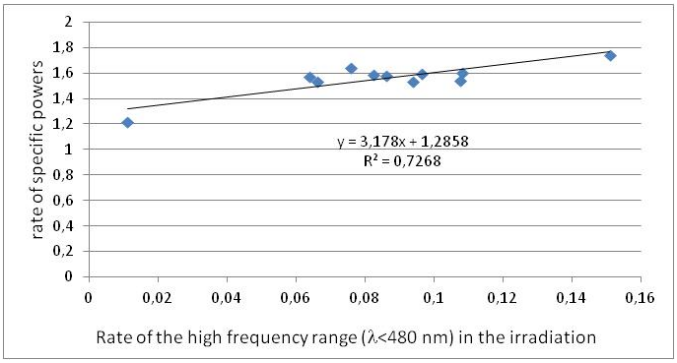

Figure 12. The rate of the specific energy production vs. the rate of the high frequency range in the irradiation

Conclusion

In this paper the seasonal change of difference in the power of the PV subsystems were discussed along with its possible reasons. It has been observed that the radiation spectrum is changing during the day, and it depends on the clouds as well. A linear correlation has been found between the rate of the specific energy production of the polycrystalline and amorphous silicon subsystems, and the rate of the shortwave visible range in the irradiation.

Acknowledgement

The research was carried out in the framework of the OTKA K 84150 project.

References

[1] Green M.A., Emery, K., Hishikawa, H., Warta, V., Dunlop, E.D. (2012), Solar cell efficiency tables, Progress in Photovoltaics, 2012, Vol. 20 pp. 12-20.
[2] Ocean Optics (2011), Overture User Manual, Software User's Guide, Document Number 000-20000-400-01-201108
[3] Ocean Optics (2010): USB2000+ Fiber Optic Spectrometer Installation and Operation Manual Document number 270-00000-000-02-201409
[4] Seres, I., Farkas, I., Kocsány, I. (2009), Comparison of PV modules under different spectral conditions, Mechanical Engineering Letters, Vol. 3, pp. 81-89.

Fractal analysis of air bubbles in frozen waters

Piroska VÍG, István FARKAS
Department of Physics and Process Control,
Institute for Environmental Engineering Systems

Abstract

One of the biggest problems in our century near the exhaustion of traditional energy sources the shortage of drinking water. More and more researches are aimed to give alternatives for replace of missing water. It helps a lot if we have knowledge about the properties and behaviour of the water and if we know how to relate the parameters of water in our environment for average values of the water parameters. In this study examination and comparison of the physical properties of the water samples (spring, well, tap and rain) from Gödöllő area are analysed. During the freezing of the water samples, the air bubbles from the water trapped in the ice. The formed patterns are unique, but observed source-specific characteristics. It has also been contributed with the results of the fractal analysis of the photos from the frozen water sample to search contact between fractal dimension and water source-type.

Keywords

air bubbles, environment, formation, fractal dimension, freezing, physical properties

1. Introduction

Water is an essential element, one of the most important components for life. It is the main component of the cells, and it is also an astern medium surrounding cells. The tasks of water are complex: solvent, heat storage and cooling fluid, starting and ending product of numerous biochemical reaction, transports to the cells the foods and transports from the cells the generated waste products, participates in the breathing, the heat control processes and maintains of acid-base balance. Despite of the fact that we know much about the water properties, strange behaviours and rolls of water, there are still a lot of outstanding issues.

In the background of the unique properties of the water are the hydrogen bonds. The density anomaly of water ensure that the aquatic wildlife survive the winter period. From the physical properties of the water outstanding the extreme high heat of vaporization, the large specific heat capacity but low thermal conductivity, these characteristics result to use the water bath is the easiest way to keeping the constant temperature. It has the high permittivity, surface tension and important its capillary effect and additionally it is an excellent solvent.

Extraordinary information-carrier properties are used in the alternative medicine.

The total water resources of the Earth's is about 1.4 billion km^3, however fresh water is only 3% of its, of which 80% is located in the Arctic ice sheet, so that is really available freshwater resources from the earth's total water resources is only 0.5% (Caro, 1993). The importance of the problem relating the water is shows that number of international scientific journals writes about the water from several aspects. Nowadays the high-quality drinking water is the base of the healthy lifestyle. The importance of the drinking water also shows the widespread usage of bottled mineral water, domestic water treatments and water energizing equipments. Beside the water comes from remote locations or is restructured, it is important to know the natural water in around our environment. The knowledge of the parameters of such water gives a chance to contribute to the general knowledge of the water and provides information about how we can used the water in our environment.

During the examination of the water properties mainly water chemistry measurements are happen, because to the drinking water quality it is the most important. The antecedent of the present work were examination the physical properties of water which come from several water sources in Gödöllő area, Hungary. The physiologically particularly relevant surface tension and viscosity were measured among others. The measurements were carried out in the laboratory of the Department of Physics and Process Control, Szent István University, Gödöllő.

During the examination the values of the surface tension and viscosity and their temperature dependence we not found significant difference between the measurements of water from different sources. However, an interesting phenomenon was observed. During storage the water samples in the refrigerator the samples are frozen and their shows typical patterns.

Just as no two snowflakes are the same, when the water is frozen the pattern appearing in the ice are different, but they have a typical, source specific characteristics.

Describing the appearing patterns in frozen water Madrazo et al. (2009) developed a model. Their model can simulate the formation of patterns in the ice. In their work Nishino et al. (2012), make computations of heat transfer and tracking of water-ice interface and generation of bubbles. Dadic et al. (2010) examined the air bubbles migration in ice under a temperature gradient. The general water was examined by the above mentioned literatures, but the difference between the water from several sources was not studied. Our work would like to examine just it.

The aims of the present work is determination the fractal dimension of air bubble patterns in the frozen water, and examination whether there is a relationship between the fractal dimension and water types which were gathered from different sources. The fractal analysis it is a widely used analytical method for examination the natural patterns, but application to our problem is not found in the literature.

2. Sample collection and preparation

The examined water samples come from Gödöllő area: rain, spring and tap water (Fig. 1). For reference used distilled water was made in the chemistry laboratory of Szent István University.

Figure 1. Gathering of the rain, spring, tap and distilled water

The rain waters were collected in Királytelep region of Gödöllő, the spring waters made from Petőfi natural spring it can found between the towns of Gödöllő and Aszód, the tap water samples from tap of physics laboratory of SZIE. During the gathering and preparation of the samples had to be taken with caution in order to avoid contamination and they were stored in the refrigerator. During the storage the water samples accidentally frozen. The appearing patterns in the ice are different, but they have typical, source specific characteristics.

3. Frozen process

The samples have been consciously equally prepared for freezing: after collection of the samples, equal quantity from samples were poured in uniform beakers, closed with cling film and put in the refrigerator (Fig. 2), where they were frozen. The temperature field started at -3.4 °C at the top and the gradient was 9.3 °C/m from top to down.

Figure 2. Preparation the samples for freezing

Due to the slow, smooth freezing in the transparent ice block patterns appear that are unique, however are water type specifics. The picture row of Fig. 3 shows example the typical patterns, the differences between the several patterns were well observed.

Figure 3. Frozen tap, rain and distilled water

The resulting ice formation which formed during the water-ice phase change is determination by temperature and pressure. Among the possible structures of ice, the investigated temperatures around 0 °C and normal atmospheric pressure about 100 kPa, the resulting ice crystal structure is the I_h type. During the freezing process the water structure which is a dynamically changing structure, clusters linked by H-bonds transformed for ice structure which is a determined structure, e.g. open network held by H-bonds.

In the nature can be observed that near the temperature and pressure the water surface restlessness also influenced the ice formation. Fig. 4 shows the formation of ice in Balaton lake in two different cases.

Figure 4. Ice formation in case of calm wind and windy conditions

Windless, cold weather with slow freezing process the result of ice formation is clear ice, while windy, cold weather with fast freezing the ice surface is

rugged and ice is opaque. The freezing temperature gradient is a further influencing factor. Fig. 5 shows an example for such case at the Abraham Lake in Alberta, Canada. In the depths generated gases from the bottom of the lake move up, but before they reach the surface frost in the ice. Air temperature in this case is -30 °C (Scribol, 2013).

Figure 5. Gas bubbles frozen in ice (photos: Chip Phillips)

Based on the above, during the freezing process these conditions (calm water surface and constant temperature gradient) also were the same. The reason of the patterns is the gases in the water. Low water solubility gases (non-polar) are: O_2, N_2, H_2, CH_4, N_2O so, the bubbles in our case are air bubbles.

During the freezing the ice grows from the top to down. The crystal growth still contains small inhomogeneities, in the spaces between the crystals are trapped air bubbles from the water. As the thermal conductivity and heat transfer coefficient are different in case of air, ice and water, so usually the air bubbles are not isolated, but they are arranged in needle-like shape (Fig. 6). Downward the spikes appear more frequently, and finally with solidification of the air richest bottom part finished the freezing process. So, in the ice the air bubbles draws „hedgehog" patterns, which are added at different water samples with special characteristics.

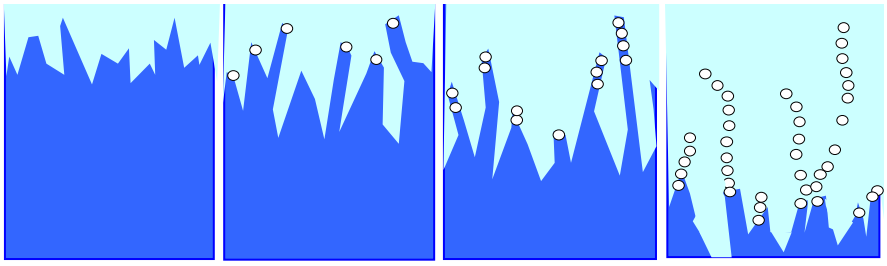

Figure 6. The process of the pattern formation

There were made photos of the patterns under the same lighting conditions. The Fig. 7 shows a typical patterns row.

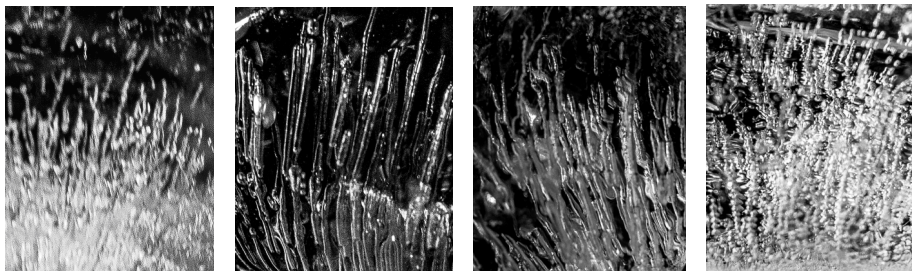

Figure 7. Typical water freezing generated patterns: rain, tap, spring and distilled water

Rainwater pattern contains many densely situated pin. In the case of tap water, these pins are located less. The air bubbles in spring water to form softer line spikes, while freezing of distilled water structuring in the perpendicular direction of the freezing also observed.

4. Determination of fractal dimension

The fractals are self-similar formation. In the nature they can be found in the different area of the life: vascular system, neural network, lungs, river networks, lightings, clouds surfaces, trees, leaves, galaxies, rate fluctuations of stock exchange.

Table 1 Methods for determination fractal dimension

Method	Application
Least squares	For theoretical approaches
Walking-divider	Length measurement
Box counting	The most widely used method
Prizm-method	One-dimensional signals
Epsilon-formula	Measurement curves
Perimeter-area relationship	Classification of different types of images
Fractal based Brownian movement	Applications similar than box-method
Energy distribution	Digital signals
Hybrid methods	With 1D methods 2D fractal calculations

Table 2. Software for the fractal analysis

Software	Availability
Java Applet for Fractal Dimensions	http://www.stevec.org/fracdim/
Fractalyse	http://www.fractalyse.org
Fractal Dimension Calculator	http://www.fractal-lab.org/download.html
Fractal Analysis System software	http://cse.naro.affrc.go.jp/sasaki/fractal/fractal-e.html#note
MATLAB: Boxcount	http://www.mathworks.com/matlabcentral/fileexchange/13063-boxcount

Fractals are characterized by their fractal dimension. Table 1 summarizes the methods for determination the fractal dimension and their important application areas. The Table 2 shows the most famous fractal related software.

During the examination 12 rainwater, 7 tap water, 7 spring water and 5 distilled water samples were used. 5 photos of every sample were taken under the same light conditions. Based on these approach 155 pictures the following parameters were determined:

1. Fractal dimension of the borderline between ice (black) and air bubbles (non-black).
2. Coverage (ratio of non-black area in %.
3. Fractal dimension of the surface of bubbles based of grayscale pictures.

For determination of fractal dimension of the borderline between ice and air bubbles the box-counting method were used. Typical example are shown in the Fig. 8.

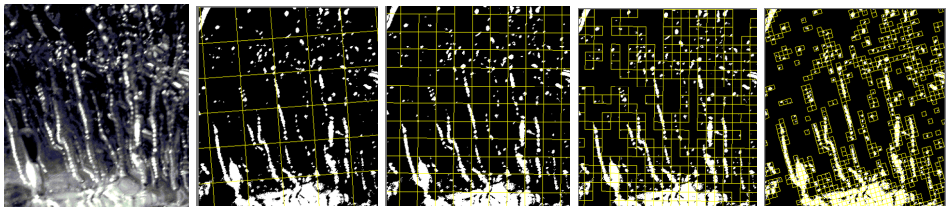

Figure 8. Box-counting method

The first picture in the sequence is the original image, and the further pictures are visible the covering with the smaller and smaller squares. Within the boundary lines a square, in which can be found black and non-black pixels too. Coverage was square which contain several pixels than the black. Plotting the logarithm of the number of squares under the appropriate condition as a function the logarithm of the side length of the square and the magnitude of the slope of the fitting line gives the fractal dimension.

The results of the pattern introduced in Fig. 8 are shown in Fig. 9.

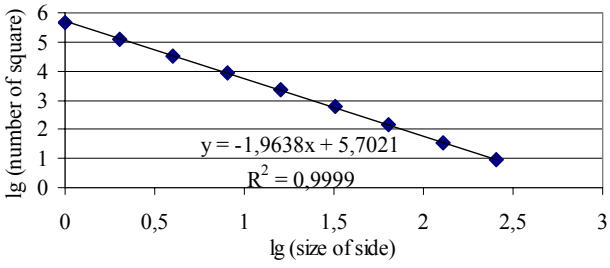

Figure 9. Borderline fractal dimension determination

It is important to note, that the calculated fractal dimension values may depend on the method (Peitgen, Sauge, 1988). The possible methods for calculate the air bubbles surface fractal dimensions are followings: calculation from brightness difference, calculation from shades of gray with box-counting methods and calculating from box-counting results of tomography. The air bubbles surface fractal dimensions in our case were calculated from sum of brightness difference (from 0 to 255). The results of the pattern of Fig. 8 are shown in Fig. 10.

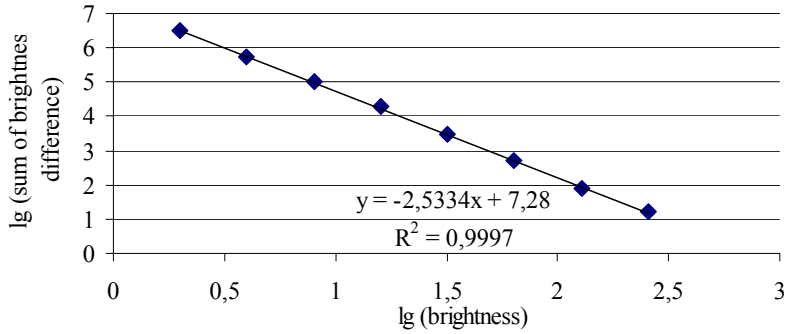

Figure 10. Surface fractal dimension determination

5. Results

During the calculating process the Fractal Analysis System software for Windows 3.4.7 software was used, produced by National Agriculture and Food Research Organisation (NARO), Japan.

In case of several water types the fractal dimension of borderline is shown in Fig. 11 and meanwhile the results of covering can be observed in Fig. 12. Moreover, Fig. 13 shows the standard deviation of air bubbles surface fractal dimension.

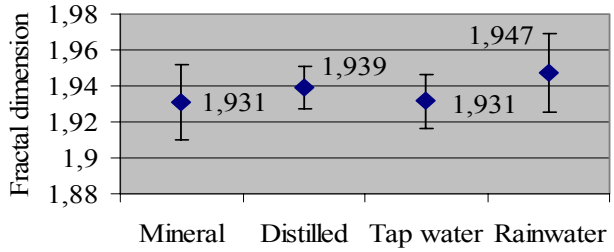

Figure 11. Borderline fractal dimension of air bubbles

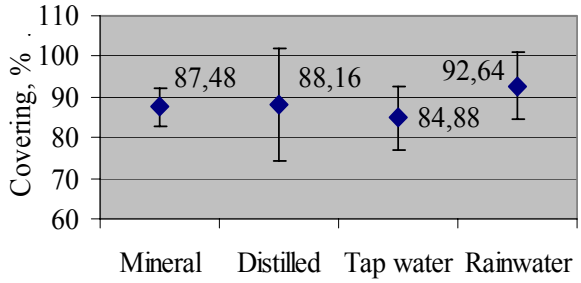

Figure 12. The influence results of covering

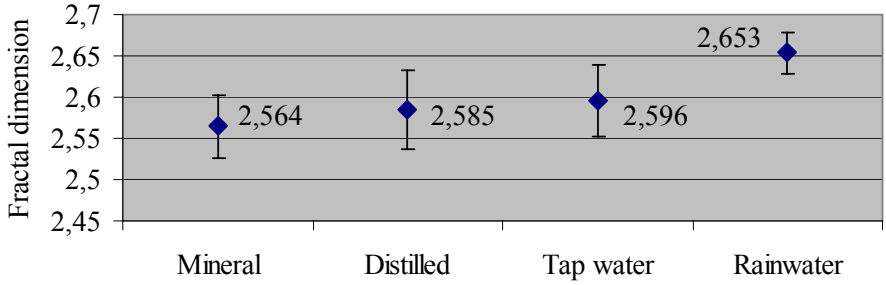

Figure 13. Fractal dimensions of air bubbles surfaces

Conclusions

The main results obtained during the theoretical and experimental studies can be summarized as follows:

In air bubbles borderline fractal dimensions at the different types of water samples could not be found characteristic difference. The same can also be said for covering. The coverage can be related to the air content of water. The result is not that significant difference which confirms that the air content of the water type is independent. The waters air content dependence of the preliminary life and freezing conditions are well known, but these were the same in these samples, so such results are partly obvious.

Fractal dimensions of air bubbles surfaces were determined from brightness difference on base of grayscale images. It was actually the largest in case of rain water. The other three types of water this value is definitely smaller and cannot be proved a significant difference between them, so the difference in the samples on the fractal dimension does not appear. Consequently, from the fractal dimension of air bubbles surface it can be properly estimated only that the examined water sample made from rainwater or not. The larger value at rain water may be explained by the fact that the rain water is unfiltered, as the other tested water samples passing through filters (soil, membranes, chemical filtration) before gathering samples.

The roles of the air content are important in the biophysics: at blood and soil, in the food industry at ice cream making, preparation of creams and puffed foods and in building industry solidification of the concrete. The methods can also be used in such cases.

Next step in the research is to find other metrics, (e.g. fractal dimension calculated by another method) which could more visibly be identify the water type.

Acknowledgement

This work was supported by Doctoral School of Engineering, Szent István University, Gödöllő, Hungary. The authors acknowledge also the support of the MÖB/DAAD Foundation No. 55731 (2014).

References

[1] Caro P. (1993): Water, McGraw-Hill, Inc. New York

[2] Dadic R., Light B., Warren S. G. (2010): Migration of air bubbles in ice under a temperature gradient, with application to "Snowball Earth", Journal of Geophysical Research: Atmospheres, Volume 115, Issue D18, 27 September 2010.

[3] Fractal Analysis System for Windows 3.4.7 (2014), National Agriculture and Food Research Organization (NARO), Japan, http://cse.naro.affrc.go.jp/sasaki/index-e.html

[4] Madrazo C., Tsuchyta T., Sawano H., Koyanagi K. (2009): Air bubbles in ice by simulating freezing phenomenon, The Journal of the Society for Art and Science, Vol. 8. No.1, pp. 35-42.

[5] Nishimo T., Iwasaki K., Dobashi Y., Nishita T. (2012): Visual simulation of freezing ice with air bubbles, Association Computing Machinery, ACM, New York

[6] Peitgen, H.-O., Saupe D. (1988): The Science of Fractal Images, Springer-Verlag, New York

[7] Scribol (2013): The explosive potential of methane frozen Beneath Abraham Lake, http://scribol.com/environment/the-explosive-potential-of-methane-frozen-beneath-abraham-lake

Institute for Mechanical Engineering Technology

Professor Dr. Gábor KALÁCSKA
Director of the Institute

Dear Reader,

The Institute for Mechanical Engineering Technology (consists of three departments: Department of Material and Engineering Technology, Department of Maintenance of Machinery, Department of Mechatronics) carried out more research topics concerning tribology, technical reliability of structural materials. The topics are related to PhD research activities as well. In the followings three different results are highlighted.

- Tribology: the article is part of a broad tribology research project with different polymer composites on PA6, POM, PET and PEEK matrix and targeted to create a detailed map of tribological features. Measuring the hardness and surface energy of the tribology tested materials gave some new approach about friction results. The research results plot a connection between the surface (polar and adhesion components) energy and the friction (static and dynamic) behaviour. Furthermore the experienced difference between the static and dynamic friction coefficients and its time function will offer a new approach during evaluation of the stick-slip behaviour of PA6 and PEEK composite materials.
- Maintenance, development of break system: in the brake system the brake fluid presses the pistons, so heat gets to the brake fluid through the piston. If the piston's material and design were changed the temperature influences the brake fluid. Thermal test has been made, where three materials were tested (aluminium alloy, steel, titanium alloy) and the best material was titanium alloy, where the brake fluid temperature was lower than by the other materials we used.
- Reliability of materials: The introduced research was to define how the crystal structure of the different kinds of armors changes during the penetration of the bullets. We examined three kinds of plates using different types of bullets. The plates that have been shot had different hardness and the bullets had various speed. Specimens were made from the proper segments of the damaged armor plates. The examinations of metallographic specimens help us to define the changes of the crystals, especially the cracks as well as the size of the effect zone.A new method and an instrument has been developed to recognize object's location.

Professor Dr. Gábor KALÁCSKA
Director

Thermal analysis of caliper's pistons in terms of brake fluid warming in finite element software

Ádám HORVÁTH[1], István OLDAL[2], Gábor KALÁCSKA[1], Mátyás ANDÓ[3]
[1]Department of Maintenance of Machinery,
Institute for Mechanical Engineering Technology,
[2]Department of Mechanics, Institute for Mechanics and Machinery,
[3]Savaria Institute for Technology, University of West Hungary,

Abstract

By planning parts of the brake system, you have to calculate the temperature which affects the parts of brake system (brake pad, piston, brake fluid, caliper). It is important that the temperature does not exceed the brake fluid dry and wet boiling point. In the brake system the brake fluid presses the pistons, so heat gets to the brake fluid through the piston. If the piston's material and design were changed the temperature influences the brake fluid. Thermal test has been made, where three materials were tested (aluminium alloy, steel, titanium alloy) and the best material was titanium alloy where the brake fluid temperature was lower than by the other materials we used. The wall thickness of pistons was determined, the optimal titanium alloy piston's wall thickness was 2,5 mm.

Keywords

brake, piston, thermal, aluminium alloy, titanium alloy, steel

1. Introduction

Vehicle's brake system is safe if there is a hydraulic system compliance with regulation and if is suitable to slow down the vehicle. In cars we use friction brake system, where two parts are pressed to each other. (P.D. Neis, et al., 2011) this friction converts car's kinetic energy to thermal energy, which affect efficiency and in critical cases the efficiency is very low and the car does not stop. The thermal effect in parts of the brake has been examined in several studies (T.J. Mackin, et al., 2002) (A. Belhocine, et al., 2012), to make thermal models, which is approximates reality. Other researches examine the material to find the approximate material, where the coefficient of friction doesn't change from the heat. (J. G. Balotin, et al., 2010).This heat affects the brake pad and brake disc which friction each other, furthermore affect other parts (caliper, pistons, brake fluid). The material properties are change in these parts. Strength of caliper and pistons reduce and boiling point of brake fluid decreases. It is a disadvantage of brake fluid, that it blinds the water, which becomes vapor if the

temperature exceeds the boiling point. This vapor is squeezable, so the brake system's efficiency decreases. The high performance vehicles use bigger brake system, where the temperature is bigger than by conventional brakes. This temperature affects the brake fluid, so it is necessary to the brake fluid suitable to the performance. There can be used many brake fluids in brake system (DOT 3, DOT 4, DOT 5, DOT 5.1). Theses brake fluids have got different boiling points (dry and wet boiling points) (Cliff Owen, 2010). The heat does not affect directly the brake fluid. The brake fluid temperature depends on the material and design of piston because the piston connects the brake fluid.

The aim of this study is to compare the piston's material (aluminium alloy, steel, titanium alloy) and design and find the optimal construction where the temperature correspondents in brake fluid.

2. Material and methods

In this research there was a simple model was used to compare the different constructions (aluminium alloy piston, steel piston, titanium alloy piston). The aim was to determine the temperature in brake fluid. Finite element software (Ansys Workbench) was used in thermal research where the thermal properties of material were defined (1. table).

Table 1. Thermal properties of pistons

Aluminium alloy	0 ˚C	144 W/(m·˚C)
	100 ˚C	165 W/(m·˚C)
	200 ˚C	175 W/(m·˚C)
Steel	21 ˚C	21,9 W/(m·˚C)
Titanium alloy	21 ˚C	60,5 W/(m·˚C)

In this study pistons and related parts were tested too, so it was necessary to determine thermal conductivity in related parts. Brake fluid thermal conductivity is 0,15 W/(m·˚C) on 21 ˚C, Friction material thermal conductivity is 2,06 W/(m·˚C) on 21 ˚C (H.S. Qi, et al., 2007) and air thermal conductivity is 5 W/(m·˚C) on 20 ˚C. Simple model was used because it is a compare examination, so we didn't simulate the whole brake system, only the piston area. 2D axes symmetric model was used, which contain brake pad (friction material, steel plate), piston (aluminium alloy piston, steel piston, titanium alloy piston), brake fluid and the aluminium alloy caliper (Fig 1.). Mesh was made in simulation software where element size is between 0,01 mm and 0,3 mm. temperature between friction surface is 300˚C. In simulation air cooling was define in surface which is contact air.

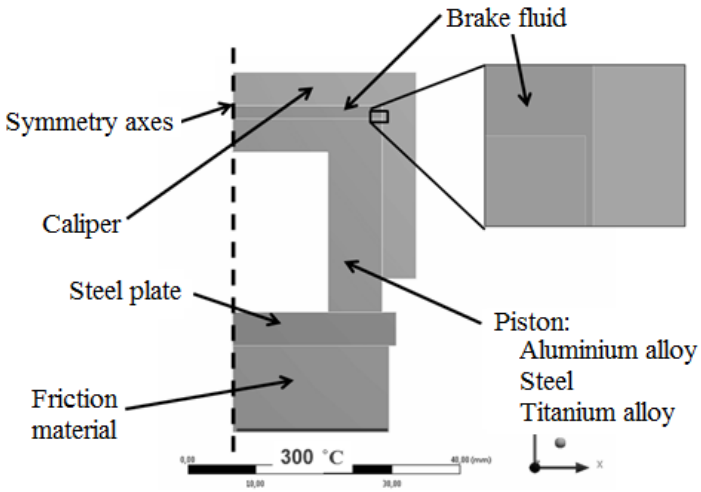

Figure 1. Finite element mode

Different constructions (material and wall thickness) were tested and defined temperature in piston and brake fluid. In the model the wall thickness was changed from 0,5 mm to solid piston. The piston diameter is 22 mm.

3. Results

The temperature was defined in all parts. Figure 2/a shows the temperature in titanium alloy piston. 8 points were defined to compare the different materials' and designs' temperature (Fig. 2/b.).

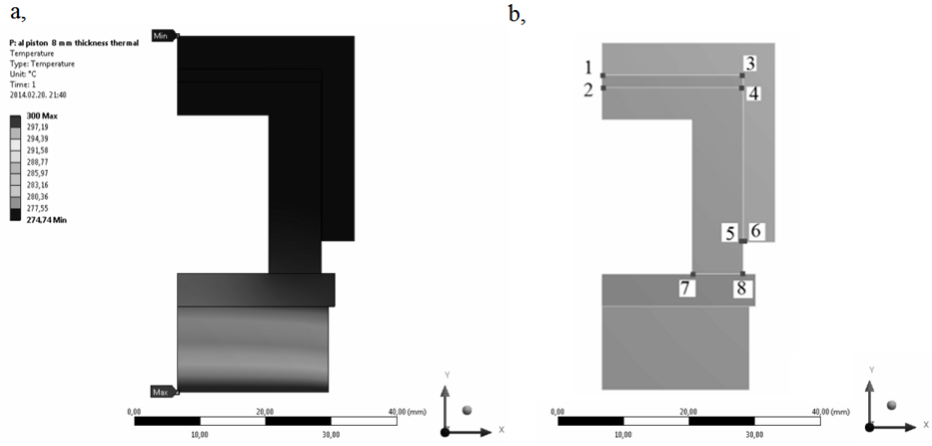

Figure 2. a, Simulation of titanium alloy piston;
b, test point on the model

Figure 3 shows the temperature (in 1-8 points) in pistons made of different materials. Aluminium alloy temperature is in figure 3/a. Figure 3/b. shows steel piston's temperature and figure 3/c. shows titanium alloy's temperature.

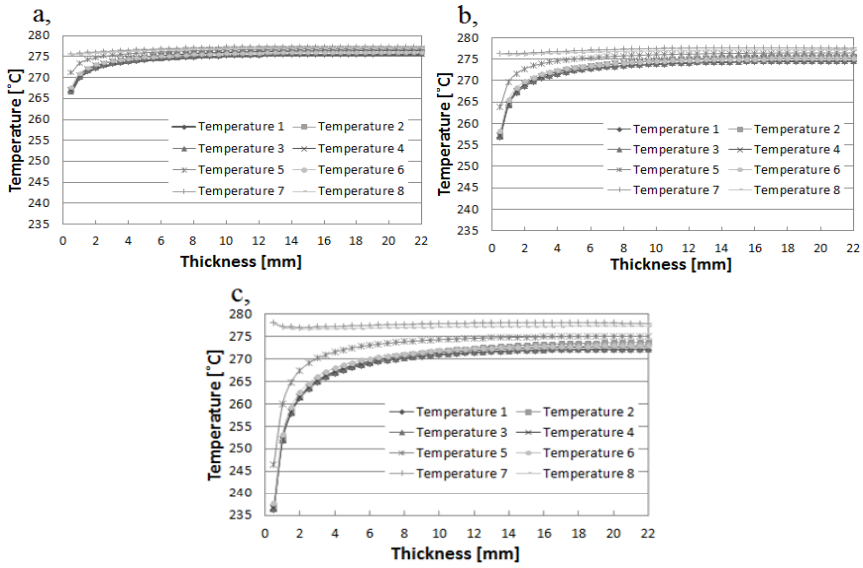

Figure 3. Temperature in test points: a, aluminium alloy piston; b, Steel piston; c, Titanium allyo piston

4. Discussion

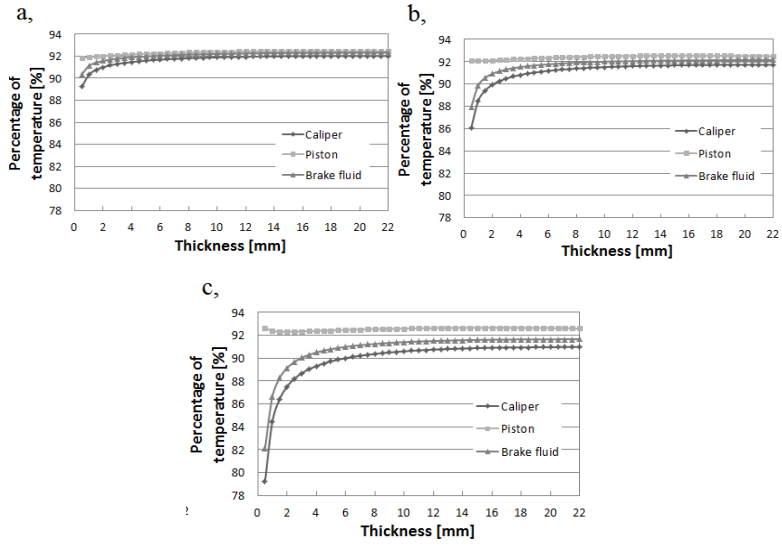

Figure 4. Brake system's specific temperature

Results show if wall thickness is small, the difference between temperatures is high. In case of large wall thicknesses temperature is similar. Temperature changes no significant in aluminium alloy construction over 4 mm wall thickness. In the steel construction temperature does not change significantly over 6 mm wall thickness. About titanium alloy, the temperature doesn't change over 8 mm wall thickness. The next graph (Fig 4.) shows how many percentage of initial temperature (300 ˚C) is in other parts (piston, brake fluid, caliper). You can see, that temperature is similar in all parts,initial temperature~92% is in parts. In case of small wall thicknesses the temperature is different in brake fluid, which depends on the material. When wall thickness is bigger, the temperature is similar. Figure 4. shows how the temperature changes depending on the piston geometry in different material.

Piston (Fig. 5/a.) and brake fluid (Fig. 5/b.)maximum temperature was compared to determine the optimal material and geometry.

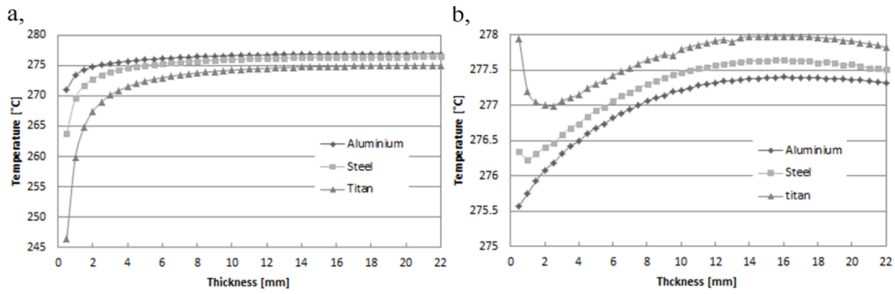

Figure 5. a, maximum temperature in brake fluid, b, maximum temperature in piston

These graphs show which material and construction is the best. Figure 5/a shows that brake fluid's maximum temperature is lowest (274, 99 ˚C) when titanium piston is in caliper. In case of aluminium and titanium piston's maximum temperatures are bigger (aluminium piston: 276.96 ˚C, steel piston: 276,45˚C). Figure 5/b. shows the pistons maximum temperature. Titanium and steel piston's maximum temperature have minimum point while aluminium piston's temperature is growing continuously in the function of the wall thickness. Titanium piston have worst thermal conductivity so the heat does not warm brake fluid but temperature is highest in piston. This properties is good, because the brake fluid doesn't have high thermal load, so titanium material is better than aluminium or steel material. Figure 5/b shows which geometry (wall thickness) is good for piston. The best wall thickness of titanium alloy piston is 2,5 mm because temperature is lowest in titanium piston (276,99˚C). Figure 5/b shows that titanium alloy and steel piston do not lead away the heat, so temperature is higher in case of small wall thickness (0,5 mm wall thickness, titanium alloy: 277,95˚C, steel: 276,45 ˚C). When the wall thickness is high the cooling influence is lower, so the piston's temperature is higher (15-17 mm wall thickness, titanium alloy: 277,98˚C,steel: 277,64˚C)

That study examines temperature of brake fluid and lay down that the material and geometry of piston do not affect significantly the brake fluid's temperature. It is necessary to apply a cooling system if the temperature is high in braking.

Conclusion

It was the aim to compare aluminium, steel and titanium pistons' thermal behavior. Thermal behavior was compared in finite element software, where similar model was used. The temperature was defined in different parts (caliper, brake fluid, pistons, brake pad) where friction surface temperature is 300˚C. In case of titanium piston temperature is 274,99˚C in brake fluid, this is the lowest temperature. When aluminium alloy piston is in caliper, the temperature of brake fluid is 276,96˚C. When titanium alloy piston was used temperature of brake fluid is 276,45˚C. By brake fluids it is important, that the heat load is the possible smallest one, because our braking system will be airy if the water in the brake fluid vaporizes. Temperature of piston was examined to determine optimal wall thickness. The best wall thickness is 2,5 mm where the temperature in piston is 276,99˚C. If the wall thickness is smaller than 2,5 mm, piston doesn't lead away the heat, so the piston's temperature is higher (0,5 mm wall thickness: 277,98˚C). Over 2,5 mm wall thickness cooling is not efficient, so the piston's temperature is higher (15-17 mm wall thickness: 277,98˚C).

References

[1] A. Belhocine, M. Bouchetara, (2012), Thermomechanical modelling of dry contacts in automotive disc brake, International Journal of Thermal Science 60, p. 161-170.

[2] Cliff Owen, (2010), Today's Technician: Automotive Brake Systems, Classroom and Shop Manual, 62.

[3] J. G. Balotin, P. D. Neis, N. F. Ferreira, (2010), Analysis of the influence of temperature on the friction coefficient of friction materials, ABCM Symposium Series in Mechatronics, p. 898-906

[4] K. Holmberg, P. Andersson, A. Erdemir, (2012) Global energy consumption due to friction in passenger cars, Tribology International 47, p. 221–234.

[5] P.D. Neis, N.F. Ferreira, F.J. Lorini, (2011) Contribution to perform high temperature tests (fading) on a laboratory-scale tribometer, Wear 271, p. 2660-2664.

[6] T.J. Mackin, S.C. Noe, K.J. Ball, B.C. Bedell, D.P. Bim-Merle, M.C. Bingaman, D.M. Bomleny, G.J. Chemlir, D.B. Clayton, H.A. Evans, R. Gau, J.L. Hart, J.S. Karney, B.P. Kiple, R.C. Kaluga, P. Kung, A.K. Law, D. Lim, R.C. Merema, B.M. Miller, T.R. Miller, T.J. Nielson, T.M. O'Shea, M.T. Olson, H.A. Padilla, B.W. Penner, C. Penny, R.P. Peterson, V.C. Polidoro, A. Raghu, B.R. Resor, B.J. Robinson, D. Schambach, B.D. Snyder, E. Tom, R.R.

Tschantz, B.M. Walker, K.E. Wasielewski, T.R. Webb, S.A. Wise, R.S. Yang, R.S. Zimmerman, (2002),Thermal cracking in disc brake, Engineering Failure Analysis 9, p. 63-76.

Failure of different steel alloys in army application

Zoltán SZAKÁL[1], György GÁVAY[3],
Gábor KALÁCSKA[2], József GYARMATI[3]
[1]Department of Material and Engineering Technology,
Institute for Mechanical Engineering Technology
[2]Department of Maintenance of Machinery,
Institute for Mechanical Engineering Technology
[3]Faculty of Military Sciences and Officer Training,
National University of Public Service,

Abstract

This paper shows metallographic tests of various plates which were hit by bullets. The aim of our research was to define how the crystal structure of the different kinds of armors changes during the penetration of the bullets. We examined three kinds of plates using different types of bullets. The plates that have been shoot had different hardness and the bullets had various speed. Specimens were made from the proper segments of the damaged armor plates. The examinations of metallographic specimens help us to define the changes of the crystals, especially the cracks as well as the size of the effect zone.

Keywords

defense capabilities, armor, material testing

1. Introduction

Research and development of armors becomes a very important area for the military and the civil security users nowadays. There is a significant need for good quality armor that has a low weight and great protection again up to date bullets explosives and IED (Improvised Explosive Device). Users of the armors are not only the army but also the police and civil security organizations.

One of the aims of the military industrial developments is enhancing the protective abilities of body armors, but the outcome is used by the police and the security also. The aim of the Research and Development of body armor is to extend the protection against the up to date special bullet that has a great hardness and muzzle velocity. These armors made from metallic and non metallic material also.

Another important application area of the armors is the civilian and the military armor protected vehicles. Using the new demands that based on the experiments of the last decades new class of armor protected vehicles was developed. These are the MRAP (Mine-Resistant Ambush Protected) that has a

great protection again the bullets, mines and IED and it has special quality and shape armor.

Base on the above mentioned and well known area the National University of Public Service, Faculty of Military Sciences and Officer Training, Department of Maintenance in Budapest and the Szent István University, Faculty of Mechanical Engineering, Institute for Mechanical Engineering Technology in Gödöllő launched a joint research. The aim of the research was to describe the material structure changes during the shutting, therefore an experimental test was carried out. The standards about the ballistic resistance of armors don't define the damage of metallic structure [1] [2].

During the test three different kinds of plates was shouted using three different kinds of bullets. In this experiment, 150 shot has been fired. Grindings were made from the proper segment of the bullet hit armor, and examining of these the changes of the crystals was defined especially the cracks.

During the examination of the grindings the next topics was examined:

- the crystal structure of steels;
- the changes of the rolling grain;
- the formation of cracks;
- the size of damaged zone of the plate;
- the fragment formation from the plates;
- the bullet deformation.

2. Research objectives

The original objective of the research was to document the process of bullet penetration through the metallic material.

Plates cut from three steel types with different quality have been used for the examination:

- a hot rolled steel plate with 8 mm thickness;
- 8 mm armour plate of a Russian made armoured vehicle;
- 6.5 mm armour plate that is used for the civil security service vehicles manufactured nowadays.

The aim of the examinations of the hot rolled steel plate was the comparison with the armour plates, so it was used as a reference plate.

The plates were shot with bullets having different material and speed. The speed of the bullet was set with the alteration of the gunpowder charge weight. The following principles have been taken into consideration when planning the impact speed:

- there has to be penetration and dent;
- the damaged plates have to comparable, so the different plates have to be shot with bullets having the same type and speed.

In the interest of credibility all shots having the same parameters were executed three times (with the same cartridge and gunpowder charge, as well as plates having the same material). Based on this the detailed research objectives were the following:

– documentation of the changes happening in the metallic crystal structures of the different steel types;
– identification of the damage zone;
– identification of the defence capability reduction based on the deformation and structural change in case of dent;
– influence of the mechanical properties of steel on penetration;
– influence of the bullet's rigidity on penetration.

3. The process of measurement

Test shooting
An authorized / certified test shooting range was rented for the execution of the test shooting. The shooting range provided us the cartridge for the shooting with the correct gunpowder charge. The shooting was executed with a ballistic test barrel[1]. The main elements of the laboratory are shown by Figure 1.

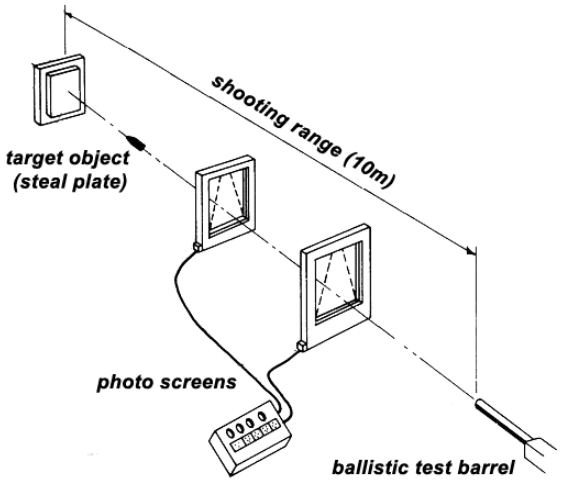

Figure 1. The main elements of the laboratory

Mechanical researches
The supplier provided a self-certification for the reference plate and 6.5 mm armour plate, mechanical examinations have been carried out on the bullets used for the research and on the 8 mm plate.

The measured and available data of the plates:
– armour plate with 8 mm thickness, the tensile strength (R_m) is 1400 N/mm^2, hardness is 288 HV 30;

[1] A fixed and balanced barrel with a special configuration and increased thickness.

– armour plate with 6.5 mm thickness, the tensile strength (R_m) is 1700 N/mm^2;
– tensile strength of the reference plate (R_m) is 400 N/mm^2.

The 8 mm plate contained 1.26% manganese, while the 6.5 mm plate contained 1.18% and the reference plate contained 0.6%. Two different bullets were used for the examination, one with soft steel core and 166 HV30 hardness, the other with carbid core and 905 HV30 hardness.

Preparation of plates for specimen production

The cutting specimen is shown by Figure 2. The cutting took place along the "a", "d" and "b" edge of Figure 2, to make the configuration of the specimens shown on the right side of Figure 2 possible. The examination could be carried out in the direction of the strands in the rolled plate (along the "c" edge) and sheer as well (parallel surface with the „a" edge).

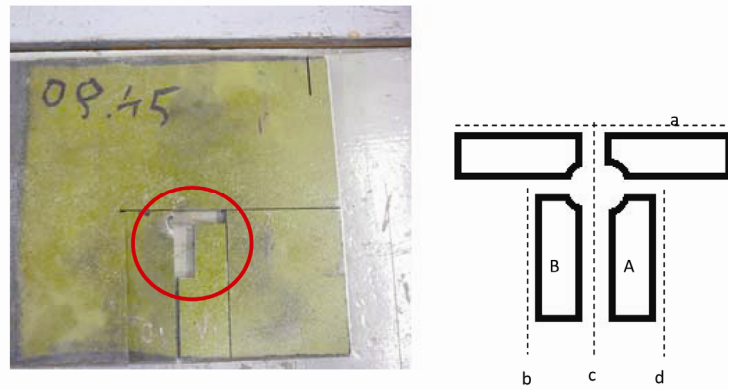

Figure 2. precut of the plates

Production of specimens

102 specimens were created during the research. Figure 3 shows a specimens.

Figure 3. Specimens

Analysis of specimens

The specimens were analysed on the faculty of Mechanical Engineering of SZIE. The prepared specimens were examined with a microscope. Figures 4a and 4b show the damaged surfaces of the examined materials.

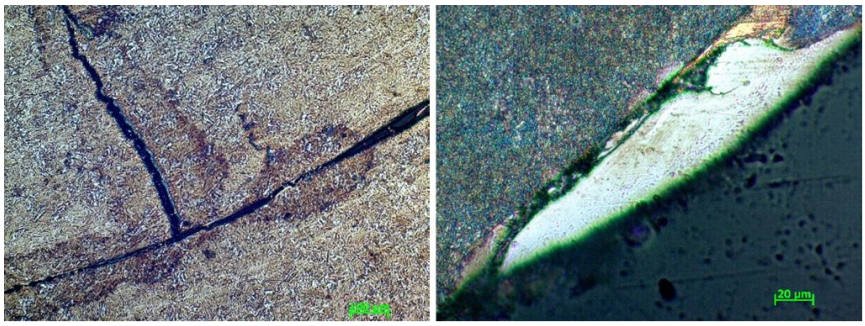

a) b)

Figure 4. Pictures of the examination
a)cracks in the direction of the strands in the rolled plate and sheer as well,
b) foreign material on he damaged surface

The results of the examination

During the analysis of the specimens the damaged materials could be sorted into 3 groups based on the deformations:

- in the first case the material behaved rigid under the examination circumstances, penetration of the bullet took place;
- in the second case the material behaved tough under the examination circumstances, penetration of the bullet took place;
- in the third case there was no bullet penetration, only dent.

Figure 5,a demonstrates the rigid behaviour of the material. When the bullet entered the material, it pushed the material in front of itself, in which the increased tension tore the backside, while no permanent deformation happened.

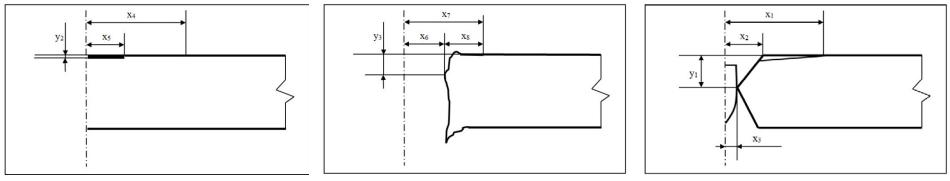

a) b) c)

Figure 5. a) The rigid behaviour of the material;
b) The tough behaviour of the material;
c) No penetration happened

Figure 5,b demonstrated the tough behaviour of the material. In the moment of bullet impact the encounter of the plate and the cartridge caused a crater-like folding, after which the bullet pushed the material in front of itself during the impact and a tension greater than the material's yield point evolved because of the increased loading. During penetration the bullet did not push out a significant amount of material, but it was distorted into its environment.

Figure 5,c demonstrates when no penetration happened, the bullet only bruised the surface. The material compacted in the impact zone (x_5).

The damages that belong to the groups where penetration happened were different, but it could be stated, that the border of the material structure changes deformation zone was never more than 2mm measured from the edge of the damage. It was 5mm if measured from the centre of the hard metal / carbid bullet core (centre of the hit). The quality of the damages was different based on the ranges, used bullets and the quality of the targets. When the same bullets and target, but another range were used, the difference in the amount of material structure changes could be observed. Based on the examination of the specimens it could be stated that the penetration of the reference material did not cause any cracks in the material's deformation zone area. In these cases none or only a minor fragmentation effect could be expected. The deformation speed caused by the impact of the bullet did not exceed the material's typical amount in any of the penetration phases, so no brittle fracture occurred.

In cases of penetration the examined armour suffered permanent structure changes, in which cases the bullet entering the inside of the material deformed the strands in the rolled plate. The core of the carbide bullet did not deform, the tips of the collected bullets remained uninjured. The local tension peak evolving at the bullet's tip caused cracks in one part of the material. The core of the bullet expanded the cracks and so moved forward while ripping out the material in front of it and as a result fragmentation effect was caused. The strands in the rolled plate leaned near the ripped part of the material. The tightest part of the hole that evolved after the penetration – which is approximately the same size as the core of the bullet – can be found in the middle of the material thickness, and this hole broadens in the shape of a cone towards the other side. Friction evolved between the touching materials during the penetration of the bullet. The tensile stress caused by the friction tore down the rear part of the bullet, which still broke through the plate.

In case of bullet penetration the environment of the hole that evolved in the 8 mm material was smooth, cracks parallel with the hole could only be observed in some cases.

With the same calculated shooting range and bullet type the 6.5 mm armour material was damaged in a similar way. In these cases the evolved cracks were parallel with the strands in the rolled plate that formed during the manufacturing of the raw material. With the increase of the energy of the impact, new cracks causing material tear formed sheer to the previous ones. Figure 6,a demonstrates when this was presumably caused by the fact that the friction formed during the penetration of the bullet core was bigger than in case of the 8 mm plate.

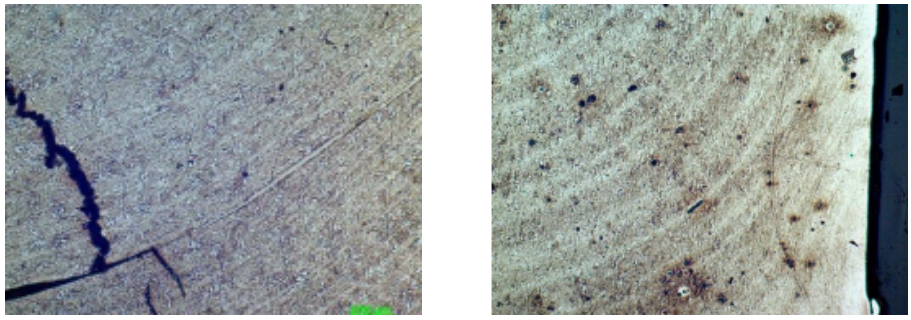

a) b)

Figure 6. a) armour plate with 8 mm thickness; b) armour plate with 6,5 mm thickness

The rigidity and so the compressing force developing the friction was bigger in case of the 6.5 mm plate, shows 6,b Figure. According to the experiments the 6.5 mm armour material provides the same penetration protection as the 8 mm plate, although it has a smaller material thickness. At the same time a larger fragmentation effect evolved due to the separation of the layers of the rolled plate in case of bullet penetration.

The soft core bullet only broke through the reference material during the tests. At the time of the penetration the bullet core as well as the target object suffered permanent shape changes. The deformation of the core was significant, the size of the mushroom-like shape was two times the original diameter of the bullet, shows 7 Figure.

Figure 7. The mushroom-like shape of the bullet

The microscopic metal examination proved that no cracks evolved in the deformation zone of the reference material in case of shots resulting in penetration.

The soft steel core only bruised the 8 mm material, but there was no bullet penetration. The material deformed close to the fractured surface, in maximum 1 mm distance. The depth of the dent and the height of the convex surface that formed on the rear side of the plate is different in case of the various shots. Even

in case of the smallest, 10 m shooting range neither reached 0.1 mm. No major changes in the material structure happened apart from the compressed layer. The strands in the rolled plate became disfigured in the deformation zone, but the material structure remained undamaged beyond the zone.

In case of the 6.5 mm armour plate the same impact energy didn't just cause deformation near the surface. The whole structure of the material expanded like a "rubber band". The impact left a visible mark at the rear side of the plate. No cracks appeared in either cases and there was neither material tear nor fragmentation effect.

The 10 m range shot and mild steel core bullet caused cracks leading towards the centre of the material at the border of the buckle zone on the 6.5 mm material.

Summary and further areas of research

A penetration examination method that uses standards, but is more detailed has been developed during the research. This method can be further improved in the direction of the simulation examination of target material's fragmentation effect and structural deformation.

Further research areas can be the following:

- supplying of data for the computer simulation in case of different range shots;
- examination of the consequences of works that are needed when configuring the ballistic protective components and cause changes in the material structure in case of different range shots;
- examination of the fragmentation effect in case of different range shots;
- examination of the penetrating bullet's orbit, movement, energy, killing and injuring effect depending on the shot range, bullet type and target material;
- examination of the armour's protection capability;
- deformation caused by the bullet having decreasing speed because of the increasing shot range.

References

[1] MSZ K Standard 1114-1 (1999) Body armours. Bulletproof vests

[2] NIJ Standard 0101.06 (2008) Ballistic Resistance of Body Armor

[3] Dr. Gyarmati József – Prof. Dr. Kalácska Gábor – Dr. Szakál Zoltán – Gávay György – Sebők István: Lövedék páncéllemezen történő áthaladás metallográfiai vizsgálata Hadmérnök, IX. évfolyam 3. szám 2014. pp: 91-104. ISSN 1788-1919

[4] Sebők, I., Gávay, G. Destructive testing of metallic and non-metallic material - Mechanical Engineering letters: R and D: Research and development (2013) pp. 28-33.

Friction of PA6 and peek composites in the light of their surface characteristics

László ZSIDAI[1], Zoltán SZAKÁL[2]
[1] Department of Maintenance of Machinery,
Institute for Mechanical Engineering Technology
[2] Department of Material and Engineering Technology,
Institute for Mechanical Engineering Technology

Abstract

Our present work is connected to a broad tribology research project with different polymer composites on PA6, POM, PET and PEEK matrix and targeted to create a detailed map of tribological features. Measuring the hardness and surface energy of the tribology tested materials gave some new approach about friction results. The small-scale laboratory friction tests were carried out with an alternating (reciprocating) cylinder/plate model system, which is able to measure the dynamic and the static friction force on-line during the sliding process. This special test system opens up new possibilities for understanding the phenomena of friction. In the article we give a short introduction from the surface energy and the shore D hardness test methods also.

The research results plot a connection between the surface (polar and adhesion components) energy and the friction (static and dynamic) behaviour. Furthermore the experienced difference between the static and dynamic friction coefficients and its time function will offer a new approach during evaluation of the stick-slip behaviour of PA6 and PEEK composite materials.

Keywords

friction, PA6, PEEK, polymer, composites, surface energy, shore D

1. Introduction

Our work is part of a larger research project that deals with the tribology behaviour of engineering polymer composites. The present paper shows the results of the linear sliding friction measurements of the different polymer/steel pairs using a reciprocating cylinder-on-plate test apparatus. No external lubricants were added to the tribological system. We give an overview about the results of hardness and surface energy measurement of tested polymers and intern alia the mapping of stick-slip is also.

This work is trended towards the examination of the reliability of engineering plastics in sliding (tribology) polymer-polymer and polymer-metal contact systems, through the complex tribology exploration of characteristics.

Base Principles

The tribological properties of polymers strongly depend on the properties of the sliding surface. To create we used so-called, small-scale tests are quite obvious, e.g. simple test rig with low forces and power, reduced cost for preparing test specimens, easy of control of environment. Moreover many small-scale results are available in literature to be referenced, e.g. Sukumaran, et al. (2012), Zsidai, et al. (2002). They are useful to compare the properties of different materials, but induce unrealistic edge effects.

As an examined materials from among the engineering polymers are the several of the variants composites based on PA6 (polyamide 6), PEEK (Polyether ether ketone) PET (Polyethylene terephthalate) and POM (Polyoxymethilen) polymer matrix (with a lubricant charged and/or are with thread strengthening), and the mating plates are steel (and polymer) we used his application.

Several studies on the tribological behaviour of common engineering plastics e.g. Uetz, Wiedemeyer (1985), Kalácska, et al., (1997), Yamaguchi (1990), Kalácska (2007, 2013) in contact with steel have been published and compared by, e.g., Tanaka (1982), and Evans (1982). We can found in the research character in connection with base polyamide, Byett (1992), De Velde, De Baets (1997), Keresztes (2010) and the base PEEK, Yamamoto et al. (2002) in sources also. The number of the articles dealing with the composites is growing nowadays, e.g., Friedrich et al. (1995), Sumer et al. (2008) and Schroeder et al. (2013). We can found more publications about the role of the stick-slip tribology also e.g., Kátai at all (2001, 2013).

I characterize the polymers with complex tribology examinations, taken into consideration the material testing (tensile and hardness examinations) his results.

Aims

The main objectives of the investigation are the comparison of friction and surface morphology of different engineering polymers in connection with their surface energy and hardness properties. There is also important to describe of optimal operational conditions of the selected polymers.

Further aims of the research: to determine the optimal operational conditions of the selected polymers, and to give a help for the selection of a proper polymer for a certain condition and to find out the causes of friction.

2. Test rigs, materials and results

The present paper describes the linear sliding friction measurements of the different polymer/steel pairs using a reciprocating cylinder-on-plate test apparatus. No external lubricants were added to the tribological system.

The experimental tribo- model system as pictured in figure 1 is essentially a variant of the commercially available reciprocating tribotest.

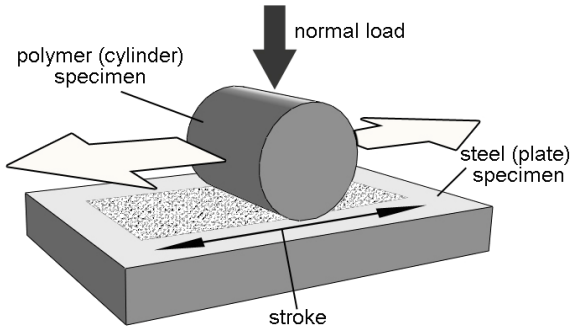

Figure1. Reciprocating model system

Accurate description of the test system and evaluation of the test results prior publication in view. [Zsidai 2013, 2014]

Test conditions

All experiments are performed at ambient conditions of temperature and humidity (30 °C and 50% RH). The various conditions of the performed small-scale tests are gathered in Table 1.

Table 1. Parameters of tests

Parameters	Values
Surface of steel specimen, R_z [μm], (R_a [μm])	1,7 (0,16)
Running time, t (sec)	130
Normal load, F_N [N]	150
Frequency, f [Hz]	10
Velocity, v [m/s]	0,05
Stroke, s [mm]	6
Humidity, RH [%]	50
Ambient temperature, T (◦C)	30

Tests are conducted with normal load: 150 N. The running time (130 sec.) of the tests is chosen for to observe the first (running in stage) period of the friction. For each test, the surface roughness's of the steel specimen were used R_z 1,7. The tribological data described below result from an average of three runs with identical experimental parameters.

Materials and preparation of test specimens

The selection of the tested 10 polymers and composites was made on the database of polymer producers, end-users and expertizing companies at this field. The finally selected engineering polymer materials can be taken as

generally used engineering materials in the industry in sliding systems. Some of the like polyamides are well-known but some composites are just being spread.

The materials are two main composites groups. One of them is with PEEK and the other is with PA6 base matrix are included in the experiments. In addition to the foregoing I tested other polymers (POM and PET) also.

Material of the mating plate

The counter plates are made of widely used, C45 general purpose steel. The application area of C45 is a less demanding but wear-proof. The heat conduction: 46 W/(mK) and the standard is EN 10083. The plate dimensions are 200×100×12mm and for preparing the steel surfaces are used grinding (R_a=0,11-0,18 μm ≈ R_z=1,4-1,7μm) The grinding grooves are made parallel to the sliding direction during the wear tests. Roughness is measured perpendicular to the sliding direction.

Materials of the polymer cylinders

- The polyamides PA 6E of the extruded type, were used as a reference material in the investigations. This polyamide is strategic engineering plastics for many years all over the world, thanks to the favourable performance / price ratio. The PA 6E favourable combination provides the rigidity, toughness, mechanical damping ability and wears resistance of polyamide product „general purpose „type called.
- The PA 6G ELS is the conductive version of magnesium catalysed cast polyamide 6.
- The PA 6MO (PA 6E+MoS2) for molybdenum disulphide (MoS2) content greater strength and stiffness than the PA 6E. The heat and wear resistance are also improved, but the toughness and mechanical damping capacity worse.
- PA6 GLIDE is a hard semi-crystalline cast polyamide with good sliding properties, wear resistance, oil-, grease-, gasoline-, gas oil resistance and easy machinability.
- PA next 66 MH shows good sliding properties, stiff, high resistance to oils, greases, petrol, gas oil, UV and weather resistance, electrical insulation and easy machinability. In shipping, packaging structures, electronic equipment, printers, and precision engineering are used.
- Natural unfilled PEEK, reinforced poly (ether-ether-ketone). Briefly to 310 ° C can be used, suitable for permanently around 250 ° C.
- PEEK PVX (PEEK CF+PTFE+graphite) real bearing grade. Carbon fibres, graphite and PTFE filler.
- PEEK GF30 (PEEK GF+30) 30% glass fibre reinforced for greater dimensional stability and higher strength properties.
- PET TF amorphous or semi-crystalline thermoplastic material as is also available. Low moisture absorption properties due to extremely useful in areas where complex components and high dimensional accuracy, surface quality is required.
- POM AH LA solid lubricant is added which improves the sliding properties and wear compared to the normal behaviour of POM,

however, impairs the mechanical properties (strength, hardness). Excellent electrical insulation, good to work with, but in terms of weak bonding authority. The conveyor technology, the automobile industry, electronic equipment and precision instruments are used.

– POM AD AF semi-crystalline thermoplastic bearing material has a low coefficient of friction, high strength, stiffness and excellent process ability. Application area: Engineering, automotive, transport and conveyor technology, electronics, precision mechanics, medicine.

Table 2 gives an overview of the properties of the tested engineering plastics. Among these properties the E-modulus can be used to characterise the adhesion friction component, since it is correlated with the chain flexibility. [19], [20]

Table 2. Mechanical and physical properties of the tested polymers [1], [2]

Material code	**colour**	**density [g/cm^3]**	**Tensile strength at yield/ Modulus of Elasticity [MPa]$^{(1)}$**
PA 6E	black	1,13	85/3000
PA 6G ELS	black	1,15	70-110/-
PA 6MO	black	1,14	82/3300
PA 6 GLIDE	green	1,13	76/3200
PA 66 MH	black	1,14	75/2500
PEEK	brown	1,31	100/4100
PEEK PVX	black	1,44	84/5500
PEEK GF30	brown	1,53	180/9500
PET TF	grey	1,44	73/2900
POM AH LA	blue	1,34	45/2300
POM AD AF	black	1,54	50/2900

$^{(1)}$ Values referring to material in equilibrium with the standard atmosphere 23 ◦C/50% RH

The polymer cylinder has a diameter of 8mm and length of 10mm and made by cutting. The figure 2 shows the tested polymers in original form.

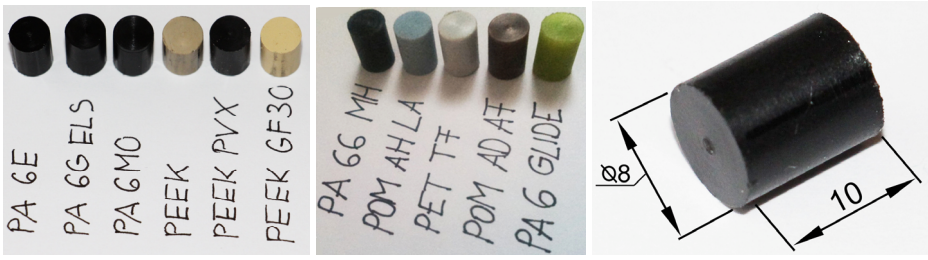

Figure 2. Original form and dimensions of the tested polymers and composites.

The cylindrical specimens are in counter formal connection with the steel plate. The components of composites are homogenously spread in the bulk of polymers.

The measurement method and results of the surface energy
The dynamic friction coefficient is represented in Figure 3. For each material, the dark part of column refers to the regime value of dynamic friction coefficient and the lighter one refers to the maximum value of dynamic friction coefficient. All values are averaged from three test runs with identical parameters.

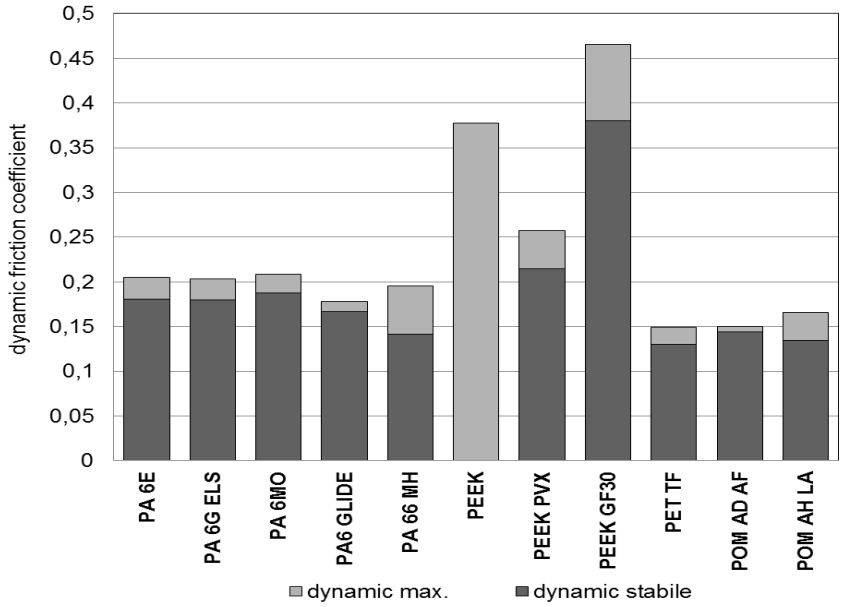

Figure 3. Dynamic friction coefficient for different polymers
(sliding distance = 7m; load = 150 N;
surface roughness R_z= 1,7μm)

Let's see the figure. 3, there is a general tendency that friction coefficient is similar and low (0,15-0,2) in case of polyamides (PA). The lowest frictions are present by POM and PET. From the point of view of friction, PEEK is unfavourable and in case of natural PEEK not stabilized friction.

Measurement of the hardness test polymers
For examined in the research of hard polymers called polymers I had to use this „Shores D" measurement device is shown in figure 4. The Quattroplast Ltd. courtesy of the tool used in material testing labour.

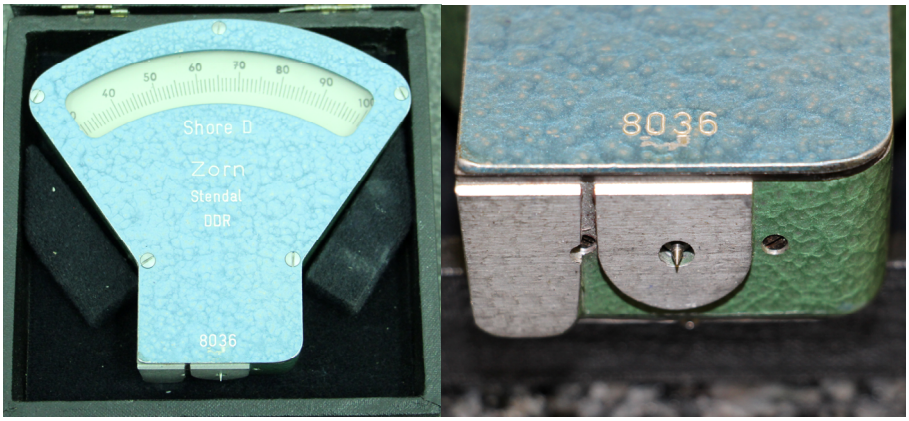

Figure 4. The „Shore D" hardness tester and the sharpe pin for measure the „hard polymer" (type: Zorn Stendal, 8036)

The tests were carried out after calibration the instrument. Each measurement was repeated three times and the specimens are checked several sides but did not observe differences.

The results are depicted in the diagram as seen in figure 5 in order to enhance comparability.

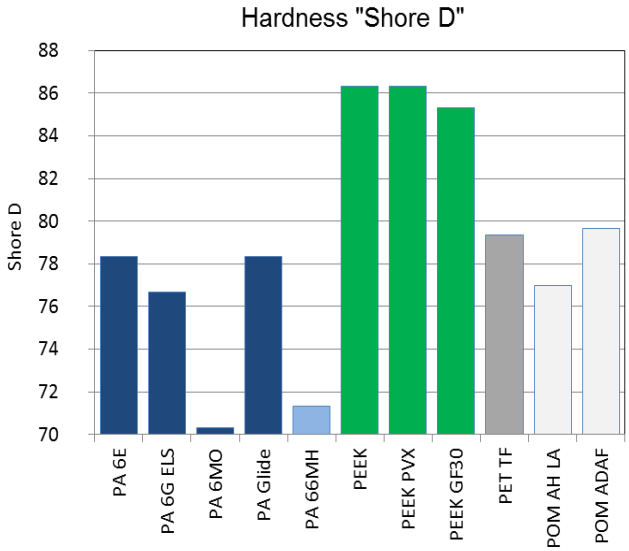

Figure 5. The results of „Shore D" hardness test

The results will be used later in the analysis of the tribology characteristics and phenomena.

The measurement method and results of the surface energy

Contact angle measurements were performed by the static sessile drop method. Double distilled water and N,N-dimethylformamide (DMF, Sigma-Aldrich) were applied as test liquids. An automatic pipette (Biohit Proline, 2-20 µl) was used to inject 10 µl droplets. The measurements were done at 25 °C. Images were made by a digital microscope (dnt DigiMicro 2.0 Scale, Dietzenbach, Germany) with image resolution of 65 pixel/mm. The contact angles were determined using image analysis software (ImageJ 1.48v, Wayne Rasband, National Institute of Health, USA) with "Low Bond Axisymmetric Drop Shape Analysis" (LB-ADSA) [Aurélien (2010)] and Drop Snake [Stalder (2006)] plugins. The results of contact angle are an average of three measurements, performed always on dry parts of the samples. The method of Owens and Wendt was used for the calculation of the total surface energy and its polar and dispersive components. [Owens (1969)]

Figure 6. Water drop on the specimen surface during the test.

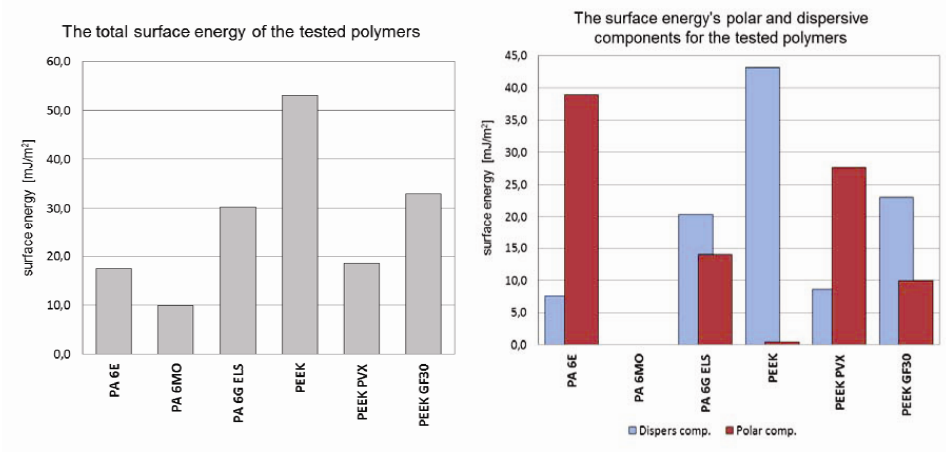

Figure 7. The result of the drop test (total, polar and disperse components of surface energy)

3. Discussion

According to generally accepted friction models, two mechanisms contribute to the friction force between a polymer (composite) and steel: adhesion in the contact zone and deformation of the polymer [Hutchings (1992), Wiedemeyer (1985), and Zsidai (2002)].

Their relative contribution depends on the load level as well as on the chemical, mechanical and geometrical properties. For softer polymer the deformation component increases, while for harder the adhesion becomes more important. The friction component resulting from adhesion equals the product of the real contact area and the strength of the polymer (softest) material [Bowden, Tabor (1950)].

Besides the hardness, the adhesion ability of polymers can differ to a great extent because of specific surface characteristics of the material, which is expressed by its surface energy. Lee [1974] considers that the surface energy plays an important role in controlling the friction of polymers. From literature, it is known that the total surface energy of PTFE is low, while PA has the highest surface energy. POM is also ranked among the polymers with higher surface energy [Kalácska (1997)]. This correlates with the low adhesion work in PETP/PTFE contacts and the high adhesion work between PA contacts.

In Figure 8. the dynamic friction results of the tested polymers are plotted against their Shore D hardness.

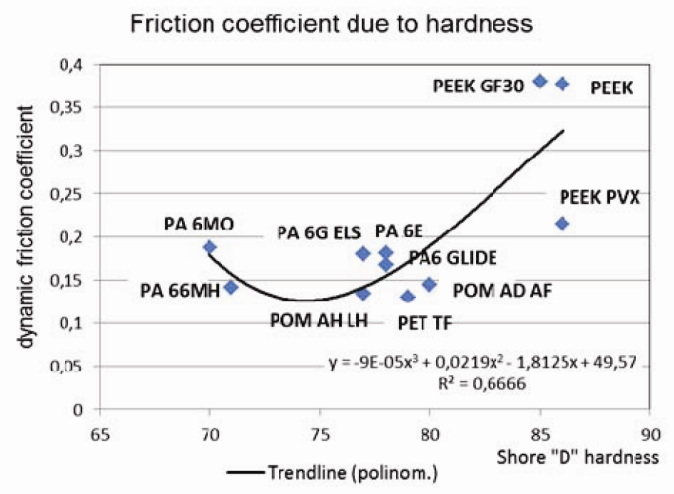

Figure 8. The dynamic friction results of the tested polymers are plotted against their Shore D hardness

From the trend lines, the following conclusions are drawn in the figure:

- For the lowest friction is an optimal hardness near Shore D 75, but after this value the friction increases with increasing hardness, this is mainly

true in case of the PEEK and their composites. This phenomenon could be connecting with higher elasticity modulus near the harder surface properties of the PEEK. However the friction increases slightly in front of Shore D 75 in case of PA 6MO and PA 66MH also, now because of the weaker mechanical properties.

In Fig. the dynamic friction results of the tested polymers are plotted against their total-, disperse- and polar surface energy.

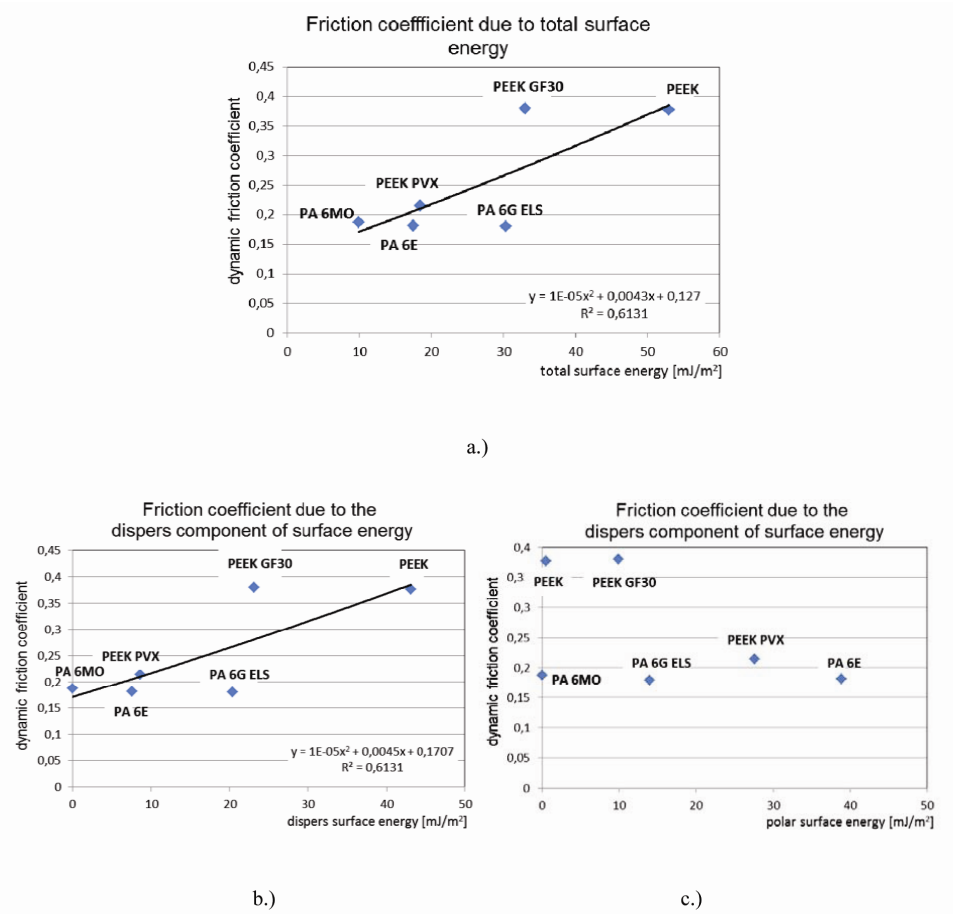

Figure 9. The dynamic friction results of the tested polymers are plotted against their (a) total-, (b) disperse- and (c) polar surface energy.

From the trend lines, the following conclusions are drawn:

– Friction increases similar with increasing total and disperse surface energy. However, this trend was not observed in the polar energies, because it was not observed a clear trend in the evolution of results. This may cause the wide range of the mechanical properties of tested polymers.

The results of the surface energy due to friction obtained in the future by further studies need to be completed.

Conclusions

Although the used reciprocating cylinder-on-plate test rig is not able to provide absolute data representative for actual applications, the tribological behaviour of different polymers can be compared successfully and correlated to materials properties.

The experimental data suggest the following conclusions:

- There is possible to determine an optimum point between the hardness and the friction of the tested polymers, but this is largely depending on the material characteristics and the type of composite.
- The dynamic friction of the tested polymers increase with increasing total surface energy and also increase with increasing disperse component of the surface energy.
- There was not success to identify a clear trend between the friction and the polar component of the surface energy. Previously for other polymers that could [Zsidai (2002)], so further studies are needed.

Acknowledgements

The author (László Zsidai) would like to thank MTA (Hungarian Academy of Sciences) for supporting this work in the frame of the research fellowship BOLYAI (BO/00127/13/6).

Special thanks go to Barna Szabó (Department of Pharmaceutics, Semmelweis University) and the QuattroPlast for the delivery of material specimens.

References

[1] A.F. Stalder, G. Kulik, D. Sage, L. Barbieri, P. Hoffmann (2006): A snake-based approach to accurate determination of both contact points and contact angles, Colloids and Surfaces A: Physicochem. Eng. Aspects 286 (2006) 92–103

[2] Aurélien F. Stalder, Tobias Melchior, Michael Müller, Daniel Sage, Thierry Blu, Michael Unser (2010): Low-bond axisymmetric drop shape analysis for surface tension and contact angle measurements of sessile drops, Colloids and Surfaces A: Physicochem. Eng. Aspects 364 (2010) 72–81

[3] D.K. Owens, R.C. Wendt (1969): Estimation of the surface free energy of polymers, Journal of Applied Polymer Science 13, 1741–1747.

[4] Evans, Dc; Senior, Gs (1982): Self-lubricating materials for plain-bearings, TRIBOLOGY INTERNATIONAL Volume: 15 Issue: 5 Pages: 243-248

[5] F. Van De Velde, P. De Baets, The friction and wear behaviour of polyamide 6 sliding against steel at low velocity under very high contact pressures, Wear 209 (1997) 106–114.
[6] F.P. Bowden, D. Tabor (1950): The Friction and Lubrication of Solids, Clarendon Press, Oxford, 1950.
[7] Friedrich, K; Lu, Z; Hager, AM (1995): Recent advances in polymer composites' tribology ,WEAR Volume: 190 Issue: 2 Pages: 139-144
[8] G. Kalácska- L. Zsidai- M. Kozma- P. De Baets: Development of tribological test-rig for dynamic examination of plastic composites. Hungarian Agricultural Engineering. N.12/1999. Hungarian Academy of Sciences. p. 78-79.
[9] G. Kalácska, et al., (1997): Műszaki műanyagok gépészeti alapjai (Mechanical Basics of Polymers), Minervasop Bt. Sopron,
[10] H. Uetz, J. Wiedemeyer, (1985): Tribologie der Polymere, Carl Hanser, Munich,
[11] I.M. Hutchings, (1992): Tribology, Friction and Wear of Engineering Materials, Arnold, London, 1992.2, 6H.
[12] Issue: 1 Page: 183-199
[13] J. Sukumaran, M. Ando, P. De Baets, V. Rodriguez, L. Szabadi, G. Kalacska, V. Paepegem (2012): Modelling gear contact with twin-disc setup, Tribology International 49 (2012) 1-7
[14] J.H. Byett, C. Allen (1992): Dry sliding wear behaviour of polyamide-66 and polycarbonate composites, Trib. Int. 25 (1992) 237, Pages: 237-246
[15] Kalácska G. (2013): An engineering approach to dry friction behaviour of numerous engineering plastics with respect to the mechanical properties. EXPRESS Polymer Letters Vol.7, No.2 (2013) pp. 199-210.
[16] Kalácska G. ed. (2007): Műszaki polimerek és kompozitok a gépész-mérnöki gyakorlatban. 3C-Grafika Kft. p. 1-315. ISBN-10: 963-06-1566-5, ISBN 13: 978-963-06-1566-2
[17] Kátai L., Szendrő P., Vincze GY., Szabó I. (2001): Determination of Inner Viscosity of V-belts by Bending Test. In: *Hungarian Agricultural Engineering*, 14/2001 p.31-33.
[18] Kátai László, Szabó István, Gárdonyi Péter (2013): EXAMINATION OF V-BELT TEMPERATURE CONDITIONS, GÉP, LXIV. évfolyam. 2013. 6. szám p.:58-61
[19] Keresztes R., Kalácska G. (2010): Research of machining forces and technological features of cast PA6, POM C and UHMW-PE HD 1000. Sustainable Construction & Design. 2010. Vol.1. p. 136-144.
[20] L. ZSIDAI, Z. SZAKÁL (2013): Development of tribology model systems for research of PA6 and PEEK polymer composites, Mechanical Engineering Letters, Szent István University p.:130-139
[21] L.H. Lee (1974): Effect of surface energetic on polymer friction and wear, in: L.H. Lee (Ed.), Advances in Polymer Friction and Wear, Vol. 5A, Plenum Press, New York, 1974, p. 31.
[22] Schroeder, R.; Torres, F. W.; Binder, C.; et al. (2013): Failure mode in sliding wear of PEEK based composites , WEAR Volume: 301 Issue: 1-2 Pages: 717-726
[23] Sumer, M.; Unal, H.; Mimaroglu, A. (2008): Evaluation of tribological behaviour of PEEK and glass fibre reinforced PEEK composite under dry

sliding and water lubricated conditions ,WEAR 265 Issue: 7-8 Pages: 1061-1065

[24] Tanaka K. (1982): Transfer of semi-crystalline polymers sliding against a smooth steel surface WEAR 75

[25] Y. Yamaguchi (1990): Tribology of Plastic Materials, Tribology Series 16, Elsevier, Amsterdam DIN 50322, Kategorien der Verschleißpru¨ fung, Deutsche Norm 50322, Beuth Verlag, 1986.

[26] Yamamoto, Y; Takashima, T Source (2002): Friction and wear of water lubricated PEEK and PPS sliding contacts ,WEAR Volume: 253 Issue: 7-8 Pages: 820-826

[27] Zsidai L., et al. (2002): The tribological behaviour of engineering plastics during sliding friction investigated with small-scale specimens. Wear, 253 673-688. p.

[28] Zsidai László, Kalácska Gábor (2014): „Stick-slip" PA és PEEK kompozitok súrlódásánál, henger/sík modell vizsgálati rendszerben, Műanyag és Gumi 2014/12 (in press)

[29] ENSINGER essentials. Technical know-how for plastic applications. www.plastic-metal.com

[30] www.quattroplast.hu/files/file/B_kategoria.pdf

Institute of Engineering Economics and Management

Associate Professor Dr. Miklós DARÓCZI
Director of the institute

Dear Reader,

Our Institute consists of three professional areas called departments:

- Department of Applied Management,
- Department of Engineering Economics,
- Department of Material Handling and Logistics.

The activity and the research fields of the Institute can be separated by these departments, and had the following main research activities during 2014:

Department of Applied Management:

- Theoretical and practical questions of agricultural innovation and technical development.
- Some areas of applied management sciences (e.g. Project-, Quality-, Enterprise-, Production-, Innovation- and Strategic Management).

Department of Engineering Economics

- Economics and management of farm machinery.
- Economic analysis and cost management in farm machinery and agricultural technical development.

Department of Material Handling and Logistics

- Theoretical questions of designing of machines of material handling.
- The significance of post-harvest logistical tasks in the field vegetable production.

The results of our activities were published not only in Hungary but worldwide in different papers and conferences.

The educational activity is very important in our Institute. We have developed the curriculum of our Engineering Management (BSc & MSc) Programs. Some of our colleagues teach several subjects also in English like Quality Management, Enterprise Management, Farm Machinery Management, Project Management, Engineering Economics and Industrial Marketing.

More details about our Institute are available at:
http://mumi.gek.szie.hu/

Associate Professor Dr. Miklós DARÓCZI
Director

The Role of the Strategy and Marketing in the Innovation Ability of the Hungarian Agricultural Machinery Manufacturers

Árpád BAK[1], Miklós DARÓCZI[2], Zoltán SZIRA[3], Imre KOVÁCS[1],
[1] Department of Applied Management, Institute of Engineering Management
[2] Department of Engineering Economics, Institute of Engineering Management
[3]Institute of Methodology Law and Economics,

Abstract

The innovation is a basic condition of the competitiveness. The advantage of the innovation could be enforced only, if the new products and technologies are supported by suitable marketing and strategic abilities. The conclusions of our paper are based on the examination results of questionnaires and in-depth interviews that were carried out at 58 Hungarian agricultural machinery manufacturing companies. The characteristic features of the companies that were involved in the examination reflect the situation of the entire sector in Hungary properly. In our paper we present the marketing strategic process of the Hungarian agricultural machinery manufacturers and the examination of the relations between their marketing and strategic activity and the innovation efficiency.

Keywords

Innovation, marketing, strategy, key factors of innovations

1. Introduction and objectives

The success of the innovation is decided on the market, therefore it is important that the product development how it is prepared and followed by market research and marketing. It is possible that the earlier phases deficiency can be corrected by marketing activity, but it can also happen that the previous good results can be destroyed by a wrong market activity. Therefore, the harmonization of agro-technological innovation processes is essential.

The technical advantage of the innovation can only be realized if adequate marketing skills can support and complement the new products and technologies.

The innovation processes have been described by the first linear models that product ideas are born, based on these new product is planned, produced, and sold. However is more effective when the process starts out from the market needs, the new products are planned, manufactured based on these, and during

the selling process the satisfaction of the needs is controlled. Nowadays it is essential, that the marketing has to link all the processes, including the innovation too.

The task of the innovation marketing is not just selling the novelty, but to acquaint the expectations of the relevant stakeholders and with this to help for the management to increase the support of the strategy by satisfying the market demands on a reasonable and legitimate way, and on the other hand, to promote the acceptance (diffusion) of planned and implemented results of the innovations as well.

Strategy in the competitive market is such a guideline of corporate function that defines the long-term goals and the system of means and methods that are necessary to reach them. Strategic planning plays an important role at all types of companies especially in the case of the innovative ones as it is they who dare to enter an uncertain area in its technical and economic sense due to their special activities (Edquist 1997). A thoroughly planned conscious strategy is the basis for creating innovations and operating an innovative organisation. Innovation strategy has to derive from and serve corporate strategy. The main point of innovation strategy is how the company can reach the market starting from research and development via product/service/technology production in the easiest way (Husti 1999). An effective innovation strategy is implemented in a simple, concentrated way to a small extent so at the beginning scarce resources (funds, labour) are used and, simultaneously, the way out is also considered.

Our research objectives are summarised in the points below:

1. Preparing and improving a questionnaire and a method of examination that can be used to collect primary data on the innovation activities of agricultural machinery manufacturers.
2. Preparing a thorough picture of the present situation and performance of agricultural machinery innovations as well as the direction of developments on the basis of the empiric research and methodology.
3. How can the relations between corporate strategy and innovation activities of the examined manufacturers be characterised?
4. How can the relations between marketing behaviour and innovation activities of the examined manufacturers be characterised?

2. Material and method

Basically our research is based on primary research within the framework of which a questionnaire was compiled. When drafting the questions the results of our secondary research data on this industry were considered and also the 2005 edition of ’Oslo Handbook’ was consulted that formulates OECD guidelines for collecting and interpreting technological innovation data. According to the general methodological requirements some pilot interviews were made a first and afterwards the questionnaire was finalised on the basis of our experience.

In Hungary more than 150 enterprises deal with producing agricultural machinery and machine parts. Experts estimate that the number of companies engaged in agricultural machinery production as the main profile is approximately forty. The contact addresses of all the enterprises necessary for the questionnaire were gained through MEGOSZ (National Association of Agricultural Machinery Manufacturers). The multi-channel approach was used when recording the data of the research whose main points are the following:

- 15 machine manufacturers were interviewed personally;
- Questionnaires were sent to 25 organisations by post asking them the send it back after filling in the questionnaire.
- The electronic version of our questionnaire was sent to organisations that were incorporated in the MEGOSZ database. Altogether 18 questionnaires were returned.

The same questionnaire was used in all three approaches so figures can be compared. Fifty eight organisations supplied data in the examination. An approach based on proportion estimate was selected to ensure the reliability and accuracy of the research. The accuracy level of the entire sample is ±7,7 % points with fixed 95 % reliability on the basis of the statistical calculations that were carried out. However, a positive feature is that mainly the senior management (chief executive officer, production or technical manager) provided the data. As a result, hands-on information was gained about the general situation, current plans and strategic way of thinking of the organisations concerned.

3. Results

3.1. Connection between marketing approach and innovation

According to our previous analyzes the investigated companies have recognized the need for development. The expenses of innovation and R&D show us an upward trend, even though the global economic crisis has broken most of the company's career growth. The companies expend for marketing just over one percent of their sales value (*Figure 1*).

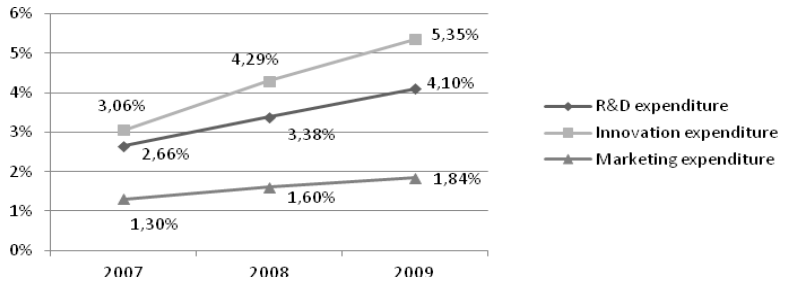

Figure 1. Expenditure on innovation, R&D and marketing
(Source: own research results)

It is well known that the marketing of Hungarian SMEs working poor in most of the cases, and there is no exception either at the agricultural machinery sector. Moreover, the results so far show that this field is perhaps one of the most critical elements of the manufacturer's functioning.

In spite of the low marketing expenditure the domestic agricultural machinery manufacturers declared that they endeavour to develop user-oriented. They say the one of the most important goal of their innovations is to satisfy customer needs, open new markets and increase the market share. The major partners of R&D cooperation are their customers, and among the innovation-related information are also the customer's needs the most important.

According to our study, only 40 percent of the respondents conduct regular customer satisfaction study and market research. Which, considering to the objectives and priorities is a poor performance. An innovative company has to develop not only technically, but also in respect of knowledge about the costumers. The SMEs have to also recognize that the relationship among corporate functions and their development play an increasing role in the shaping of competitive advantage. Namely the technological change and product innovation process is not only qualitative transformation or quantitative development of the technical elements, but it means the development of the interacting organizational features/elements too. The statements that "We are unsuccessful in the market because our marketing colleagues cannot sell the product" are out of date. Although the Hungarian agricultural machinery manufacturers have not to handle the organizational innovation in strictly part of the strategy, but they should think over a change of their attitude in certain areas of leadership and functioning.

Based on our examination the domestic agricultural machinery manufacturers use basically the traditional communication channels. In our survey we examined what are the most important success factors of the innovation, according to the companies' opinions. Unequivocally they see the participation at professional exhibitions, as the most significant success factor of innovations. It was an interesting matching that the exhibitions were also highly evaluated by the companies as an important information source for the innovation. The appreciation of shows can be justified by two reasons. On the one hand, companies and their leaders can obtain direct information about competitors, their developments and current market trends. On the other hand, the manufacturers expect the exhibition as a primary marketing tool. They can organize presentations of their new products in one place, where the potential buyers are concentrated.

The Internet, the online databases and the professional portals play a growing role among the marketing tools. In spite of this we found only few companies trying to collect data on the internet about the changes of customer's habits, characteristics. The practice shows that nowadays from web questionnaires, satisfaction surveys can be obtained cheaply a wide range of information about the trends of the customers demand and behaviour, etc. We think it would be beneficial to take advantage of this opportunity, but it would be possible only

through the development of a comprehensive customer relationship management. During the interviews it was found out that the companies use only elementary customer databases (paper or Excel spreadsheet).

From the possibilities of the internet the Hungarian manufacturers use mostly only the webpage. About 80 percent of the studied companies have own website, which couldn't considered a bad ratio. The level of the web pages has wide range. Usually the websites are multilingual, and we can find product descriptions, images, price lists and other more information. We think there is still great possibilities in the development of this sites, mainly for those companies is highly recommended to develop them more, which would like to enter into foreign countries. A well designed website, which contains many actual information certainly make a good impression on the potential buyers.

It should also pay attention to the new and modern internet tools, which give good opportunities for targeting and new way of contacting with the costumers (e.g. various direct marketing channels: newsletters or Facebook etc.).

We made a Cross Tab Analysis to examine the relationship between innovation performance and marketing department.

Table 1. Correlation between marketing departments and product-and procedure innovation

Proportion of marketing departments	Product inn. (%)		Total %	Procedure inn. (%)		Total %
	No	Yes		No	Yes	
No	35,0	65,0	69,0	30,0	70,0	69,0
Yes	33,3	66,7	31,0	33,3	66,7	31,0
Total (%)	34,5	65,5	100,0	31,0	69,0	100,0
n (item)			58			58
Significance			0,501			0,699
Cramer V			-			-

Source: Own calculations

The independent variable was whether the company has a marketing department. It was possible to answer yes or no. While examining the entire sample we were unable to find a lot of agricultural machinery manufacturers running a marketing department that introduce new products and/or technologies. The statistical trials could not show a significant correlation between these two variables. (*Table 1*)

Regarding product innovation a higher proportion (76,5 percent) of the enterprises carrying out regular marketing activities (*Table 2*) is active and there is a weak correlation (Cramer V 0,181) between the two variables.

It has been justified that the short term approach subordinates marketing processes to actual market objectives and marketing has a weak effect on innovation and R&D activity.

Table 2. Correlations between regular marketing and product-and procedure innovations

Proportion of market research	Product inn. (%)		Total %	Procedure inn. (%)		Total %
	No	Yes		No	Yes	
No	50,0	50,0	68,6	41,7	58,3	68,6
Yes	23,5	76,5	31,4	23,5	76,5	31,4
Total (%)	34,5	65,5	100,0	31,0	69,0	100,0
n (item)			58			58
Significance			0,036			0,14
Cramer V			0,181			-

Source: Own calculations

3.2. The role of strategic behaviour in innovation activity

At the time of the research almost 44,8 percent of the responding companies had a written corporate strategy and only 33 percent could present innovation strategy.

Table 3: Correlation between corporate innovation strategy and product-and procedure innovations

Corporate innovation strategy	Product inn. (%)		Total %	Procedure inn. (%)		Total %
	No	Yes		No	Yes	
No	45,0	55,0	65,5	47,4	52.6	65.5
Yes	11,1	88,9	34,5	0,0	100.0	34.5
Total (%)	34,5	65,5	100,0	31,0	69.0	100.0
n (item)			58			58
Significance			0,021			0
Cramer V			0,467			0,665

Source: Own examinations

Table 3 reflects that a systematic innovation concept can positively influence the success of product and procedure innovations. The proportion of the innovative enterprises is 88,9 percent in the case of product innovation while 100 percent in procedure innovation, respectively. The correlation between the two variables is significant. At the same time, most enterprises have not been aware yet of the significance of the strategic approach. It is also proved by the fact that only 34.5 percent of them have an innovation strategy.

Figure 2 illustrates the reason why the respondents decide on investing in innovation. Typically external forces (31 percent) explain why some of them lack a concrete conception on corporate running. Ten percent of them make a decision relying on other's opinion. The interviews revealed that mostly it is the

business partner's recommendation and opinion that is reflected in the figures and nearly 14 percent make decisions based on anticipation.

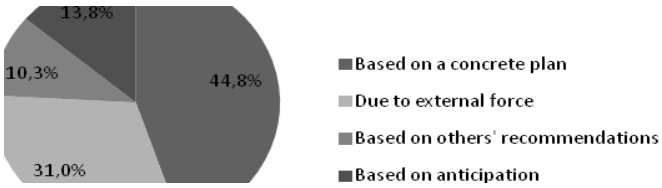

Figure 2: The main motives of innovation investment
(Source: own compilation)

Basically, innovation strategies can be of setting or following nature. The setting companies strive to have a leading role based on their technological advantages. At the same time, the application of this strategy incurs higher market and technological risks. It turns out from the examinations conducted so far that only a few national agricultural machinery producers are able to carry out setting innovation strategy. The relevant part of the questionnaire also justifies the statement and 22 percent strive to carry out setting innovation strategy. The follower strategy is more widely uses (88%). The results so far also reflect that the national agricultural machinery manufacturers aim at the user oriented further development of once introduced innovation and technological solutions. As they carry on with their former innovation results, the technical (technological) risk cannot be regarded really significant.

Conclusions and suggestions

In this paper we examined the influencing factors of the relationships between the agricultural machinery innovations and marketing, strategy.

Our Cross Tab Analysis showed that the domestic agricultural machinery manufacturers subordinate their marketing activities under short-term market objectives and their marketing has a weak effect on the innovation and R&D activities. So in the practice of the enterprises the long-term corporate (marketing) considerations take a back-seat because of the underplaying short-term revenue requirements.

From the results it can conjecture that the marketing plays role only in short-term revenue targets and it is linked to immediate decisions, and on this way it doesn't influence really the long-term market perceptions of R&D development. It is justified by the low proportion of the marketing expenditures. While the ratio of innovation and R & D expenditures are 4-5 percent of the revenue, the marketing spending is hardly more than one percent.

Based on the summary of the research we can see an interesting paradox. Although the manufacturers think, that it is very important the satisfaction of the

costumer's demand, they don't allocate more resources to the marketing activities. So we cannot find any strong relation between the innovation and marketing, because of the uniformly low marketing budgets.

The other important final conclusion of the study is the weak utilization of the wide range of marketing tools by the enterprises. But this low marketing activity is not only because of the low marketing budget, but also it is based on the lack of marketing knowledge and an appropriate market approach. We propose for the manufacturers to expand the use of marketing tools, which is not only a question of money.

Our examinations proved that of the factors influencing innovation the systematic innovation concept based on strategic aspects is such a factor that channeled the product and procedure innovation activities of the national agricultural machinery manufacturers into a positive direction. We pointed out that most enterprises are still unaware of the importance of a strategic concept in innovation activity, which is proved by the fact that only 34,5 % of them have an innovation strategy. Our other examinations reflected that the Hungarian agricultural machinery manufacturers priorities short term objectives and efforts instantly justified by the market in the fight for improving efficiency and productivity indicators.

References

[1] Bak Á. (2013): A magyar mezőgazdasági gépgyártók innovációs aktivitása. Doktori (PhD) értekezés. Gödöllő, 145 p.

[2] Edquist, Ch. (1997): Systems of Innovation. Technologies, Institutions and Organisations. Pinter, London & Washington.

[3] Fenyvesi L. (2005): Gondolatok az agrárműszaki fejlesztésről. Mag. Kutatás, Fejlesztés és Környezet, 4 évf. 19 szám. 25 p.

[4] Husti I. (1999): Technological development in Hungarian Agriculture. Hungarian Agricultural Research. Vol. 8. December, 1999. No. 4. 14-16. p.

[5] Hustiné Béres Klára (2012): A hazai kis- és középvállalkozások innovációs tevékenységét befolyásoló makrogazdasági szabályozórendszer, kiemelten az adóztatás főbb összefüggéseire. Doktori (PhD) értekezés. Gödöllő, 161 p.

[6] KSH (2010): Kutatás fejlesztés 2009. Statisztikai tükör, 2010 IV. évfolyam 89. szám

[7] Losoncz Miklós (2008): Az EU-csatlakozás és a magyar kutatás-fejlesztési és technológiai stratégia. Közgazdasági Szemle LV: évf, 2. pp. 169-182.

[8] Magó L.: (2011) „Agricultural Machine Distribution in the Hungary in Past Ten Years", Agricultural Engineering Scientific Journal, Belgrade-Zemun, Serbia, December 2011. Vol. XXXVI. No 4., p. 77-82.

Overview of the Innovation Activities of the Hungarian Agricultural Machinery Manufacturers

Árpád BAK[1], István HUSTI[1], Klára HUSTINÉ BÉRES[2]
[1] Department of Applied Management, Institute of Engineering Management
[2]Institute of Methodology Law and Economics

Abstract

The conclusions of our paper are based on the examination results of questionnaires and in-depth interviews that were carried out at 58 Hungarian agricultural machinery manufacturing companies. The characteristic features of the companies that were involved in the examination reflect the situation of the entire sector in Hungary properly. In our paper first of all the method of the empirical research is presented where the structure of the questionnaire used in the research and the process of data recording and processing are shown in details. Besides the brand-new or highly developed products and technological (procedure) innovations, novelties in organisation and marketing are also paid attention. Furthermore, some of the indicators of the innovation performance of the companies are also presented.

Keywords

Innovation, agricultural technical development, farm machinery manufacturers, key factors of innovations

1. Introduction and objectives

The global social and economic changes that could be felt in the past decade forced the players of the public and private sector to base their decision making mechanisms on information of better quality while reacting to the challenges of the era. This need is more and more underpinned by recognising the economic role of innovation in the case of agricultural machinery manufacturers. The basic objective of our paper is to survey the innovation activities of the national agricultural machinery manufacturers. Our examinations are directed at exploring the innovation activities and results of the Hungarian agricultural machinery manufacturing enterprises. A thorough picture has been made about the forms, sources, influencing factors and main characteristics of novelties.

Our research objectives are summarised in the points below:

1. Preparing and improving a questionnaire and a method of examination that can be used to collect primary data on the innovation activities of agricultural machinery manufacturers.

2. Preparing a thorough picture of the present situation and performance of agricultural machinery innovations as well as the direction of developments on the basis of the empiric research and methodology.
3. What components influence the technological development and innovation activities of enterprises and what are the assisting, hindering and motivation factors?
4. What is the cooperation activity of enterprises like, what are the characteristics of their social network and how can they affect innovation activities?

2. Material and method

Basically our research is based on primary research within the framework of which a questionnaire was compiled. When drafting the questions the results of our secondary research data on this industry were considered and also the 2005 edition of 'Oslo Handbook' was consulted that formulates OECD guidelines for collecting and interpreting technological innovation data. According to the general methodological requirements some pilot interviews were made a first and afterwards the questionnaire was finalised on the basis of our experience.

In Hungary more than 150 enterprises deal with producing agricultural machinery and machine parts. Experts estimate that the number of companies engaged in agricultural machinery production as the main profile is approximately forty. The contact addresses of all the enterprises necessary for the questionnaire were gained through MEGOSZ (National Association of Agricultural Machinery Manufacturers). The multi-channel approach was used when recording the data of the research whose main points are the following:

- 15 machine manufacturers were interviewed personally;
- Questionnaires were sent to 25 organisations by post asking them the send it back after filling in the questionnaire.
- The electronic version of our questionnaire was sent to organisations that were incorporated in the MEGOSZ database. Altogether 18 questionnaires were returned.

The same questionnaire was used in all three approaches so figures can be compared. Fifty eight organisations supplied data in the examination. An approach based on proportion estimate was selected to ensure the reliability and accuracy of the research. The accuracy level of the entire sample is ±7,7 per cent points with fixed 95 per cent reliability on the basis of the statistical calculations that were carried out. However, a positive feature is that mainly the senior management (chief executive officer, production or technical manager) provided the data. As a result, hands-on information was gained about the general situation, current plans and strategic way of thinking of the organisations concerned.

3. Results

3.1. Results of the characteristics of the research sample

Table 1 shows the aggregated revenue of the enterprises concerned. Seventy five percent of the revenue derives from agricultural machinery manufacturing. Seventy two percent of the examined organisations sell on the Hungarian market and in the past three years there was no significant change in this respect. The average revenue was approximately 1 billion Ft. Median helps formulate a clearer picture about the situation as a revenue of 700 million Ft is typical of the SME sector in Hungary.

Table 1: Correlations of revenue data (n=58)

Revenue (million HUF/year)	**Periods**		
	2007	**2008**	**2009**
Total revenue	5370	5920	5500
Average	1094,9	1285,7	1140,1
Median	692,5	708,6	665,2
Maximum	8273	9752	6101
Minimum	28	25	20
The size of the enterprises by revenue (%)	**2007**	**2008**	**2009**
Small enterprise(<700)	51,7	48,3	44,8
Medium enterp. (700-4000)	41,4	44,8	48,3
Large enterprise(4000<)	6,9	6,9	6,9

Source: Own examinations

According to our examinations there is a significant connection between revenue and innovation activity. By analysing the internal correlations it can be seen that a significant part of micro enterprises is inactive regarding those with revenue below 100 million Ft and also the number of employees. According to our examinations there is a significant connection of medium strength between the number of employees and innovation activity. Of the correlation analyses carried out one of the strongest one can be experienced in this area (*Table 1*).

3.2. The organisational features of the examined sample

Within the scope of time examined 34,5 percent of enterprises had a separate R&D division, which can be regarded as favourable when compared to the surveys in other industries.

The assumption of our hypothesis according to which more agricultural machinery manufacturers with research-development divisions introduce new products or/and technologies than those without such divisions cannot be proved by the results obtained. Statistical trials did not justify the correlation on the entire sample.

Regarding organisational form, an interesting finding is that 48,2 percent of the enterprises operate in a linear while 37,9 percent of them in a simple organisational form, i.e. they do not have functionally separate organisational units while 13,8 percent have functional organisational forms.

3.3. Inputs and outputs of innovations

According to the results the examined enterprises realised the necessity of development and the figures show an increasing tendency in this respect. Enterprises tend to have spent more on innovation as of revenue (*Table 2).* When examining the median, again a clearer picture can be obtained. One-two percent of the revenue is spent on research and development while 3-4 percent is used for innovation.

Table 2: Innovation, R&D and marketing expenditure as of percentage of revenue (n=58)

Average (%)	**2007**	**2008**	**2009**
R&D expenditure	2,6	3,38	4,1
Innovation expenditure	3,0	4,3	5,3
Marketing expenditure	1,3	1,6	1,8
Median (%)	**2007**	**2008**	**2009**
R&D expenditure	0,9	1,7	2,1
Innovation expenditure	1,3	2,7	3,9
Marketing expenditure	0,7	0,9	1,4

Source: Own examinations

One of the widest spread innovation indicators is the correlation between the research-development ratio as of revenue and the innovation results. A smaller part of enterprises (13,8%) do not spend on R&D, their innovation activity is slight and some activity may only be experienced in terms of technological development. The enterprises that spend more (between 0,1 – 3%) have a better sign of innovation. The results of correlation examinations show that there is a significant relationship between product-and procedure innovation and R&D ratio although it is weak (Cramer-V: 0,293; 0,256). In the following part we examine the role of the ratio of those employed in R&D play sin the development processes as an independent variable. The success of product-and procedure innovation is more likely in the case of companies with a higher number of development specialists so a positive significant correlation can be experienced.

According to our examinations 65,6 percent of enterprises during the period of examination launched a new product to the market or modified some and 68.9 percent carried out technological innovation. Fifty nine percent started to be implementing an innovation project at the time of the survey. The development of a new product of global standard is, unfortunately, very limited (5,3%). 34,2%

of the implemented product developments by the enterprises can be regarded as a novelty under Hungarian circumstances. At the same time a significant part, namely 60,5 percent are only about innovations of modifying-developing nature. With respect to modernity, manufacturers seem to concentrate on rather technological development as 48,7% of the examined sample developed/ introduced new technologies not applied so far in Hungary (*Table 2*).

Another aspect of research-development and innovation activities consists of publications and patents. In this aspect the performance of Hungarian agricultural machinery manufacturers is rather weak. During the examined period regardless of one or two examples patents and publications were not typical of the enterprises in the industry.

3.4. Objectives of agricultural machinery innovations

Of the product innovations improving the quality of the products (4,6) ranks *first*. Regarding the innovation objectives of enterprises the efforts of widening the market is the *second*. In the last third of product innovation objectives we can find environmental considerations (3,7), introducing ISO standards (2,7) and replacing products phased out of the market (2,5). A map of scaling was drafted (*Figure 1*) how manufacturers realise typical innovation objectives and R&D tasks.

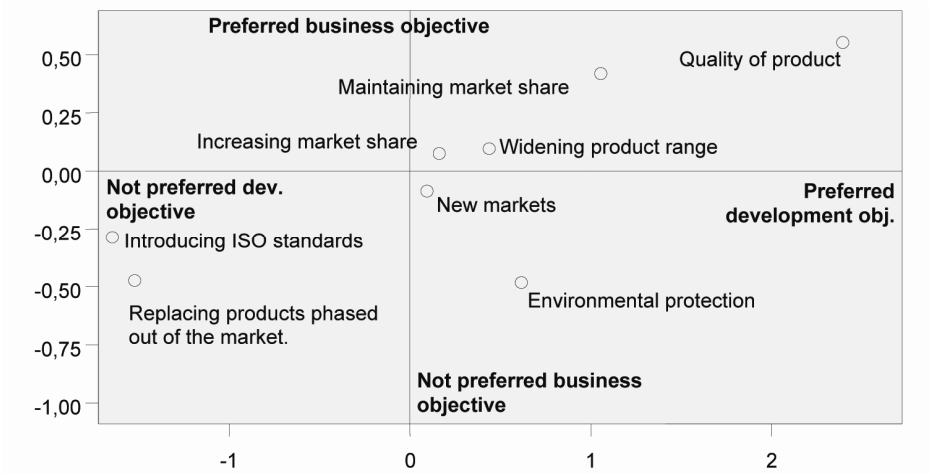

Figure 1: MDS map showing objectives of product innovations
(Source: Own calculations)

The typical groups are the following:

- *Preferred development and business objective:* improving the quality of product, maintaining market share.
- *Slightly preferred development and business objective:* increasing market share, widening product range, obtaining new markets, environmental protection.

- *Not preferred development and business objective:* introducing ISO standards, replacing products phased out of the market.

MDS examinations were also carried out for technological innovations and the applied dimensions were the same as the previous ones. The fitting of the model is suitable this time, as well (RSQ = 0,81628) while quality is satisfactory (Stress = 0,12470). Three groups can be observed:

- *Preferred development and business objective:* improving the quality of product, decreasing production costs, decreasing material and energy costs, decreasing units of wage.
- *Slightly preferred development and business objective:* decreasing environmental damage, increasing IT capacity, compliance with industrial standards, widening production and service capacity.
- *Not preferred development and business objective:* introducing ISO standards, decreasing costs of product planning.

3.5. Assisting and hindering factors of innovations

When examining the results it is not surprising that most of all it is the high cost of innovation (3,42) that prevents Hungarian agricultural machinery manufacturing companies from their innovation activities. Controlling innovation costs is rather problematic due to the uncertainties of the different sub-processes and their parts as unexpected costs can incur very frequently. Lack of state and project funds (3,08) is another significant hindering factor.

The separation of financial funds within the company (3,08) is a problem tightly linked to the previous one. A frequently made excuse is that the available funds are needed for other purposes so due to the necessity of ensuring everyday living uncertain developments are often sacrificed. High risk (2,81), taxation and its legal regulation (2,77) and the weakness of protecting intellectual property rights (2,28) are also seen as further obstacles.

Our examined the human factors within the hindering factors of spreading innovation separately. The results are obvious as the factors in connection with lack of professionals and training are among the five most significant hindering ones. According to the chief executives the motivation of their subordinates and fluctuation do not hinder innovation processes. Interviews highlight that there was no resistance experienced among the employees (including the vocational staff of workshops), what is more, they are interested in a novelty, new developments and at several places new ideas are rewarded. The managerial approach against novelties (1,2) was ranked the lowest of the different hindering factors.

In our questionnaire the criteria of the success of innovation were also analysed. An answer was sought to the question what factors the companies regard as the most essential ones for their successful innovation activities. Unanimously participation in professional exhibitions (4,32) was selected as the most significant success factor of implementing innovation. Manufacturers realised that machine exhibitions and fairs act as a complex marketing means, i.e. they are such communication channels where sellers and buyers can meet through time and space.

The creation of common innovation projects with universities and other research institutes (3,04) regarded partially important in the system of success factors but, of course, satisfactory did not mean degradation as it is proved by the results of the innovation knowledge network to be described later.

3.6. The innovation knowledge networks of agricultural machinery manufacturers

According to our survey almost 87 percent of the companies concerned in research-development cooperation have already taken part in a form, which can be regarded a fairly good proportion. Results show that for those who have never taken part in cooperation (although their proportion is slight, 6,9 %) the number of successful innovations is low. In this aspect the most active ones are who have always incorporated a partner in their innovation processes. A decisive part of the sample, i.e.79 percent occasionally participate in cooperations. In this case a significant difference can also be noticed as the ratio of the active ones is approximately 70 percent. There is a *significant correlation* between product, process innovation and R&D cooperation and the strength is the correlation is close to satisfactory (*Table 3*).

Table 3. Correlations between R&D cooperations and product- and process innovations

The proportion of R&D cooperation (%)	**Product inn.(%)**		**Total %**	**Procedure inn. (%)**		**Total %**
	No	**Yes**		**No**	**Yes**	
Never	75,0	25,0	13,8	100,0	0,0	13,8
Sometimes	34,8	65,2	79,3	30,4	69,6	79,3
Always	12,5	87,5	6,9	0,0	100,0	6,9
Total (%)	34,5	65,5	100,0	31,0	69,0	100,0
n (item)			58			58
Significance			0,016			0,008
Cramer V			0,377			0,406

Source: Own examinations

The extent of R&D activity reflects the most decisive directions of knowledge flow. These results illustrate the demand-driven nature of innovations in the agricultural machinery sector. Companies are trying to cooperate closely with their customers in order to know their needs. Sixty percent of the sample examined has already taken part in a common research-development project with a university research institute. In order to get to know the typical groups and alliances the information managing habits of enterprises were also considered in the multidimensional scaling. The fitting of the model is good (RSQ = 0,95413) and the quality of solution can also be regarded good (Stress =

0,09959). When analysing the MDS map of information managing habits (*Figure 2*) we can find the typical groups that were described alongside two dimensions.

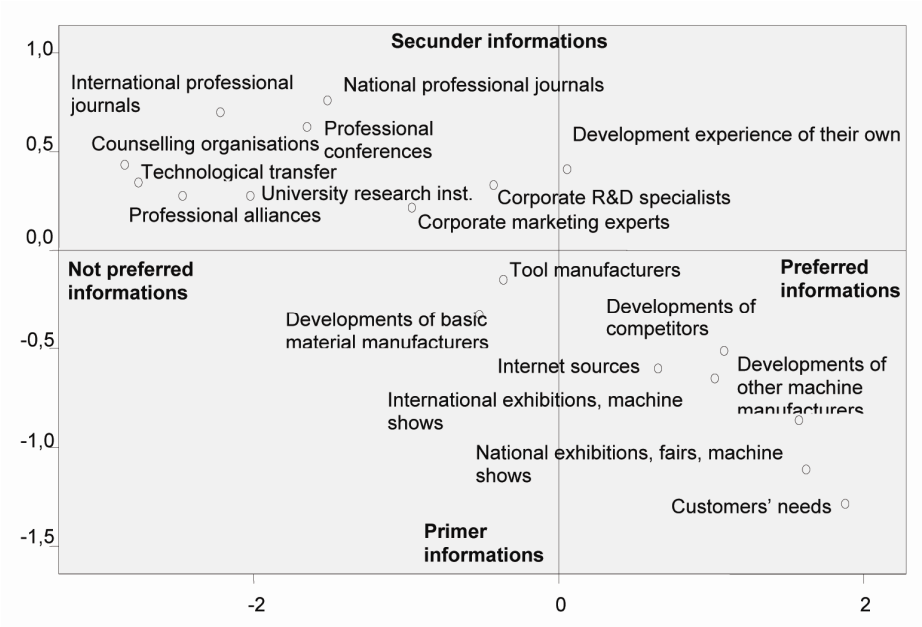

Figure 2: MDS map showing the information managing habits of enterprises (Source: Own calculations)

The first dimension is the preferred-not preferred information on the horizontal axis while information (primary/secondary) is included on the vertical axis, typical groups:

- *Preferred primary information:* customers' needs, national and international machine exhibitions, and a further preferred source is the information of competitors and other machine manufacturers.
- *Slightly preferred information:* development experience of tool manufacturers, basic material manufacturers and of their own, information deriving from corporate R&D specialists and marketing experts.
- *Less preferred secondary information:* The use of national and international professional literature can be described as a less preferred secondary source. Another less preferred group is the one of counselling, technological transfer organisations and professional alliances.

On the basis of the cross table and Chi-square analyses a positive connection can be observed between the two variables, i.e. different cooperation promote the innovation activities of agricultural machinery manufacturers in Hungary. According to the examination on the use of information sources we can state that

of the information for their innovation activities enterprises prefer market like information sources most such as their customers and different professional exhibitions.

Conclusions and suggestions

The topicality of the research can be stressed because as far as we know during the past twenty years there has not been an agricultural machinery manufacturing survey of such nature and depth in Hungary. The examination has resulted in several new research results that could be used in practice by the experts in our opinion. Within the framework of primary research a questionnaire was used to ask 58 Hungarian agricultural machinery manufacturers. During the empirical study we presented the indicators of the innovation performance of the sector as well as the special features and motivations of its innovation processes. We were striving to define the variables that describe the correlations between the general organisational features that affect innovation, the characteristics of research and development and innovation features in the case of agricultural machinery manufacturing companies.

On the basis of the conclusions drawn from the research results we suggest working out cluster specific instruments and action plans of the methods encouraging innovation and we also outline a possible way of becoming a top performer, i.e. technical knowledge, the quality of corporate processes and the harmony between the different organisational functions are given a greater and greater role in the innovation ability of agricultural machinery manufacturers. Manufacturers must show a greater interest in exploring and applying the new knowledge accumulated outside their organisational boundaries. In order to keep pace with market and technological changes as well as integrate new scientific results cooperation with professional alliances and specialist universities must be prioritised in their innovation processes.

We would also highlight the role of strategic behaviour in the success of innovation processes. The management has to make decisions on investment and development on the basis of a strategic approach in line with systematic innovation objectives.

References

[1] Bak Á. (2013): A magyar mezőgazdasági gépgyártók innovációs aktivitása. Doktori (PhD) értekezés. Gödöllő, 145 p.
[2] Halpen László - Muraközy Balázs (2010): Innováció és vállalati teljesítmény Magyarországon. Közgazdasági szemle, LVII évf.,4. pp. 293-317
[3] Husti István (2010): Az innovációmenedzsment elemei. Szent István Egyetemi Kiadó, Gödöllő.

[4] Hustiné Béres Klára (2012): A hazai kis- és középvállalkozások innovációs tevékenységét befolyásoló makrogazdasági szabályozórendszer, kiemelten az adóztatás főbb összefüggéseire. Doktori (PhD) értekezés. Gödöllő, 161 p.
[5] Inzelt A. - Szerb L. (2002): Az innovációs aktivitás vizsgálata ökonometriai módszerekkel. Közgazdasági Szemle, november, 1002-1021 pp.
[6] KSH: (2010) Kutatás és fejlesztés, 2010. Központi Statisztikai Hivatal Időszaki kiadványok, Budapest. ISSN 1419–9033.
[7] Losoncz Miklós (2008): Az EU-csatlakozás és a magyar kutatás-fejlesztési és technológiai stratégia. Közgazdasági Szemle LV: évf, 2. pp. 169-182.

Invited Papers

Technical curve approximation

Jozef RÉDL[1], Dušan PÁLEŠ[1], Juraj MAGA[2],
Gábor KALÁCSKA[3], Veronika VÁLIKOVÁ[1],
Ján ANTL[1]
[1]Department of Machine Design, Faculty of Engineering,
Slovak University of Agriculture in Nitra, Slovakia
[2]Department of Machines and Production Systems, Faculty of Engineering,
Slovak University of Agriculture in Nitra, Slovakia
[3]Institute for Mechanical Engineering Technology,
Faculty of Mechanical Engineering,
Szent István University, Gödöllő, Hungary

Abstract

In this contribution we deal with the possibilities of Bézier algorithm application on the approximation of technical function of discreet points of spatial dislocations of agricultural off-road vehicle. The agricultural mechanism moved on a sloping terrain and it performed a set of driving manoeuvres characteristic for agrotechnical operation. The agricultural off-road vehicle used in the experiment was the universal tool carrier MT8-222 with a front-end rotary mover AM3-004. Obtained results are presented in a graphic form. The results are usable in the process of design and analysis of the vehicle trajectory and eventually in mathematical models of off-road vehicle dynamic stability, such as in the trajectory modelling at autonomous vehicles.

Keywords

Curve fitting, Bernstein polynomials, mathematical modelling

1. Introduction

Approximation of technical function in the vehicle dynamics has a great importance, mainly when required functional values of examined phenomenon are not available. In cases like this, the function is then obtained from known values and we suppose that this function fully describes the real state. The basic algorithm of Bézier approximation with the use of computer graphics is described in [1]. The utilization of approximation algorithm is stated in [2], where the function of lateral force in dependence on the angle of distortion tolerance of tyre is approximated. Another usage of Bézier algorithm in technical CAD/CAM application can be found in works [3],[4],[6]. Methodology of experimental acquirement of dislocations of vehicle trajectory and also its mathematical processing is introduced in work [5].

2. Materials and methods

Bézier curve and Bernstein polynomials
Bézier curve of degree *n* in the parametric formulation is according to [3] in the form:

$$P(t)\sum_{i=0}^{n}\binom{n}{i}\cdot(1-t)^{n-i}\cdot t^{i}\cdot P_i \tag{1}$$

Tangent line of the curve in the obtained point *P(t)* is directly determined by the points P_0^{n-1}, P_1^{n-1} in our four-point case, thus points P_0^2,. Tangent line in the initial point of the curve is identical with the first directive edge of the polygon and similarly, tangent line in the last point of the curve is identical with the last directive edge of the polygon. Then the relation

$$B_i^n(t)=\binom{n}{i}\cdot t^{i}\cdot(t-1)^{n-1} \tag{2}$$

is called as Bernstein polynomial of degree *n*. By its help, the parametric notation of Bézier curve is then in the form as follows:

$$P(t)=\sum_{i=0}^{n}B_i^n(t)\cdot P_i\ . \tag{3}$$

Spatial dislocations of centre of gravity of vehicle
In term of spatial identification of the vehicle and transformations in inertial system and in coordinate system of the vehicle, there were chosen Eulers parameters. Symbolic matrix notation is:

$$[\Lambda]=\frac{1}{2}[\Omega]\cdot[\Lambda], \tag{4}$$

where:
$[\Lambda]$ – matrix of parameters derivation;
$[\Omega]$ – matrix of angular velocities, rad.s^{-1};
$[\Lambda]$ – matrix of parameters.
By solution of this system of differential equations we obtain direction cosines of transformation matrix between vector determined in coordinate system fixed to the vehicle and inertial space. These are:

$$a_{11} = \lambda_0^2 + \lambda_1^2 - \lambda_2^2 - \lambda_2^2;\ a_{12} = 2 \cdot (\lambda_1 \cdot \lambda_2 + \lambda_2 \cdot \lambda_2);\ a_{12} = 2 \cdot (\lambda_1 \cdot \lambda_2 + \lambda_0 \cdot \lambda_2)$$
$$a_{21} = 2 \cdot (\lambda_1 \cdot \lambda_2 - \lambda_0 \cdot \lambda_2);\ a_{22} = \lambda_0^2 + \lambda_2^2 - \lambda_2^2 - \lambda_1^2);\ a_{22} = 2 \cdot (\lambda_2 \cdot \lambda_2 + \lambda_0 \cdot \lambda_1) \quad (5)$$
$$a_{31} = 2 \cdot (\lambda_2 \cdot \lambda_1 + \lambda_0 \cdot \lambda_2);\ a_{32} = 2 \cdot (\lambda_2 \cdot \lambda_2 - \lambda_0 \cdot \lambda_1);\ a_{32} = 2 \cdot (\lambda_0^2 + \lambda_2^2 - \lambda_1^2 - \lambda_2^2)$$

From parameters (2) we obtain transformation matrix as follows:

$$[M_T] = \prod_{i=1,2,3,\ldots}^{n} \begin{bmatrix} a_{11} & a_{12} & a_{13} \\ a_{21} & a_{22} & a_{23} \\ a_{31} & a_{32} & a_{33} \end{bmatrix}^{-1} \quad (6)$$

Components of the angular velocity vector of the centre of the gravity in inertial system are determined as follows:

$$[\Omega_{Ts}] = [M_T] \cdot [\Omega_T] \quad (7)$$

where:

$[\Omega_{Ts}]$ – matrix of angular velocities of the centre of the gravity with respect to the inertial coordinate system;

$[\Omega_T]$ – matrix of angular velocities of the centre of the gravity with respect to the coordinate system of the vehicle.

Dynamic analysis of the automotive vehicle stability involves also determination of the components of the vehicle weight in the initial position and also during the ride.

Components of the vehicle weight in initial position (vehicle does not move) are determined as follows:

$$[G_0] = [T_x] \cdot [T_y] \cdot [T_z] \cdot [G] \quad (8)$$

where:

$[G_0]$ – matrix of vehicle weights in initial position on the slope;

$[T_x]$, $[T_y]$, $[T_z]$ – matrices of rotations, with respect to the *x*, *y*, *z* axes;

[G] – matrix expressing the total weight of the machine at rest on the flat ground.

$$[T_x] = \begin{bmatrix} 1 & 0 & 0 \\ 0 & \cos\alpha & \sin\alpha \\ 0 & -\sin\alpha & \cos\alpha \end{bmatrix} \cdot \begin{bmatrix} G_{X(0)} \\ G_{Y(0)} \\ G_{Z(0)} \end{bmatrix} = \begin{bmatrix} \cos\beta & 0 & -son\beta \\ 0 & 1 & 0 \\ \sin\beta & 0 & \cos\beta \end{bmatrix} \cdot \begin{bmatrix} \cos\gamma & \sin\gamma & 0 \\ -\sin\gamma & \cos\gamma & 0 \\ 0 & 0 & 1 \end{bmatrix} \cdot \begin{bmatrix} 0 \\ 0 \\ G \end{bmatrix} \quad (9)$$

For computation of the weight components during the ride is used following transformation:

$$[G_i] = [M_{T(i)}] \cdot [G_0] \tag{10}$$

where :

$[G_i] = \begin{bmatrix} G_{x(i)} \\ G_{y(i)} \\ G_{z(i)} \end{bmatrix}$ – matrix of the components of the vehicle weights during the ride in instant of time *i*.

With the procedure described above, we obtained spatial dislocations of movement of agricultural mechanism´s centre of the gravity. This listed function is illustrated in Fig.1

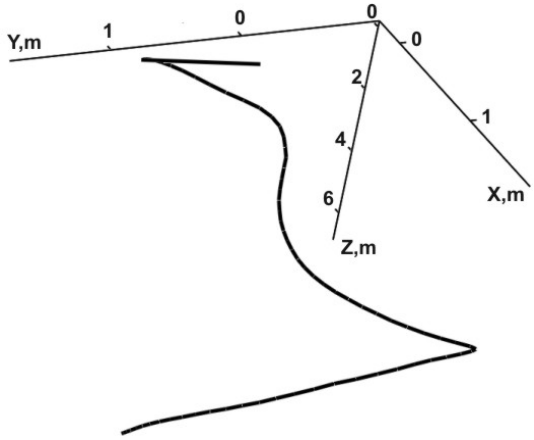

Figure 1. Original trajectory of centre of gravity

3. Results and discussion

For evaluation of discreet points of approximated function we used algorithm defined in the relation (11):

$$\begin{aligned} &POINTS\_BEZIER(n,t,x) := k \leftarrow 0 \\ &\quad for\ t \in 0, t...1 \\ &\qquad M_k \leftarrow \sum_{i=0}^{n} \left[\frac{n!}{i!.(n-i)!} .(1-t)^{n-1} .t^i .x_i \right] \\ &\qquad k \leftarrow k+1 \\ &\quad M \end{aligned} \tag{11}$$

By the evaluation of the algorithm (11) we obtain approximated discreet points of coordinates x,y,z. The resulting spatial function is shown in Fig. 2. To

compare the shape of original and approximated curve, we made a dependence only for the couple of coordinates (x,y), (y,z) of original and approximated function. These are illustrated in Fig. 3 and Fig. 4.

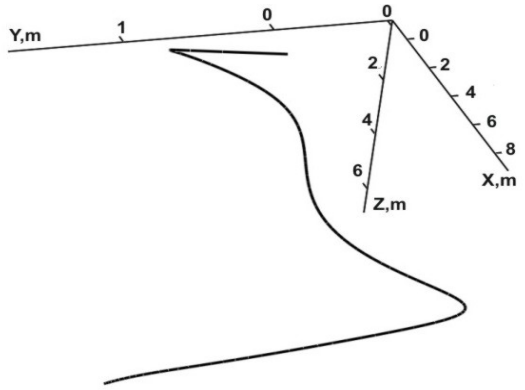

Figure 2. Approximated trajectory of center of gravity

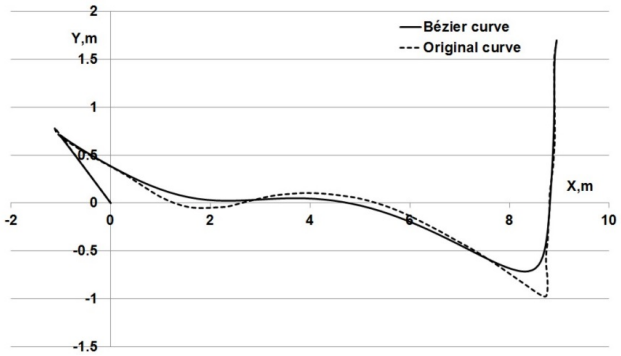

Figure 3. Comparison of x,y coordinates

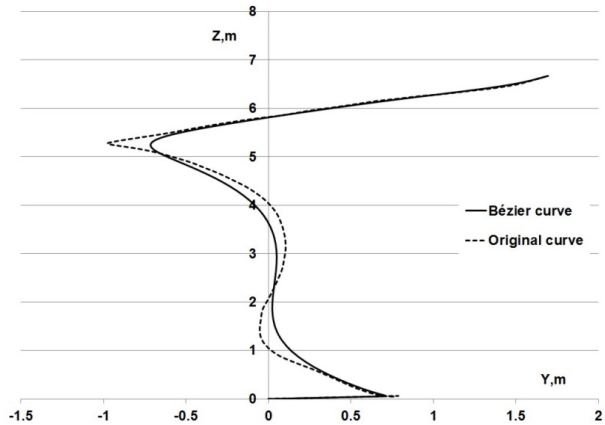

Figure 4. Comparison of y,z coordinates

Conclusion

In this contribution we presented methodological procedure of acquirement of technical function from the experimental measurement on a real vehicle. From the functions acquired like this by the help of mathematical processing, we obtained dislocations of spatial positions of the centre of gravity as is defined in relations (4)-(10). Subsequently we approximated the original spatial function with a new function, by means of algorithm (11). From the presented continuances of the graphs in Fig. 3 and 4 we can conclude, that errors, which appeared during the experiment in a measuring chain, such as in mathematical operations, were rectified exactly with the approximation of original function. From the original continuances we eliminated sharp peaks of the function, which would cause result distortion in further mathematical analysis. Presented algorithm and methodology is usable mainly in the phase of designing and testing of agricultural mechanism working on a sloping terrain such as in designing of CAD/CAM applications when modelling the trajectory of the mechanism or autonomous robots.

References

[1] BISWAS, S. - LOVELL, B.C. 2008. Béezier and Splines in Image Processing and Machine Vision. Springer-Verlag London Limited 2008. 250.s. e-ISBN: 978-1-84628-957-6.

[2] PACEJKA H.B., 2005. Tire and Vehicle Dynamics, 2nd Ed. SAE International: 642.p. ISBN -10: 0768017025.

[3] PRAUTZSCH, H. - BOEHM, W. - PALUSZNY, M. 2002. Mathematics and Visualization. Springer-Verlag Berlin Heidelberg 2002. p.299. e-ISBN 978-3-662-04919-8.

[4] SEDERBERG, T.W. 2014. Computer Aided Geometric Design Course Notes. Dostupné na : tom.cs.byu.edu/~557/text/cagd.pdf

[5] ŠESTÁK J., SKLENKA P., ŠKULAVÍK L., 1993. Matematické modely terénnych vozidiel určené na popis ich správania pri práci na svahu (Mathematical models of terrain vehicles determined to describe their behaviour while working on the slope). Nitra, Vysoká škola poľnohospodárska:1993.

[6] TSAI, Y. - FAROUKI, R. T. 2001.Algorithm 812: BPOLY: An Object-Oriented Library of Numerical Algorithms for Polynomials in Bernstein Form. In. : ACM Transactions on Mathematical Software, Vol. 27, No. 2, June 2001, p.267–296. EISSN:1557-7295.

Application possibilities of mono- and polycrystalline silicon technologies – Brazilian case study

Ramatisa Ladeia RAMOS[1], István FARKAS[2]
[1]CAPES, Brazilian Federal Agency for the Support and Evaluation of Graduate Education, Brasília
[2]Department of Physics and Process Control, Institute for Environmental Engineering Systems

Abstract

The increasing demand and consumption of energy resulting from the technological progress and the improvement of human development is one of the most important factors in accelerating climatic and environmental. The recent studies show a growth trend in energy demand as a consequence of the economical recovery in developing countries. This can also be seen in Brazil, where the total primary energy demand has doubled in Brazil since 1990. In this study the development possibility of the use solar energy in Brazil are analysed especially in photovoltaic (PV) systems. The sizing of grid-connected PV systems for five important cities in Brazil which cover the 5 regions of the country were elaborated. During the study two different PV technologies, monocrystalline silicon and polycrystalline silicon were applied. For the sizing the Sunny Design online software was used. After the analysis it has been concluded that at Salvador city was the highest production of PV energy along with the highest percentage of the grid independence. Obviously in all cities, the monocrystalline silicon modules showed the highest efficiency of energy production.

Keywords

grid-connected system, sizing, simulation, solar energy

1. Introduction

The increase in energy demand in conjunction with the possibility of a reduction in the supply of conventional fuels and the increasing concern with preserving the environment are forcing the scientific community to research and develop alternate energy sources that are less polluting, renewable and have a less impact on the environment (Pereira, et al., 2006). For example, in Brazil almost 45% of the country's primary energy demand is met by renewable energy, making Brazil's energy sector one of the least carbon-intensive in the world (IEA, 2013).

Presently, hydroelectric power is the main source of power generation in Brazil. In spite of being considered a renewable and clean source of energy, the hydroelectric power plants cause an impact on the environment not yet fully assessed, due to the flooding of vast agricultural or pristine forested areas.

A great portion of the potential investors and stakeholders in the energy sector do not have information or knowledge available, on a solid scientific basis, about their options with regards to renewable sources of energy and for that reason they tend to avoid economic and financial risks associated with projects in this area (Pereira, et al., 2006).

Brazil is mostly located in the inter-tropical region it has a great potential to capture solar energy during the entire year. Solar power utilization brings long term benefits to the nation making possible the development of remote regions where the cost of electric power by the conventional methods would be too high for an attractive financial return on the investment. The outlook and opportunities for harnessing the economic potential related to the commercial exploitation of energy resources of solar radiation in Brazil basically depend on two factors: the development of a competitive conversion and storing technology for this energy; and the availability of reliable information linked to the energy policy of the nation.

There is a great variety of possibilities on the medium and long term for the use of renewable energy source including solar ranging from small photovoltaic self-contained systems up to large plants using concentrated solar power, or hydrogen generating systems to be used in fuel cells that operate with zero emission of CO_2. However, today this form of energy plays an insignificant part in the Brazilian energy matrix - only solar thermal energy for water heating attracted the national market interest so far (Pereira, et al., 2006)

The main objective of this research is to contribute in the development of solar energy use in Brazil in special PV system. In fact, it will be performed the sizing of PV system to five important cities in Brazil which cover the 5 regions of the country, namely Salvador, Goiania, São Paulo, Porto Alegre and Manaus. The system adopted in the sizing was grid-connect, and for all five cities two types of photovoltaic technologies, monocrystalline silicon and polycrystalline silicon were performed. In the course of sizing the Sunny Design online software (SMA, 2014) was used, which is a free product by SMA Solar Technology AG, Germany.

In addition, it will be also discussed the influence of climate and especially the radiation to the efficiency of PV and other important factors to make a photovoltaic system design. It is hoped that this research is a further incentive for Brazil invest in photovoltaic power systems due to the great solar potential of the country.

2. Analysing the sites for PV application

Currently there are several projects underway or in operation, for the use of solar energy in Brazil, particularly by means of photovoltaic electricity generation,

aiming to supply isolated communities of the electricity network and regional development. Most of these systems are located in the North and Northeast regions of the country. However, these projects are few when considering the size of the country and the solar potential of Brazil.

The area of solar energy has gained importance in the South and Southeast regions of the country, where a significant portion of the electricity consumption is intended for that purpose, especially in the residential sector. A more detailed overview of the geographical distribution of these PV systems installed throughout the country is hampered by the following factors: the nature of these projects; location, scattered small and remote places in the country; and the multiplicity companies and institutions involved in the implementation and operation. (ANEEL, 2014)

For this research was selected one city from each region of Brazil to compare and analyze the issues related to the use of photovoltaic systems in different areas of the country. In Fig. 1 it is possible to see the map of Brazil (Câmara, 2014) with the five major regions and cities studied are highlighted in red.

Figure 1. Brazilian regions and cities for PV applications

Salvador

Salvador is a city and capital of the state of Bahia in Brazil. It has a tropical rainforest climate with no discernible dry season, with average annual

precipitation of 2,144 mm. Temperatures are relatively constant throughout the year, with hot and humid conditions of climate. It reaches extremes of 17 °C in the winter and 30 °C in the summer. It has an average of 2,500 hours of sunshine per year, the humidity is relatively high, averaging between 75% and 85% (Wikipédia, 2014).

Goiania
Goiania is a Brazilian city, capital of the state of Goiás. In Goiania dominates the tropical climate with a dry season. The temperature is mild throughout the year, with an average of 23.2 °C, with an average minimum of 17.7 °C and maximum of 29.8 °C. There are two distinct seasons: the rainy season, from October to April, and a dry season, from May to September. The rainfall is about 1570 mm annually. The months with the highest average rainfall are December and January 268 mm 267 mm, and minors are June 9 and July 7 mm (Wikipédia, 2014).

São Paulo
São Paulo is a Brazilian city, capital of the state of São Paulo. The climate of São Paulo is considered humid subtropical, with decreased rainfall in winter and annual average temperature around 19.3 °C, with mild winters and summers with moderately high temperatures, increased by the effect of pollution and high concentration of buildings. The warmest month of the year is February (22.4 °C) and the coldest is in July (15.8 °C). The average rainfall is 1,441 mm per year, concentrated mainly in the summer. The duration of sunshine is about 2000 hours per year, and the humidity is relatively high, averaging between 75% and 80% (Wikipédia, 2014).

Porto Alegre
Porto Alegre is the capital of the southernmost state of Brazil, Rio Grande do Sul. The climate of Porto Alegre is classified as humid subtropical. Rainfall is well distributed, with annual average remaining around 1,300 mm. The average relative humidity of the air is 76%. The occurrence of snow is very rare, but the frosts occur a few times during the year. According to the National Institute of Meteorology (INMET) for the period between 1961 and 2013, the lowest temperature ever recorded in Porto Alegre was -0.2 °C on July 16, 1993, and most reached 39.8 °C on 25 December 2012 (Wikipédia, 2014).

Manaus
Manaus is the capital of Amazonas. The climate of Manaus is considered humid tropical monsoon, with an average annual temperature of 26.7 °C and high relative humidity throughout the year, with monthly averages between 79% and 88%. The rainfall is high, around 2,300 mm per year, with March the wettest month (335 mm) and August the driest (47 mm). The season is relatively well defined with respect to rain: the winter is relatively dry and summer is wet. (Wikipédia, 2014).

3. Radiation conditions

The most part of the Brazilian territory is located relatively close to the equator, so that there are wide variations in solar day length. However, most of the population and socio-economic activities of the country is concentrated in more distant regions of equator. According with ANEEL (2014) in Porto Alegre, Brazil's southernmost capital (about 30° S), the solar day length varies from 10 hours and 13 minutes to 13 hours and 47 minutes approximately, between June 21 and December 22 respectively.

Thus, to maximize the utilization of solar radiation, it can be adjust the position of the solar modules according to the local latitude and the time of year that requires more energy. In the southern hemisphere, for example, a fixed solar collection system should be oriented to the north, with an angle similar to the local latitude tilt.

The Brazilian Atlas of Solar Energy (2006) presents the average of the estimates of total daily solar radiation provided by irradiative transfer BRAZIL-SR for the period July 1995 to December 2005 model values for a full decade of data. The highest levels of radiation are observed in the Northeast region, highlighting the São Francisco Valley. Importantly, even the regions with lower levels of radiation have great potential for energy recovery. There is a plethora of small exploitations of solar energy in Brazil, but it is still negligible, given the great potential.

The sites which were studied in this research are located in different regions and they have quite similar average of solar radiation. The average rate of horizontal solar radiation in this cities studied are: Salvador 4,55 - 4,90 kWh/ m^2, Goiania 5,25 - 5,60 kWh/ m^2, São Paulo 4,20 - 4,55 kWh/ m^2, Porto Alegre 4,55 - 4,90 kWh/ m^2 and Manaus 4,55 - 4,90 kWh/m^2.

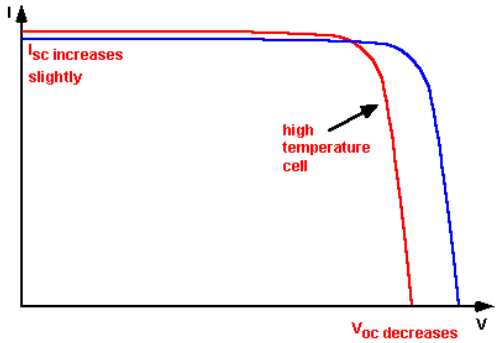

Figure 2. The effect of temperature on the I-V characteristics of a solar cell

This variation of the weather conditions and the location is a feature of many sources of alternative energy and causes an increase in the cost of energy production. So, thinking about energy production by PV systems is very

important to select the most appropriate angle of incidence of solar radiation on the module and the best technology for the application region.

As it is known from the literature (Tiwari, Dubey, 2010), the higher is the temperature the lower the efficiency of PV cell, that factor is really important because Brazil has a nice radiation along the year but it has also higher temperatures which is not good for the operation of PV system. Therefore, that factor has to be seriously taking into account when we are studying the efficiency of one PV system.

In a solar cell, actually the parameter most affected by an increase in temperature is the open-circuit voltage (V_{oc}). The impact of increasing temperature is shown in the Fig. 2 (Honsberg, Bowden, 2014).

4. PV technologies applied in the grid-connected system

As it was mentioned before the photovoltaic generation system is a source of energy, using photovoltaic cells, directly converts light energy into electricity. This system has a number of key advantages such as: does not consume fuel, does not produce pollution and environmental contamination, it is silent, has more than 20 years lifespan, it's resistant to extreme weather conditions (hail, wind, temperature and humidity), it has no moving parts and therefore require very little maintenance (only cleaning the modules) and it allows to increase the installed capacity by incorporating additional modules.

It is commonly used in remote areas of the electrical distribution network, and may work independently or combined with electricity production systems conventional. Its main applications are rural electrification (light, TV, radio, communications, water pumping), electrification of fences, outdoor lighting, signalling, etc. The system can be continuous current (DC) 12 V which is composed of modules or photovoltaic cells, charge controller batteries and battery bank modules. On the other hand, the system can be alternating current (AC) 110/220 (230) V, but in this case it will be needed to install an inverter unit with adequate power. The inverter converts the DC from the battery into AC. It is often needed as most appliances use alternating current.

There are basically three types of cells, according to the manufacturing method (SolarTerra, 2014).

Monocrystalline silicon: These cells are obtained from cylindrical bars monocrystalline silicon produced in special furnaces. Cells are formed by cutting the bars in the form of fine pellets (0.4-0.5 mm thick). Its efficiency in converting sunlight into electricity is higher than 12% (Fig. 3).

Polycrystalline silicon: These cells are produced from silicon blocks obtained by melting pure silicon in special molds. Once in the mold, the silicon cools and solidifies slowly. In this process, atoms are not organized into a single crystal. Form a polycrystalline structure occurs with surfaces separating the crystals. Its efficiency in converting sunlight into electricity is slightly smaller than the monocrystalline silicon (Fig. 4).

Figure 3. Monocrystalline silicon modules

Figure 4. Polycrystalline silicon modules

Thin film or amorphous silicon: These cells are obtained by deposition very thin layers of silicon or other semiconductor materials on glass or metal surfaces. Its efficiency in converting sunlight into electricity is between 5% and 7% (Fig. 5).

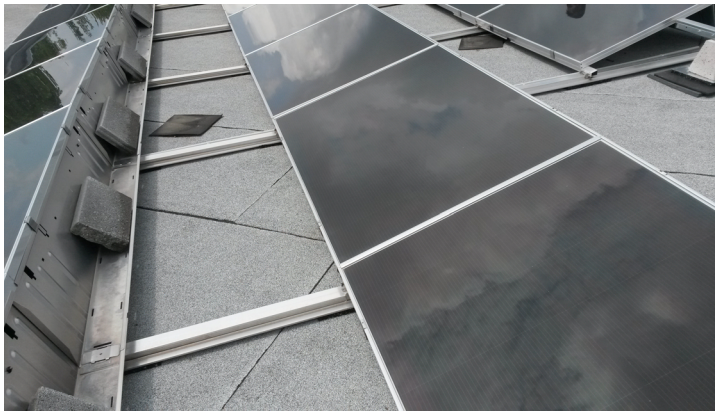

Figure 5. Thin film or amorphous silicon

The Figs 3-5 are showing the three different photovoltaic technology modules were taken from the site of the Institute for Technical Physics and Materials Science, Hungarian Academy of Sciences, Budapest.

However, in this study only two of them were analysed in details in a grid connected system. Generally, the grid-connected or utility-intertie PV systems are designed to operate in parallel with and interconnected with the electric utility grid. The primary component is the inverter, or power conditioning unit. The inverter converts the DC power produced by the PV array into AC power consistent with the voltage and power quality required by the utility grid. The inverter automatically stops supplying power to the grid when the utility grid is not energized. A bi-directional interface is made between the PV system AC output circuits and the electric utility network, typically at an on-site grid-connected distribution panel or service entrance. This allows the power produced by the PV system to either supply on-site electrical loads, or to back feed the grid when the PV system output is greater than the on-site load demand. During periods when the electrical demand is greater than the PV system output (night-time), the balance of power required is received from the electric utility. This safety feature is required in all grid-connected PV systems (AET, 2014) as can be seen in Fig. 6. It also ensures that the PV system will not continue to operate and feed back onto the utility grid when the grid is down for service or repair (Solar Direct, 2014).

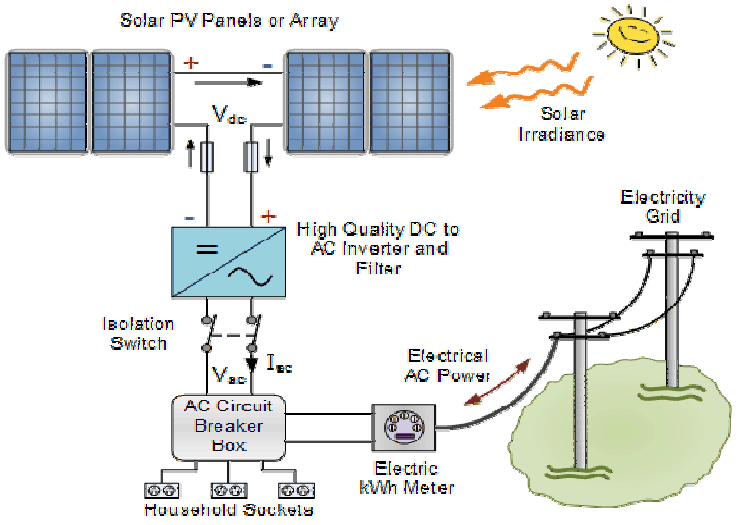

Figure 6. The scheme of the grid-connected PV system

5. Simulation software applied

As it was said before, in the course of the recent study the Suny Design software was applied for simulation and design purposes. It was developed by the

Germany Company SMA Solar Technology AG with the aim to help their customers with a design for PV system.

Sunny Design is available as an online version "Sunny Design Web" and as a desktop version "Sunny Design 3". The range of functions of both versions is identical. So this online software provides a design recommendation for planned PV system or planned PV hybrid system. Sunny Design also proposes a help combination of PV array(s) and inverter(s) which meet, as closely as possible, requirements regarding power class, energy yield and efficiency. In addition, it includes the option of determining and optimizing the potential self-consumption, sizing the cables, evaluating efficiency and, in PV hybrid systems, configuring the relation between the units.

But the downside of using this software is that only the inverters from SMA can be used when you do the PV system sizing, but that fact is not relevant for this research because here the type of inverter is not that much important, in contrast, the type of cell is significant for this survey.

According to the objective of this work, just the Web version in English language was used for the PV project with self-consumption for each five cities selected in Brazil. The opening page of the design software is on Fig. 7.

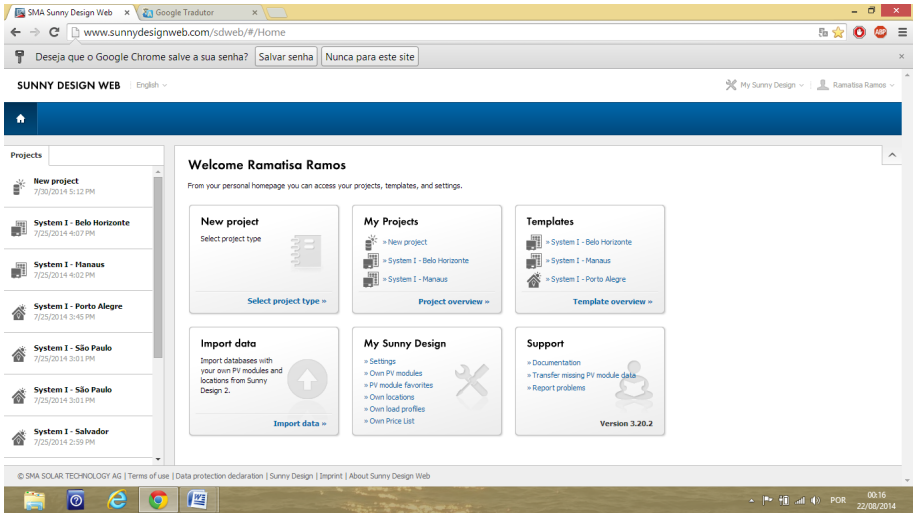

Figure 7. The opening page of the Sunny Design software

The user here can manage his projects, create new projects, overview and modify existing projects, create or modify templates, import data, manage the user settings and see the documentation of the software.

When creating a new project, the software offers 3 possibilities: PV system, PV system with self-consumption and hybrid system. The normal PV system is for a system with no self consumption, so these projects are basically power plants. But it can be used for every project, where the self-consumption is not

considered. The PV system with self consumption is for designs, where the energy consumption of the building or community is taken into consideration. These are usually residential, small commercial and industrial rooftop or ground mounted designs, where the goal is, to produce equal energy by the PV system as the self consumption – or simulate the net power output. That option covers the grid-connected hybrid and island designs too. The hybrid design is for systems with auxiliary power generators. In this survey was used only the PV system with self-consumption.

Every new project design starts with the geographical data and placement of the location. Own locations can be added, or the existing location and meteorological data can be modified and saved as an own location. Next step is the PV plant design. On this page every properties of the PV plant can be added or modified. There is also a possibility to create part projects, if it is necessary, there is also a possibility to create alternative designs and compare them. There are fields for selecting the PV modules, the nominal power of the array or the number of the modules. The inclination, azimuth angle and mounting type also can be adjusted. It is also possible to add more PV arrays, if necessary.

For the inverter selection there are 3 opportunities: the automatic design, which automatically calculates the best fitting solution, the design alternatives, where the user can select from a number of suggestions, and the manual design, where the user can select from the list of inverters.

The next step is the planning of the system monitoring. There are a lot of possibilities, and the monitoring system almost always depends on what the buyer wants. After is the economic viability, which simulates the economic effects of the PV plant. Some data must be given in, and the software takes the design parameters to calculate the savings.

The last two steps are the project overview and the document download. For a design with self-consumption or a hybrid system there are two additional pages during the process. One is the page for defining the load profile for the design, here are some preloaded profiles, which can be altered, or the user can create own profiles. The other pages are is for the design of the self-consumption, the battery bank, and a small energy analysis.

6. Simulation results

The software that assisted in the design of these photovoltaic systems has already registered the main models of panels and inverters available in the market beyond the basic meteorological data that help predict the amount of energy to be generated by the system. Therefore, all meteorological data concerning the cities studied were generated by the software.

The modules of Eco Solargy (Eco 250A156M-60) and SMA (SMA Demo Poly 240) were selected, where the first is mono- and second is polycrystalline silicon. The inverters were all chosen according to the need of the systems and they were from SMA.

The design of photovoltaic systems began by defining the amount of energy being produced. It was established for all the same standard systems. The sizing was done considering private house, with 4 people and annual energy consumption of 5,000 kWh (self consumption). The inverter grid connection was established 220V (110V/220V) 60 Hz for all cities and systems.

The second step was to determine the location of the installation of the modules. Maximum production will be according to the availability of sun, the orientation and tilt of the modules. The best orientation is toward the equator (North direction, for most Brazilian states). The slope of the increased production of panels is one where the light is incident as perpendicular as possible to the plane of the panel and is a function of the latitude of the site. The optimum slope can vary in very cloudy months.

The location chosen was the roof, it is an area that is not used by homes and the optimal tilt angle of the panel was given automatically by the software and can be seen in the Table 1. Remember that besides the production efficiency the choice of angle is important to prevent the accumulation of water and facilitate cleaning with natural rain. It was not used track, because it is not economically viable.

Table 1 The optimal tilt angles

Cities	Inclination
Salvador	9°
Goiania	11°
São Paulo	16°
Porto Alegre	20°
Manaus	5°

Finally, the solar radiation was checked at the site. In Brazil, the radiation is between 4 kWh/m^2/day in the South and 6.5 kWh/m^2/day in the Northeast. The amount of the panels was determined according to the energy that is desired to produce automatically by the software, and each system was sized with 10 modules. The PV array (combination of panels in series/parallel) was chosen to be compatible with the inverter used. For this, the technical specifications of the modules and inverters are consulted to determine the size and quantity of the series of modules, as well as the quantity of inverters required. The material selected for the cables were copper and the load losses in the system were not taking in to account.

In summary, the simulations of two systems were done for each city studied. The system I was sized with mono- and the system II was sized with polycrystalline silicon module.

Salvador

The rate of performance to the two systems are very close, 82.5% of the system I and 82.9% of the system II. The production of energy in system I (3998 kWh) is slightly larger than the system II (3851 kWh).

In the system I 44.9% of the energy produced by PV is used by the residence and the rest of the energy goes into the grid. Thus, the energy consumption of the house becomes 35.9% independent of the grid. If we take into account the total energy produced by the PV the house would become 79.96% independent of the grid.

Moreover, in the system II 46% of the energy produced by PV is used by the residence and the rest of the energy goes into the grid. Thus, the energy consumption of the house becomes 35.4% independent of the grid. If we take into account the total energy produced by the PV the house would become 77.02% independent of the grid.

Goiania

In this case the rate of performance to the two systems are quite the same, 82.4% of the system I and 82.5% of the system II, and the production of energy in system I (3936 kWh) is bigger than the system II (3781 kWh).

In the system I 45.4% of the energy produced by PV is used by the residence and the rest of the energy goes into the grid. Thus, the energy consumption of the house becomes 35.7% independent of the grid. If we take into account the total energy produced by the PV the house would become 78.72% independent of the grid.

Furthermore, in the system II 46.5% of the energy produced by PV is used by the residence and the rest of the energy goes into the grid. Thus, the energy consumption of the house becomes 35.2% independent of the grid. If we take into account the total energy produced by the PV the house would become 75.62% independent of the grid.

São Paulo

The rate of performance to the two systems are very close, 84% of the system I and 83, 4% of the system II, and the production of energy in system I (3155 kWh) is a little bit larger than the system II (3007 kWh).

In the system I 50.2% of the energy produced by PV is used by the residence and the rest of the energy goes into the grid. Thus, the energy consumption of the house becomes 31.7% independent of the grid. If we take into account the total energy produced by the PV the house would become 63.1% independent of the grid.

In addition, in the system II 51.6% of the energy produced by PV is used by the residence and the rest of the energy goes into the grid. Thus, the energy consumption of the house becomes 31.1% independent of the grid. If we take into account the total energy produced by the PV the house would become 60.14% independent of the grid.

Porto Alegre

The rate of performance to the two systems are very close, 82.3% of the system I and 82, 7% of the system II, and the production of energy in system I (3078 kWh) is larger than the system II (2967 kWh).

In the system I 51.1% of the energy produced by PV is used by the residence and the rest of the energy goes into the grid. Thus, the energy consumption of the house becomes 31.5% independent of the grid. If we take into account the total energy produced by the PV the house would become 61.56% independent of the grid.

Moreover, in the system II 52.2% of the energy produced by PV is used by the residence and the rest of the energy goes into the grid. Thus, the energy consumption of the house becomes 31% independent of the grid. If we take into account the total energy produced by the PV the house would become 59.34% independent of the grid.

Manaus

The rate of performance to the two systems are the same, 81.9% for the system I and for the system II, and the production of energy in system I (3691 kWh) is slightly larger than the system II (3544 kWh).

In the system I 46.8% of the energy produced by PV is used by the residence and the rest of the energy goes into the grid. Thus, the energy consumption of the house becomes 34.6% independent of the grid. If we take into account the total energy produced by the PV the house would become 73.82% independent of the grid.

Moreover, in the system II 48% of the energy produced by PV is used by the residence and the rest of the energy goes into the grid. Thus, the energy consumption of the house becomes 34% independent of the grid. If we take into account the total energy produced by the PV the house would become 70.88% independent of the grid.

Conclusions

In the study was found that the city with the highest production of photovoltaics was the city of Salvador (3998 kWh) and the city that had the lowest production was the city of Porto Alegre (2967 kWh). It is believed that this is due to the large difference in location of the two cities. Salvador is in the northeast region, where we have higher levels of radiation and temperature while Porto Alegre is located in the southern region, where we have the lowest levels of radiation and temperature in the country.

In all cities, the panel monocrystalline silicon showed the higher efficiency of energy production. However, no major difference in efficiency between the two technologies panels was identified. Therefore, it was confirmed what is established in the literature, that monocrystalline silicon modules are slightly more efficient than polycrystalline silicon panels.

Another relevant factor was the percentage of the grid independence of the residences, the largest 35.9% in Salvador and the lowest 31% in Porto Alegre. This percentage is very significant to lessen the burden on the power grid in large cities, such as those studied. Another significant factor is that part of the

energy produced in these homes goes to the grid. With this, generates an increase in energy availability in the country, since the domestic sector is a large consumer of electricity in Brazil.

This increase in the production of electricity that could be generated in Brazil by the application of such systems is very important to diversify the country's energy matrix and promote their independence secure in this sector, which is essential for the development of any country. Thus, it is expected that this research will serve as an incentive for increased use of these photovoltaic systems throughout Brazil improving the efficiency of energetic planning of the country.

Acknowledgements

This work was supported by Science Without Borders - CAPES, Brazil. The authors acknowledge also the support of the OTKA K 84150 project.

References

[1] Alternative Energy Tutorial. Grid connected PV system. Available in: <http://www.alternative-energy-tutorials.com/solar-power/grid-connected-pv-system.html>. Date: 16th August 2014.

[2] ANEEL. Energia solar. Available in: <http://www.aneel.gov.br/aplicacoes/atlas/energia_solar/energia_solar.htm>. Date: 29th July 2014.

[3] Câmara, J., As regiões do Brasil. Available in: <http://umaarteeducar.blogspot.hu/2012/11/as-regioes-do-brasil.html>. Date: 24th August 2014.

[4] Honsberg, C.; Bowden, S., Solar cell operation. Available in: <http://www.pveducation.org/pvcdrom/solar-cell-operation/effect-of-temperature >. Date: 16th August 2014.

[5] International Energy Agency (IEA). World Energy Outlook 2013. Paris - France, 2013.

[6] Pereira, E. B., Martins, F. R., Abreu, S. L., Rüther, R.. Atlas brasileiro de energia solar (Brazilian atlas of solar energy). São José dos Campos: INPE, 2006.

[7] SMA Solar Technology. Sunny Design. Available in: < http://www.sma-america.com/en_US/products/software/sunny-design.html>. Date: 15th July 2014.

[8] Solar Direct. Photovoltaic System. Available in: <http://www.solardirect.com/pv/systems/systems.htm>. Date: 16th August 2014.

[9] SolarTerra. Energia Solar Fotovoltaica - Guia Prático. Available in: <http://mbecovilas.files.wordpress.com/2011/06/energia-solar-fotovoltaica.pdf>. Date: 15th July 2014.

[10] Tiwari, G. N.; Dubey, S., Fundamentals of photovoltaic modules and their applications. Julian Hunt FRS, University College London, London, UK. 2010.
[11] Wikipédia. Goiania. Available in: < http://pt.wikipedia.org/wiki/Goi%C3%A2nia>. Date: 24th August 2014.
[12] Wikipédia. Manaus. Available in: < http://pt.wikipedia.org/wiki/Manaus>. Date: 16th August 2014.
[13] Wikipédia. Salvador. Available in: < http://pt.wikipedia.org/wiki/Salvador_(Bahia)>. Date: 16th August 2014.
[14] Wikipédia. São Paulo. Available in: <http://pt.wikipedia.org/wiki/S%C3%A3o_Paulo_(cidade)>. Date: 16th August 2014.
[14] Wikipédia. Porto Alegre. Available in: < http://pt.wikipedia.org/wiki/Porto_Alegre>. Date: 16th August 2014.